PB 81-210734

U.S. Department
of Transportation
**Federal Railroad
Administration**

Wind Tunnel Tests of Trailer and Container Models

Office of Research
and Development

Washington, D.C. 20590

Determination of the Independent Influence of Height and Gap Spacings and Trailer Undercarriage Shielding on Aerodynamic Forces Occurring During Railroad Transport

FRA/ORD-80/51

March 1980

A. G. Hammitt

Document is available to the U.S. public through the National Technical Information Service, Springfield, Virginia 22161

Technical Report Documentation Page

1. Report No.	2. Government Accession No.	3. Recipient's Catalog No.
FRA/ORD-80/51		

4. Title and Subtitle
Wind Tunnel Tests of Trailer and Container Models to Determine the Independent Influence of Height and Gap Spacings and Trailer Undercarriage Shielding on Aerodynamic Forces Occurring During Railroad Transport.

5. Report Date
March 1980

6. Performing Organization Code

7. Author(s)
Andrew G. Hammitt

8. Performing Organization Report No.
12-101-80

9. Performing Organization Name and Address
Andrew G. Hammitt Associates
30813 Marne Drive
Rancho Palos Verdes, CA 90274

10. Work Unit No. (TRAIS)

11. Contract or Grant No.
DOT-FR-8058

12. Sponsoring Agency Name and Address
U.S. Department of Transportation
Federal Railroad Administration
Office of Research and Development
Washington, D. C. 20590

13. Type of Report and Period Covered
Final letter report
Sept. 1979 - March 1980

14. Sponsoring Agency Code

15. Supplementary Notes
See also Aerodynamic Forces on Various Configurations of Railroad Cars for Carrying Trailers and Containers, FRA/ORD-79/39 and Aerodynamics of Freight Trains, FRA/ORD-76/295 Volumes I through IV.

16. Abstract
A series of wind tunnel tests have been run on scale model trains of 40 ft. containers and trailers. The models were 1/43 scale. A train of five models was used with forces and moments measured on the center model. A variety of spaces were used between the models. The height of the container models was varied and the undercarriage of the trailers was protected with shields of different heights. These tests are the latest in a series designed to determine the aerodynamic forces on containers and trailers on flatcars. This series provides additional information on the effect of different container block height and gap spacings and the effect of spacing on the forces on trailers with different amounts of shielding up to large values of yaw angle.

The tests showed that axial force initially increased with yaw angles up to 30 to 40° and then decreased. This decrease is caused by the axial component of the wind velocity decreasing with increasing yaw angle until it becomes zero at 90° yaw angle. The side forces increase with yaw angle reaching a maximum at about 60°. The moment data shows that the side force is applied about half way up the block at a point a little forward of the center. On the trailers, the point of application is still about half way between the top of the trailer and the ground for all shieldings used and either ahead of or behind the centerline depending on the amount of shielding.

17. Key Words	18. Distribution Statement
Intermodal, TOFC, COFC, Piggyback Aerodynamics, Train Resistance and Wind Tunnel Testing of Railcars	This document is available to the public through the National Technical Information Services, Springfield, VA 22161.

19. Security Classif. (of this report)	20. Security Classif. (of this page)	21. No. of Pages	22. Price
Unclassified	Unclassified	90	

Form DOT F 1700.7 (8-72)

METRIC CONVERSION FACTORS

Approximate Conversions to Metric Measures

Symbol	When You Know	Multiply by	To Find	Symbol
	LENGTH			
in	inches	*2.5	centimeters	cm
ft	feet	30	centimeters	cm
yd	yards	0.9	meters	m
mi	miles	1.6	kilometers	km
	AREA			
in^2	square inches	6.5	square centimeters	cm^2
ft^2	square feet	0.09	square meters	m^2
yd^2	square yards	0.8	square meters	m^2
mi^2	square miles	2.6	square kilometers	km^2
	acres	0.4	hectares	ha
	MASS (weight)			
oz	ounces	28	grams	g
lb	pounds	0.45	kilograms	kg
	short tons (2000 lb)	0.9	tonnes	t
	VOLUME			
tsp	teaspoons	5	milliliters	ml
Tbsp	tablespoons	15	milliliters	ml
fl oz	fluid ounces	30	milliliters	ml
c	cups	0.24	liters	l
pt	pints	0.47	liters	l
qt	quarts	0.95	liters	l
gal	gallons	3.8	liters	l
ft^3	cubic feet	0.03	cubic meters	m^3
yd^3	cubic yards	0.76	cubic meters	m^3
	TEMPERATURE (exact)			
°F	Fahrenheit temperature	5/9 (after subtracting 32)	Celsius temperature	°C

*1 in = 2.54 (exactly). For other exact conversions and more detailed tables, see NBS Misc. Publ. 286, Units of Weights and Measures, Price $2.25, SD Catalog No. C13.10:286.

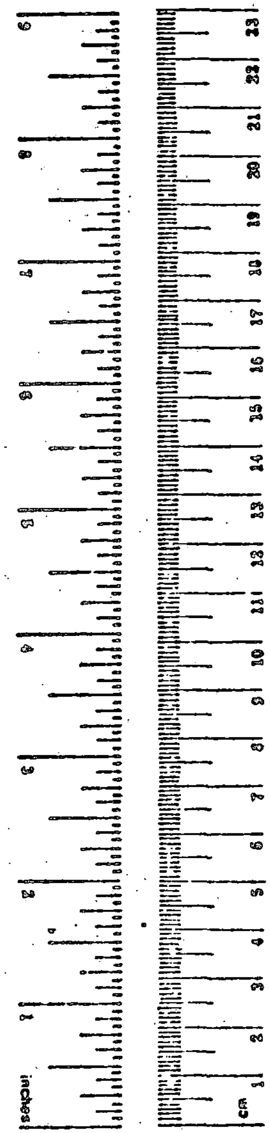

Approximate Conversions from Metric Measures

Symbol	When You Know	Multiply by	To Find	Symbol
	LENGTH			
mm	millimeters	0.04	inches	in
cm	centimeters	0.4	inches	in
m	meters	3.3	feet	ft
m	meters	1.1	yards	yd
km	kilometers	0.6	miles	mi
	AREA			
cm^2	square centimeters	0.16	square inches	in^2
m^2	square meters	1.2	square yards	yd^2
km^2	square kilometers	0.4	square miles	mi^2
ha	hectares (10,000 m^2)	2.5	acres	
	MASS (weight)			
g	grams	0.035	ounces	oz
kg	kilograms	2.2	pounds	lb
t	tonnes (1000 kg)	1.1	short tons	
	VOLUME			
ml	milliliters	0.03	fluid ounces	fl oz
l	liters	2.1	pints	pt
l	liters	1.06	quarts	qt
l	liters	0.26	gallons	gal
m^3	cubic meters	35	cubic feet	ft^3
m^3	cubic meters	1.3	cubic yards	yd^3
	TEMPERATURE (exact)			
°C	Celsius temperature	9/5 (then add 32)	Fahrenheit temperature	°F

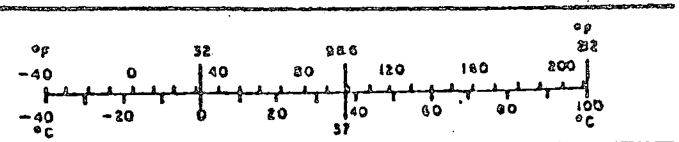

TABLE OF CONTENTS

LIST OF ILLUSTRATIONS

LIST OF ILLUSTRATIONS (continued)

LIST OF TABLES

NOMENCLATURE

$C_A A$	Axial force area
$C_Y A$	Side force area
V_R	Wind velocity relative to vehicle
V_T	Train velocity
V_w	Velocity of actual wind (relative to ground)
α	Direction of actual wind
ψ	Angle of yaw, degrees
Model height	Expressed as multiples of model width
Gap spacing	Expressed as multiples of model width
GALCIT	Graduate Aeronautical Labotsyoty, California Institute of Technology Institute of Technology

INTRODUCTION

This report is the sixth in a series of reports on the aerodynamic forces on railroad freight cars. Tests were performed on standard and modified TOFC and COFC configurations, Reference 1, and on a variety of freight car and developmental TOFC and COFC configurations, Reference 2. A general investigation of the forces on a train of blocks of standard shapes was also carried out in References 1 and 2. The purpose of these tests was to gain general information on the aerodynamic forces on a train of blocks with particular interest in the interference effects between the blocks. The present tests are a continuation of this general investigation using models of containers and trailers. The particular objectives of these continuing tests are to investigate how the aerodynamic forces are effected by the gaps between the models, the height of the models, and, for the case of trailers, the shielding of the space beneath the trailers. The sponsor anticipates the utilization of this data in intermodal railcar design work where the parameters of height, gap and shielding are to be established and where quantitative knowledge of their effects can be used in trade-off studies against the other design-related components of overall train resistance.

TEST PROGRAM

The aerodynamic test program was run in the GALCIT 10 foot wind tunnel at the California Institute of Technology following the procedures which had been developed in the previous wind tunnel tests on rail freight configurations. The configuration used in the previous tests was modified for these tests in two ways. In these tests a yaw angle range up to 90° was desired. The yaw table, however, has a maximum rotation of 50°. In order to obtain data at angles up to 90° it was decided to run the tests using two different configurations, 0° to 48° using a mounting system lined up with the flow when the yaw table was set to 0° (Configuration A) and 42° to 90° using a mounting set at 90° to the flow when the yaw table was set to 0°

(Configuration B). This arrangement was the best that could be accomplished with reasonable costs but required the tests over the full range of yaw angles to be broken into two parts and run separately. The mounting system for these tests is shown in Figures 1a and b.

The other modification in the test configuration that was made was to provide a metric plate flush with the surface on which the container block and trailer models were mounted. The advantage of this arrangement was that the container models could be mounted directly on this plate without the possibility of the metric model contacting the non-metric surfaces. The only possible contact was between the metric plate and the non-metric surfaces and proper clearances could be established for all tests and monitored by checking electric continuity between the metric elements and ground. This configuration is shown in Figure 2 and a photograph of the partially assembled parts in Figure 3.

The models for these tests consisted of the same trailer models which were used in previous tests and a series of container blocks of different heights. Drawings of the models are shown in Figures 4a and b. The models are all to 1/43 scale. In plan view the blocks are all the same, representing a full scale size of 40 feet by 8 feet. The height of the container block models varies from 1 times the width to 2.4 times the width. The 1.7 widths high model was considered the basic model since it had the same height as the trailers. More tests were run on this model than on any of the others. Four shielding pans were provided to mount under the trailers to shield the undercarriage. These are shown in Figure 5. The trailers and the shielding pans were mounted directly on the metric plate. Therefore, the forces measured consisted of the forces on the trailers, the surface of the metric plate, and the shielding pans when used. While these tests could have been run with the shielding pans and plate surface non-metric, the merit of the use of the shielding pans can only be evaluated when the forces on the pan as well as the trailer are measured.

Aerodynamic theory and practice has established that aerodynamic forces on objects scale as the dynamic pressure of the air flow, one half the air density times the velocity squared. Tests at different velocities can be correlated if the actual forces are divided by the dynamic pressure to form a number which has the dimensions of area. Once this force area has been determined for tests at one velocity it can be used to predict forces at any velocity by multiplying the force area by the appropriate dynamic pressure. This same concept can be applied to moments. In this case the number obtained by dividing the moment by the dynamic pressure has the dimensions of area. To facilitate in this process Table 1 shows dynamic pressure as a function of relative wind velocity for sea level conditions. For instance, if the axial force area were 20 square feet, the axial force at 50 mph would be 6.384 pounds per square foot times 20 square feet equalling 127.7 pounds. At 70 mph, the dynamic pressure would be 12.513 pounds per square foot and the force 250.3 pounds.

WIND TUNNEL TESTS

The wind tunnel test matrix is shown in Table 2. The first runs were made with the Configuration A allowing tests to be run up to 50° yaw angle. The plan was to limit most of the tests to the yaw angle range of 0° to 30°. However, tests at gap spacings of 0.2, 0.5, 1.0 and 2.0 were to be carried out up to 90° (using Configuration A from 0° to 48° and Configuration B from 42° to 90°). The first tests that were run were for block heights of 1.0, 1.4, 2.0, and 2.4. These were run as described. After these tests were completed, some of the data had become available and had been examined. The conclusion was reached that there was not much variation between the results at the different gap spacings, especially those with a change of 0.1 between 0.1 and 1.0. For later tests some of these spacings were left out. Since it was decided to leave out the 0.5 spacing, the 0.4 spacings were carried out to 48°. These reduced sets of spacings were used for the 1.2 and 1.7 high blocks.

Configuration B allowing testing at yaw angles of 42° to 90° was not installed until near the end of the test series.

Sufficient time was available for completing tests only on the 1.2 and 1.7 high blocks in the 42° to 90° range. The series of tests made on the 1.7 high blocks with different gap spacings ahead and behind were all carried out in the range of 0° to 48° yaw angle.

Photographs of the test configurations used for the uniform spacing ahead of and behind the metric block are shown in Figures 6 through 11. Both Configurations A and B are shown when used. The axial force areas for these configurations are shown in Figures 12 through 17 and the side force areas are shown in Figures 18 through 23. The data at all spacings has not been shown on these figures since the curves lie too closely together to properly show in the figures. This is particularly true on the side force data where there is only a small effect of spacing.

The axial force data shows that the axial forces increase with spacing as expected. At the higher yaw angles, the axial force decreases and actually becomes negative near 90° yaw angles. This behavior is not unexpected since at 90° yaw angle the axial force is at right angles to the wind direction. As the component of the wind in the axial direction decreases, it is to be expected that the force will also decrease. This behavior is best seen in Figures 13 and 15 where the tests have been extended up to 90° yaw angle.

For the low blocks, 1.0 and 1.2 in height, a somewhat erratic behavior seems to exist at small yaw angles and spacings of 0.4 and 0.8. Peaks appear in the axial force near 12° yaw angle especially for the 1.0 high block.

For the higher blocks, 2.0 and 2.4, negative axial forces occur at small gap spacings. The reason for this appears to be that at angle of yaw the side forces were sufficient to roll the blocks a significant amount. This rolling was observed during the tests but could not be accurately monitored or recorded. To obtain some more quantitative results, a mechanical side force was applied to the block while the tunnel was shut down. The amount and location of this force was adjusted to produce the same side force, roll and yaw moments observed during an actual test run. Lateral displacements both at the top and bottom of the block were recorded. These measurements allowed an estimate of the lateral displacement of the metric block with respect to the block ahead and behind. The mechanical tests indicated that the principle motion was caused by a twisting of the balance which was located below the base of the model. A displacement up to about .05 inches was obtained as the worst condition. It seems possible that this displacement caused higher pressures on the rear of the metric block than on the front leading to the negative axial forces. Negative axial forces were obtained in previous tests, Reference 2, when a block higher than the metric block was located behind the metric block.

The side forces show little change with spacing. In general, an increase in the spacing causes an increase in the side force but this does not always appear to be true. The results are close enough together so that random variations between the tests may be causing some confusion, but the repeatability seems good enough so that this should not be true. From a practical point of view, the variations measured should not be of great importance.

The next set of tests involved different spacings ahead of or behind the metric block than for the rest of the blocks in the train of blocks. Photographs of the blocks in the tunnel are shown in Figures 24 and 25. The axial force area for variable spacing behind the metric block is shown in Figures 26 through 29 and the side forces in Figures 30 through 33. Similar results for variable spacing ahead of the metric block are shown in Figures 34 through 37 and Figures 38 through 41. The effect of increasing the space behind the metric block is to increase the axial force for low yaw angles but to decrease the force at higher yaw angles, sometimes even to negative values. The most likely reason for this is that at the larger gaps and higher yaw angles a vortex is formed in the larger gap and the pressure on the rear of the metric block is increased. The effect on the side force is much less. All of the curves tend to lie on top of each other. For this reason only the extreme curves have been shown and the others lie between. The effect of increasing the front gap is more pronounced than that found for the rear gap. This result is consistant with previous tests, Reference 2, that have shown that the size of the forward gap is more important than the rear gap and that the effect of both gaps is approximately the sum of the two effects taken individually. The effect of the front gap size on side force is also larger than that of the rear gap, however, the effect is not particularly large.

Figure 42 shows the effect of changing both front and rear gaps for the larger gap sizes. This figure shows that the front gap is more important than the rear gap in determining the axial force. The side forces for these configurations are shown in Figures 43 and 44. While not as important for the side forces, the size of the front gap is still more important than the rear gap.

Photographs of trailers with different spacings and shields under the trailers are shown in Figures 45 through 49. The shield consists of a pan with different heights of sides varying from 0 to 100% of the height to the underside of the trailer. The shields under all of the trailers in any configuration are the same but may not look so in the photographs because of different light reflection. The axial force areas for these different trailer configurations are shown in Figures 50 through 54. The forces measured are those on the trailer, the shield, and the ground plane under the trailer. The axial forces increase with yaw angle and gap spacing as might be expected from previous results. There is some peculiar behavior for gap spacings of 0.8 and 1.0 near zero yaw angle for 0 and 25% shields. Comparing the figures for different shields shows that the larger the shield the less the axial force area. The shielding of the undercarriage is more important than the actual increase in frontal area caused by the shield. The side force areas are shown in Figures 55 through 59. There is very little effect of either gap size or shield size on the side force.

Figures 60 and 61 show the results for one set of runs with the trailers facing backward and no shield. The axial forces are increased somewhat over those for the forward facing trailers but the side force is not effected appreciably. This result is consistant with previous tests on trailers on flatcars facing both directions, Reference 1.

The moments about the three axis were measured in these tests. The moments of particular interest involve the roll and yaw of the vehicle. If the assumption is made that the side force is the only one which contributes to the roll and the yaw moments, then it is possible to establish the point of application of this force. This approach is considered to be a useful one in that it gives a result that is more easily understood and correlated than the moment results. It is reasonable to expect that the lift and axial forces make only a minor contribution to these moments. Actually, no error is introduced if the result presented is considered to be the quantity obtained by dividing these moments by the side force which has the dimension of length. These lengths can then be thought of as describing the approximate location at which the side force is applied.

The data for the various configurations tested has been analyzed in this way. The results for the height of application of the side force are shown in Table 3. The results for the different height blocks run at uniform gap spacing ahead and behind are shown in Part A. There appeared to be no systematic variation with either yaw angle or block spacing. For each block height the results have been averaged for all runs at different yaw angles and spacing and the average value and standard deviation are given in the table. In calculating this average, all data at 0° yaw angle and some data at 3° yaw angle that gave results not in keeping with general trends has been excluded. This was done because the side forces and rolling moments are small at these small yaw angles and small errors in each can make the ratios unreliable.

This point of application divided by the block height does seem to have a significant trend with respect to block height.

The height of the point of application plotted against block height is shown in Figure 62. There is a small but significant increase with respect to block height. The reason for this is not clear. One suggestion is that the higher blocks are less influenced by the boundary layer on the ground plane. One would expect this to cause an opposite effect, a higher relative point of application on the lower blocks instead of the higher blocks. Another cause could be the change in height to width ratio of the blocks. For instance, if part of the effect was due to the lift force, its effect might be different as the block became relatively narrower.

The data for the tests on the 1.7 high blocks at different spacings ahead and behind shows no significant trends with the changes in these parameters. The results averaged over all yaw angles and for all blocks with the same fixed values of forward or rearward spacings are shown in Table 3, Part B. There appear to be no significant variations between the results at different fixed spacings. Therefore, the results at the different fixed spacings have been averaged. This result is shown in the table and also plotted in Figure 62 where it compares favorably with the other results at this block height.

The tests on the trailers have also been treated in this same way. These results are shown in Table 3, Part C. The height of the point of application is shown averaged over yaw angle and trailer spacing for the different shield configurations. There does not appear to be a systematic effect of shield height so these results have been averaged again over all shield heights. Since the overall height of the trailers is the same as the 1.7 high blocks, the point for the trailers has been shown in Figure 62 at this value of the abscissas and corresponds favorably.

The longitudinal distance to the point of application of the side force has been considered in a similar way. However, there is a correlation between the longitudinal location of the point of application and the gap spacing. Increasing the spacing moves the point of application forward. This same result was found in the tests presented in Reference 1. These results are shown in Figure 63 both for the blocks of different heights and for the trailers with different shielding heights. The point of application for the forward facing trailers is further back than for the blocks and further ahead for the aft facing trailers. This change might be related to the greater lateral area near the end of the trailer where the wheel bogie is located. The negative slope with increasing spacing that occurs with the aft facing trailer is hard to explain. This slope is contrary to the slope that occurs for all other configurations.

RESULTS

The axial force initially increases with yaw angle up to values of 30° to 40° and then decreases. This increase has been observed in all the previous tests of objects in trains and is apparantly caused by the decrease in the shielding between the objects as the yaw angle increases. Previous tests had only been up to yaw angles of 30° so the drop off above this value was not observed. This decrease is undoubtedly caused by the decrease in the axial component of the wind as the yaw angle increases. At 90° this axial component is zero resulting in low axial forces. For yaw angles around 80° a negative axial force often occurs. The axial force increases with block height and frontal area.

The side forces depend upon yaw angle and increase with yaw angle up to a maximum at about 60° and then continue or decrease somewhat as the yaw angle increases up to 90°. Increasing the height increases the side force but there is only a small effect of gap size observed in these tests. At small yaw angles the side force increases more rapidly than proportionately with yaw angle. In Reference 1 the theory for the side force was presented and comprised terms proportional to the first and second powers of the yaw angle.

The roll and yaw moments have been interpreted as the point of application of the side force based upon the assumption that these moments are principally caused by the side force. The result is that the point of application of the side force is about at the mid-height and a little forward of the centerline of the block. The height of application seems to be independent of all parameters except for a slight dependence on block height. The longitudinal position depends upon the spacing, moving further forward at greater spacings. For the trailers the height of the point of application is the same as for the blocks and is independent of the height of the shielding pan. The longitudinal location follows the same trend with gap spacing but also depends on the amount of shielding. At 100% shielding the location is similar to that for the blocks, but moves towards the rear as the shielding is reduced so that at 0% shielding it is behind the center of the trailer. Since the wheel bogie is at the rear of the trailer, this behavior can be ascribed to the greater exposure of this bogie as the shielding is reduced. For the aft facing trailer with 0% shielding the point of application is well forward and rapidly moves aft as the spacing increases. This behavior for the aft facing trailer seems inconsistent with the behavior observed for the other configurations and cannot be readily explained.

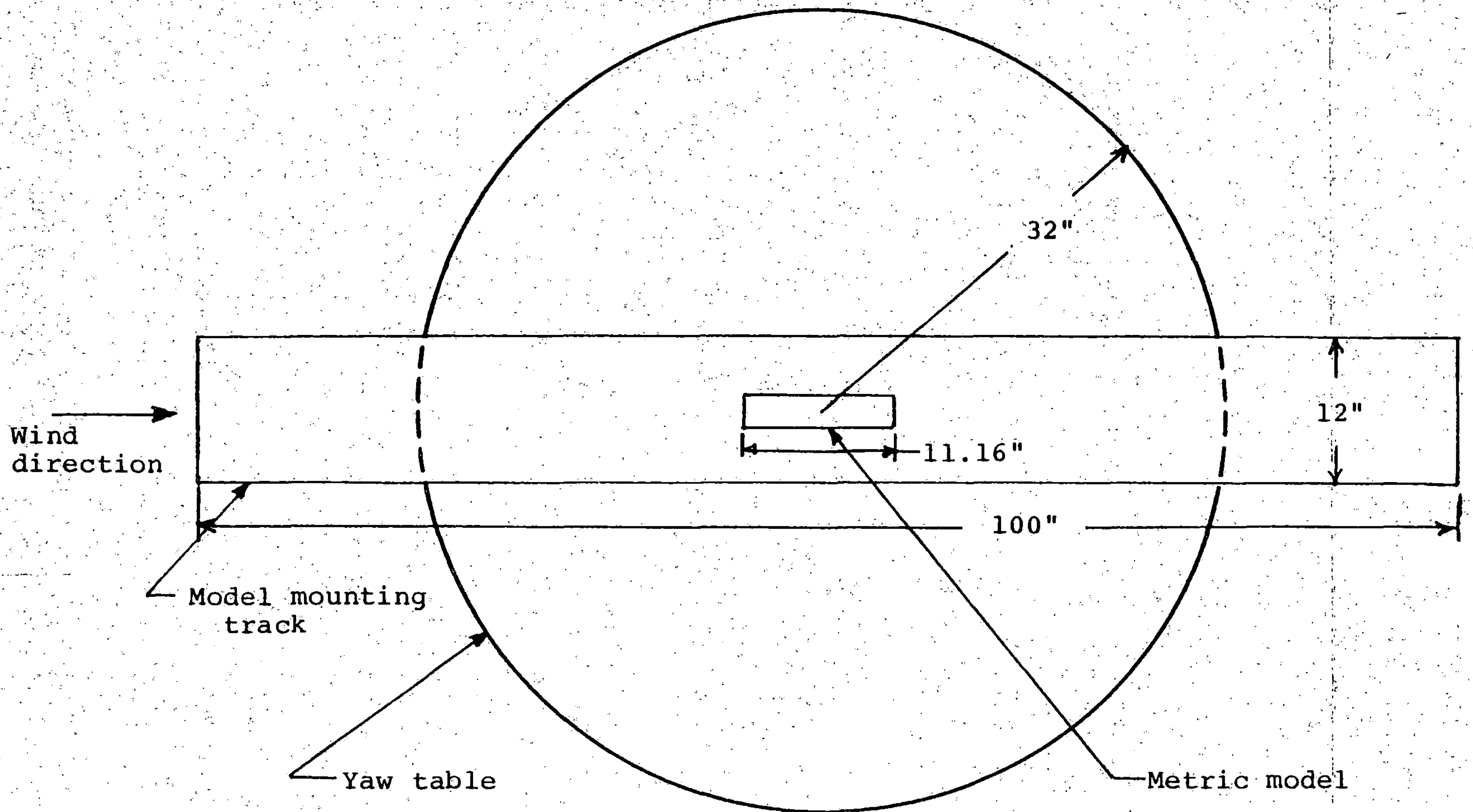

Figure 1a. Model Mounting Arrangement in Wind Tunnel. Arrangement for 0° to ±50°, Configuration A.

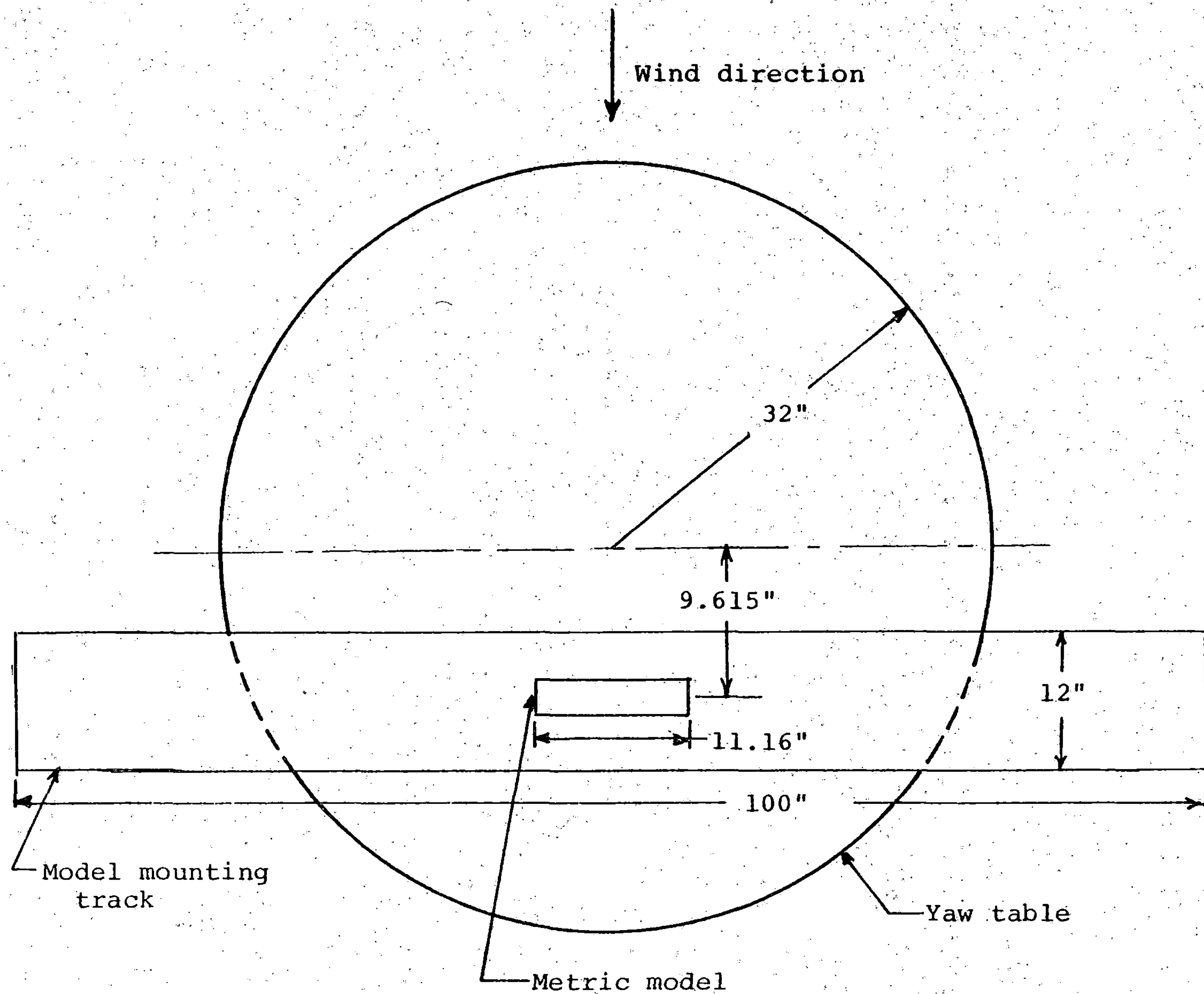

Figure 1b. Model Mounting Arrangement in Wind Tunnel. Arrangement for 40° to 90°, Configuration B.

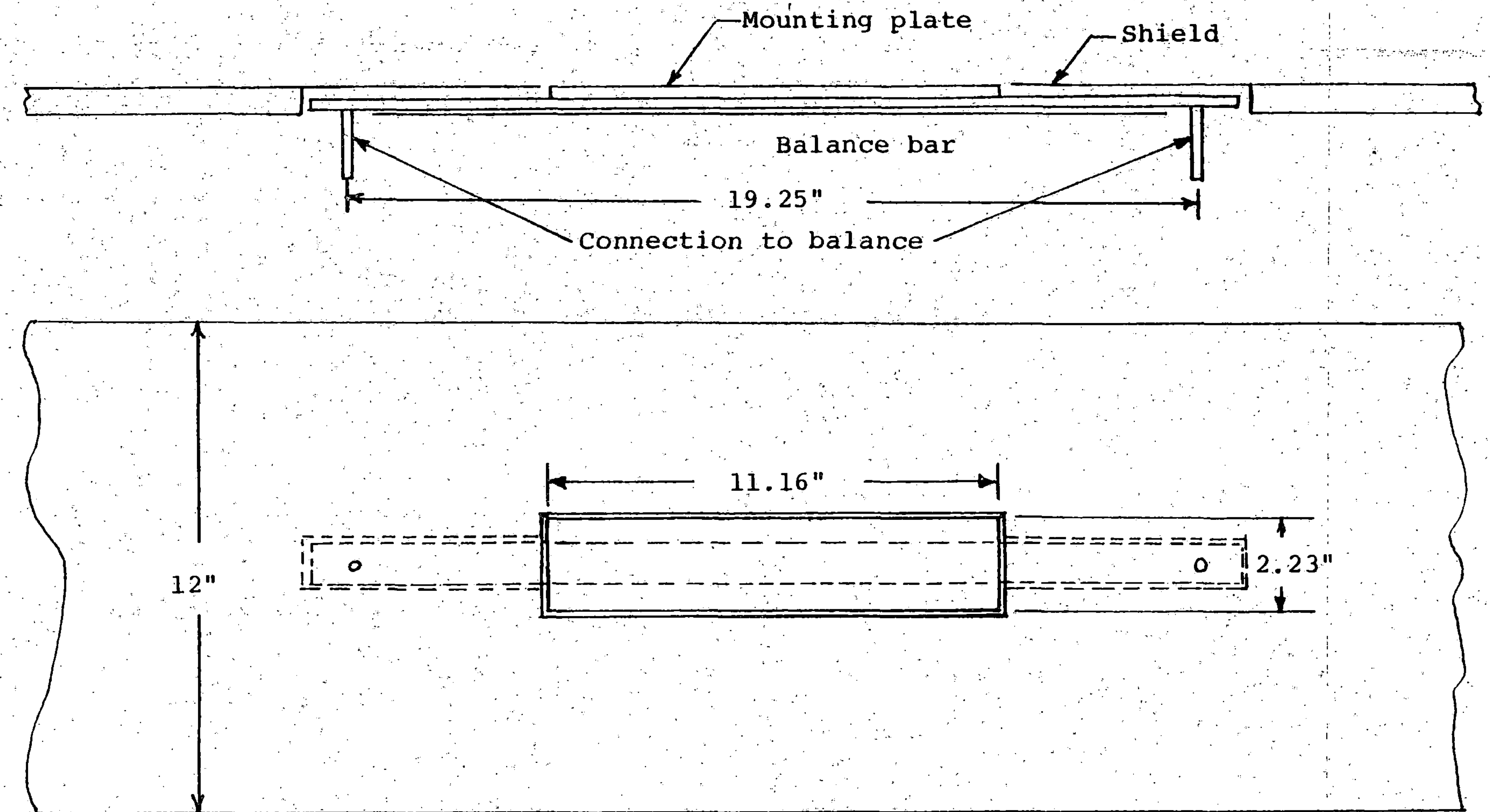

Figure 2. Detailed View of the Mounting of the Metric Element on Balance.

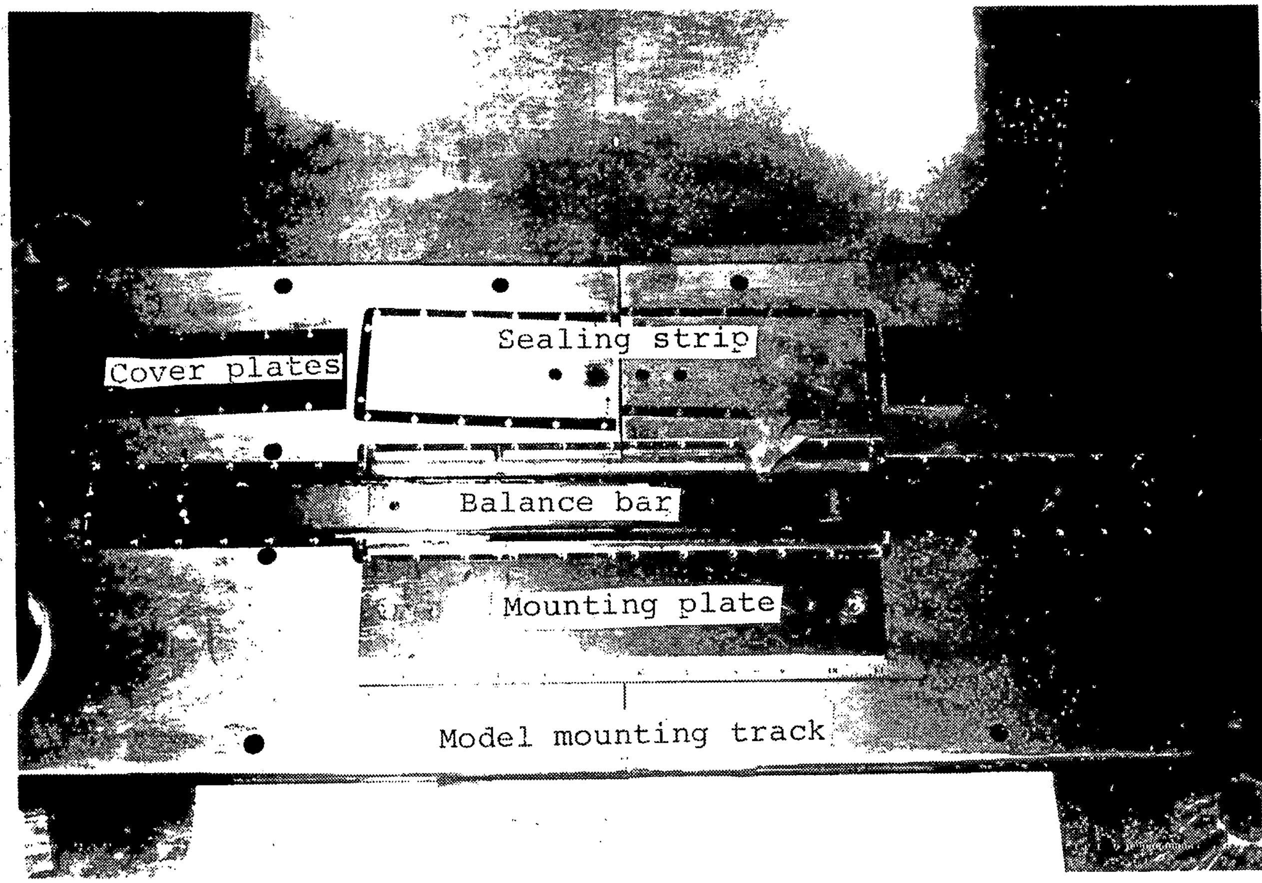

Figure 3. Photograph of Metric Element.

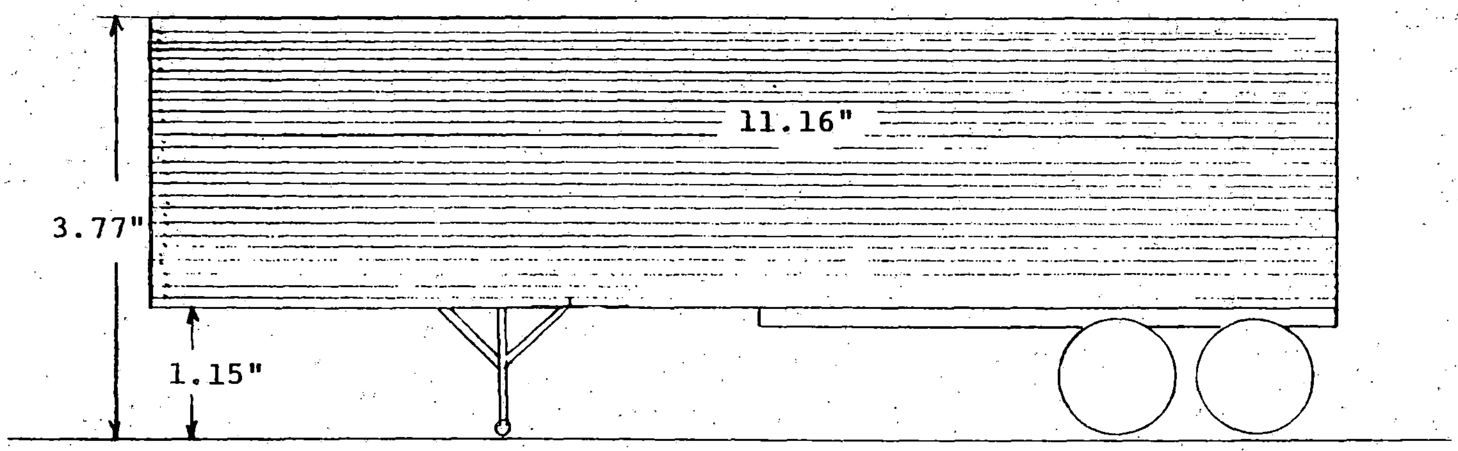

Figure 4a. Drawing of Trailer Model.

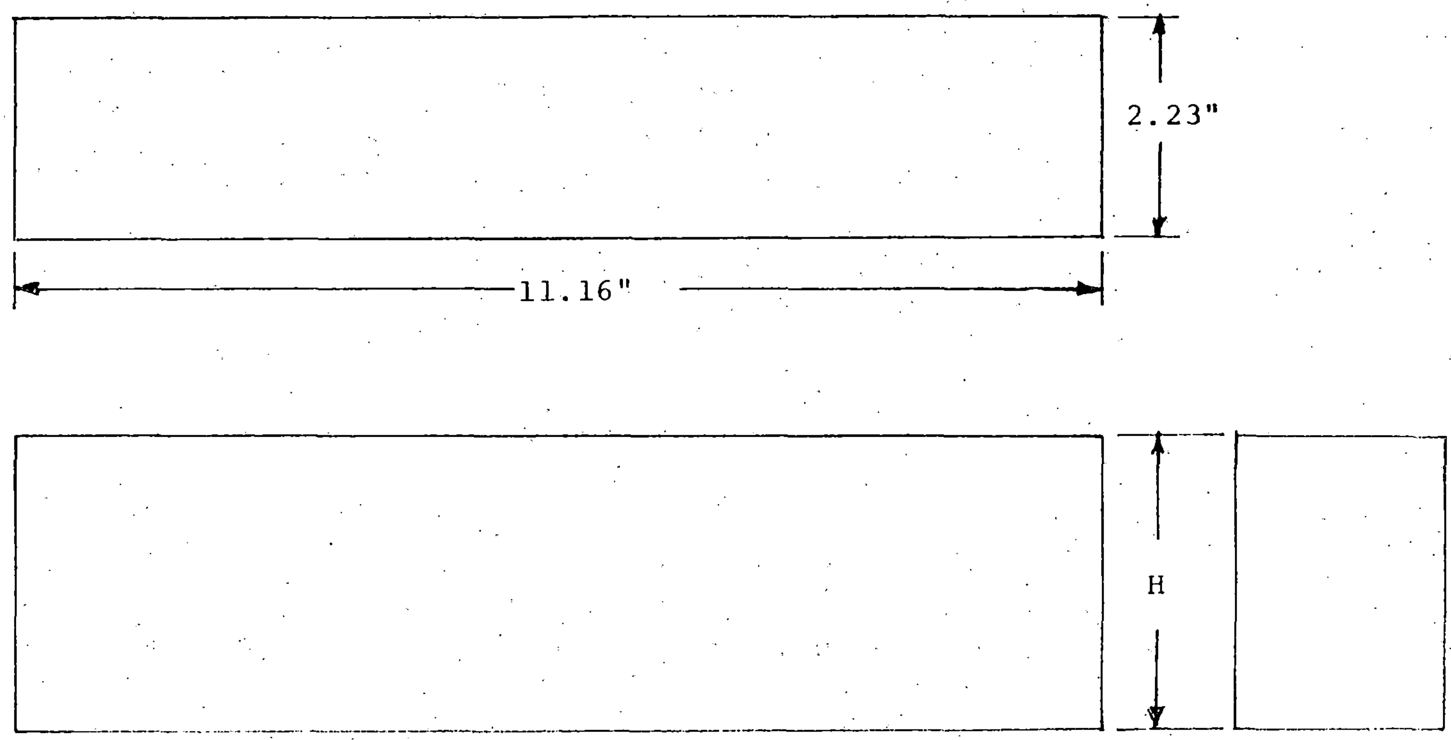

H = 2.23", 2.67", 3.12", 3.79", 4.46", 5.35"

Figure 4b. Drawing of Container Models.

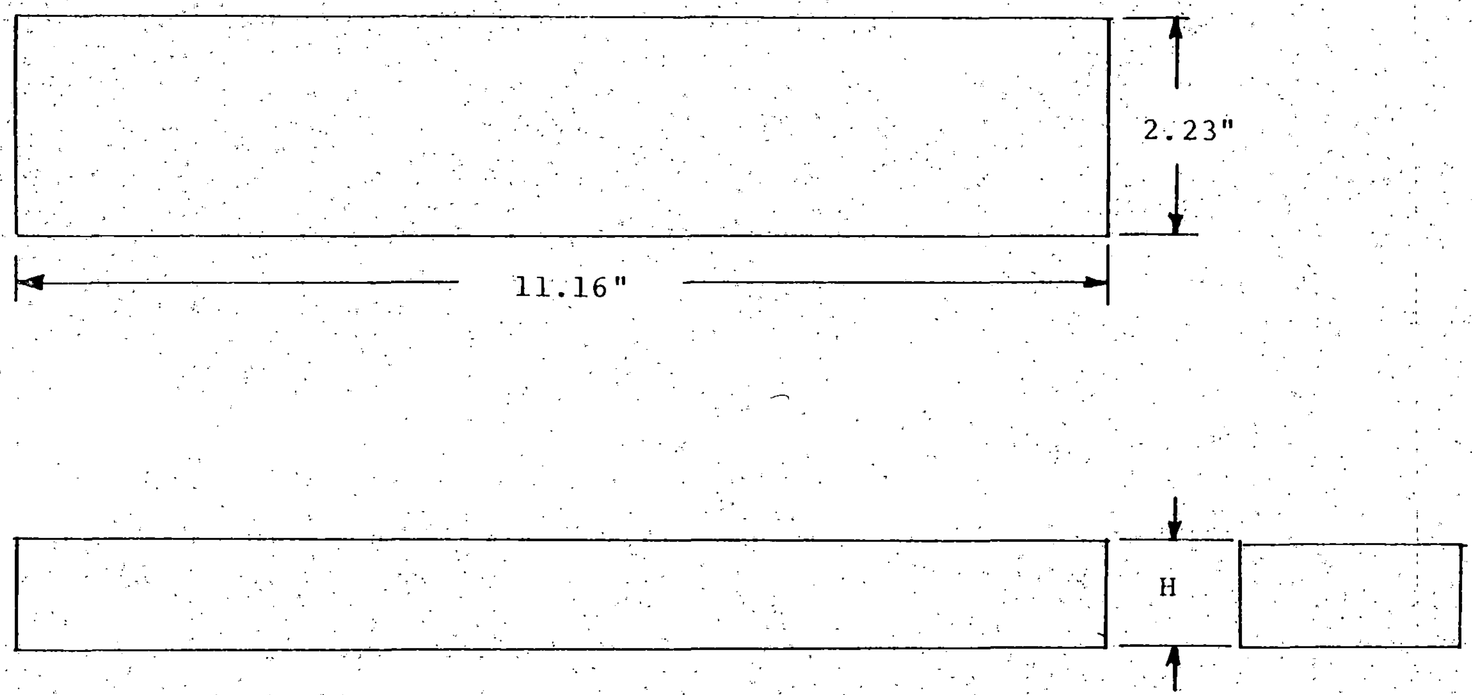

H = 1.15", 0.86", 0.57", 0.29"
(100%) (75%) (50%) (25%)

Figure 5. Drawing of Shields for Use With Container Models.

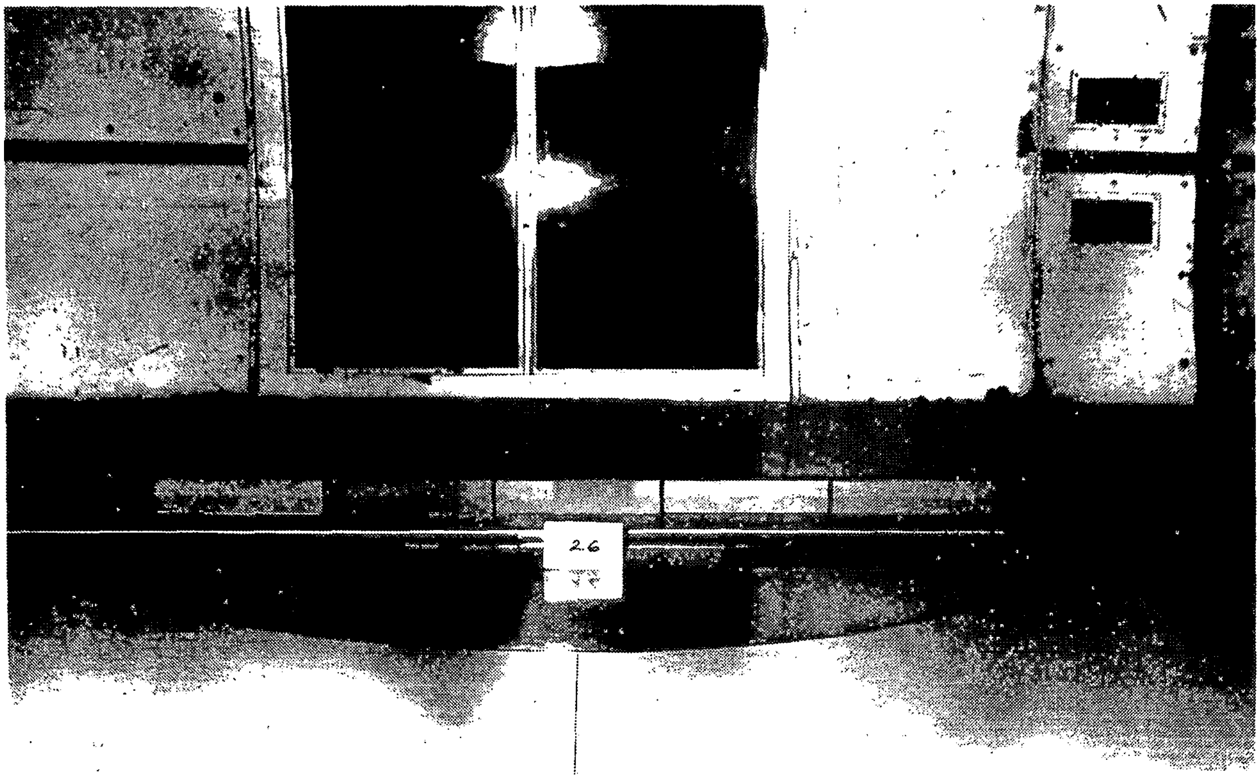

Figure 6. Photograph of 1.0 High Blocks at Equal Spacing of All Gaps of 0.1.

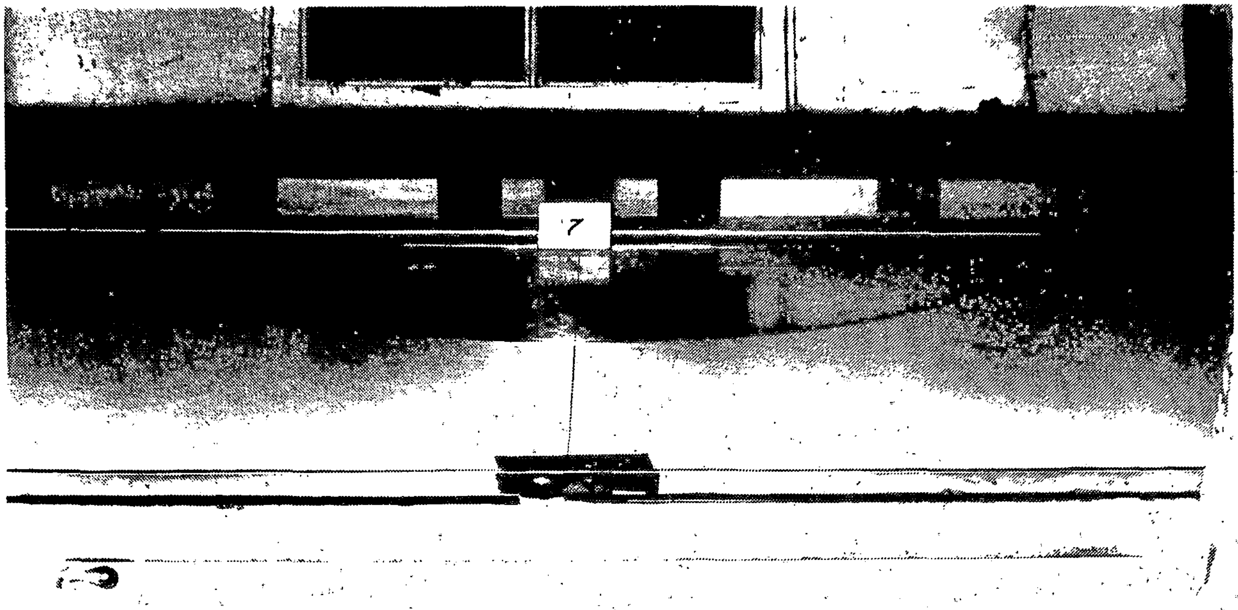

Configuration A (0°)

Configuration B (90°)

Figure 7. Photograph of 1.2 High Blocks at Equal Spacing of All Gaps of 2.0.

Figure 8. Photograph of 1.4 High Blocks at Equal Spacing of All Gaps of 0.3.

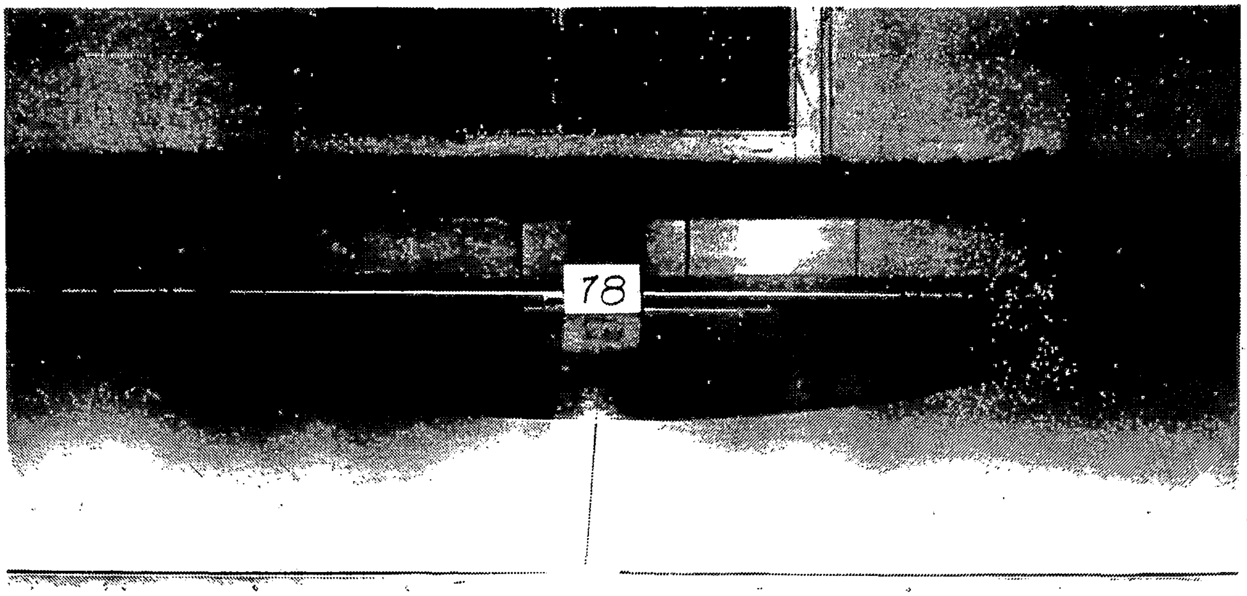

Configuration A (0°)

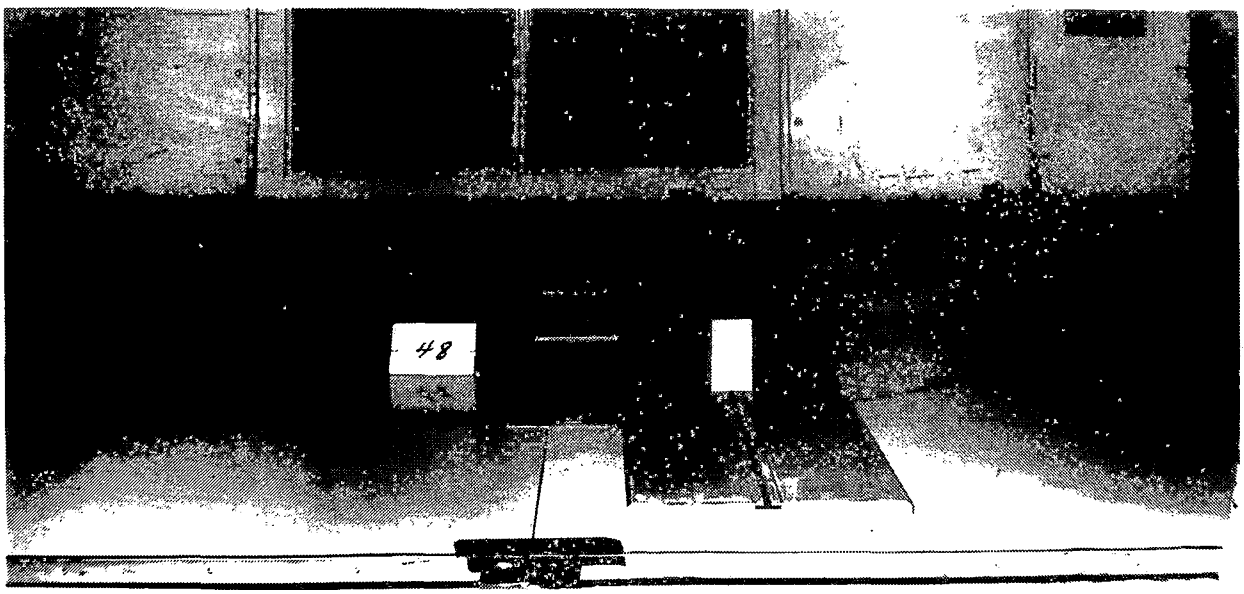

Configuration B (90°)

Figure 9. Photographs of 1.7 High Blocks at Equal Spacing of All Gaps of 0.1.

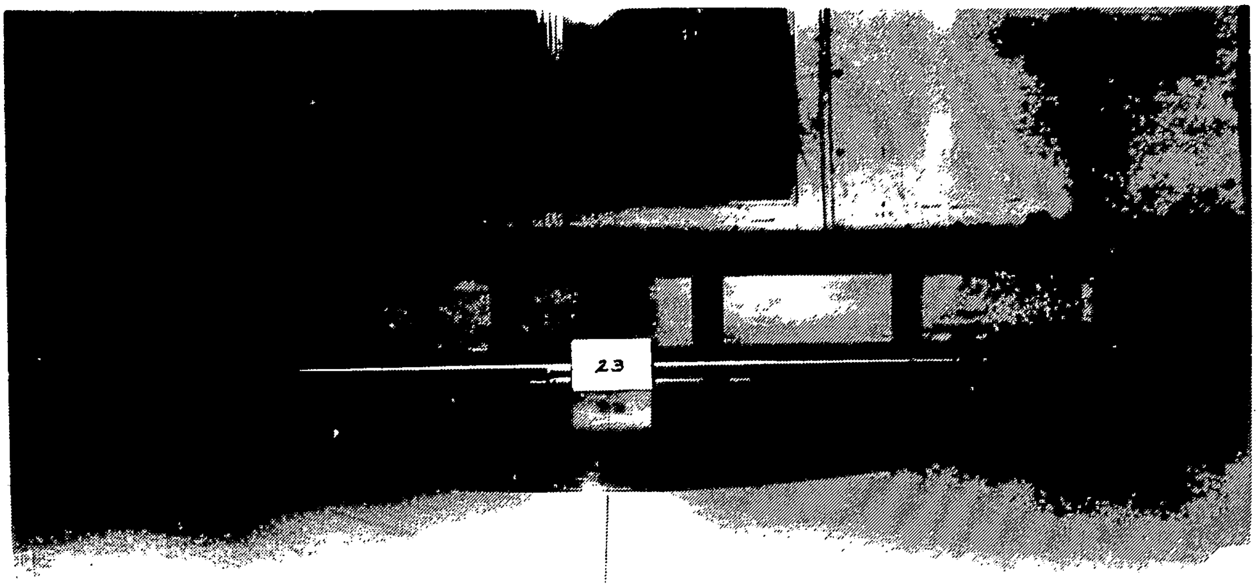

Figure 10. Photograph of 2.0 High Blocks at Equal Spacing of All Gaps of 0.9.

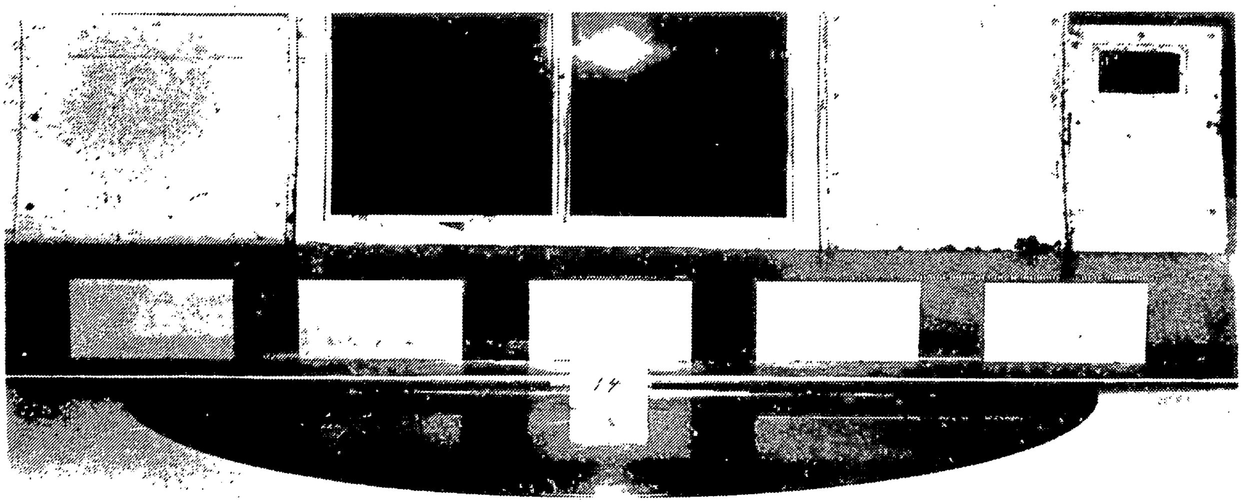

Figure 11. Photograph of 2.4 High Blocks at Equal Spacing of All Gaps of 2.0.

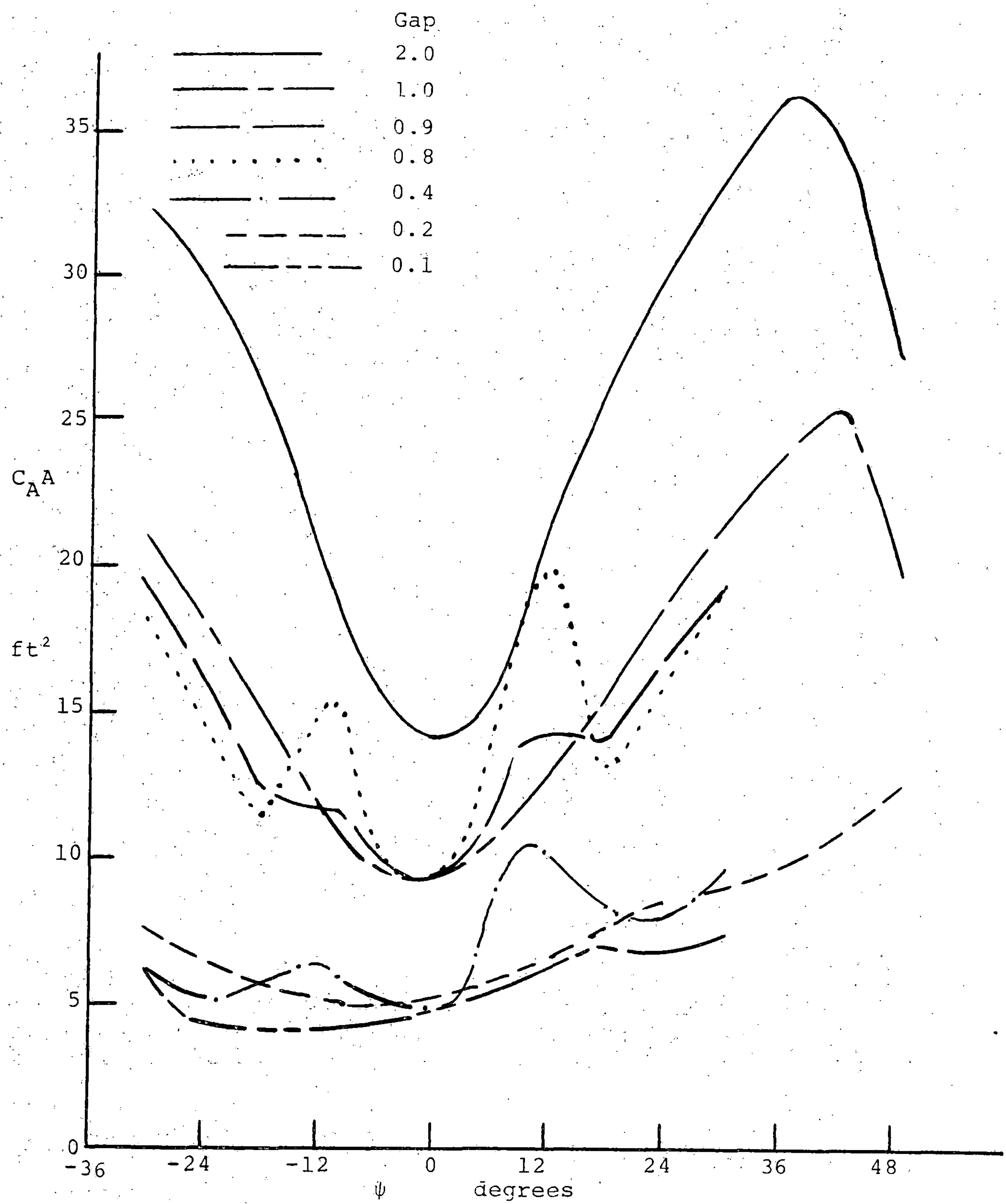

Figure 12. Axial Force Area Versus Yaw Angle for 1.0 High Blocks With Equal Spacing of Gaps Ahead and Behind.

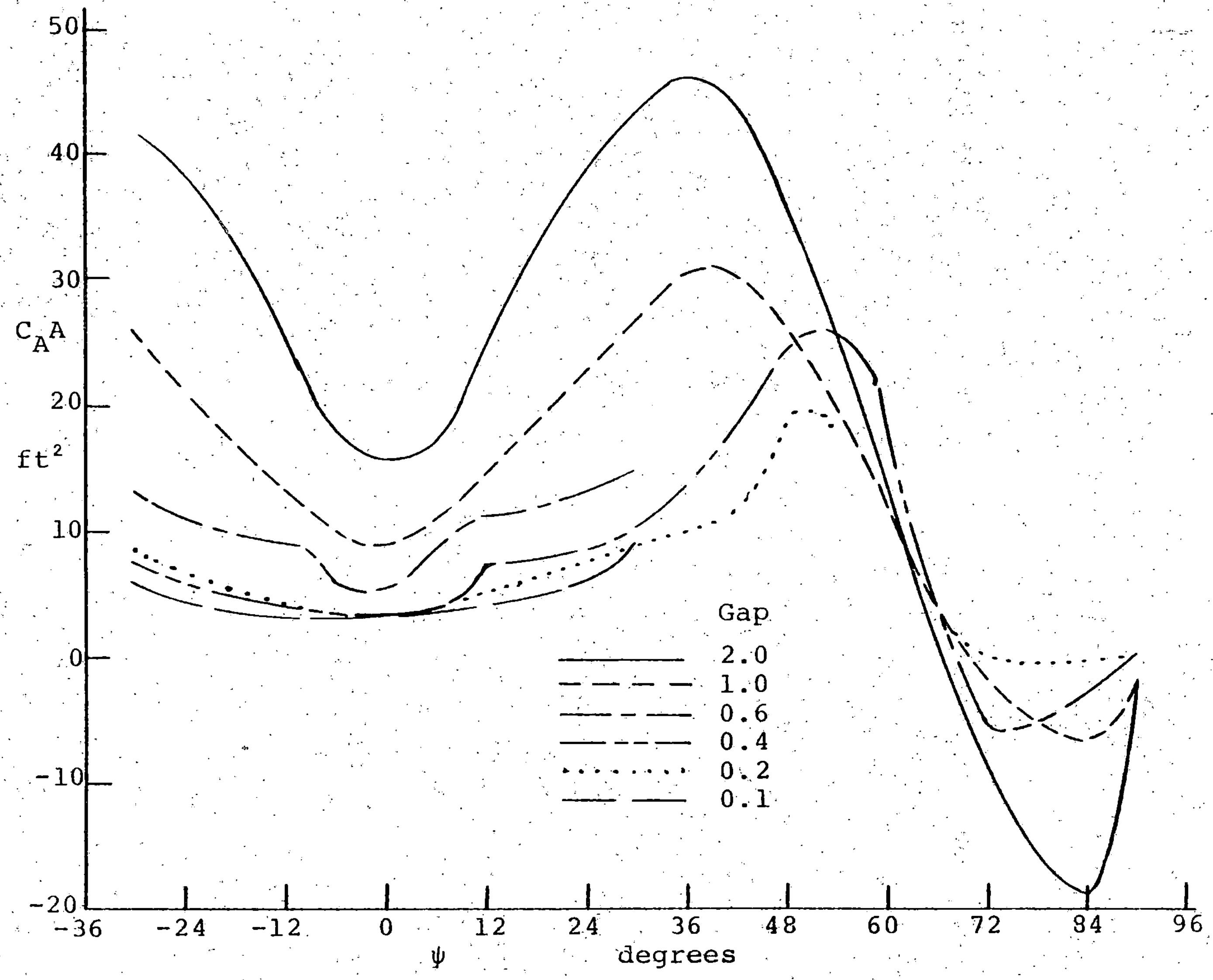

Figure 13. Axial Force Area Versus Yaw Angle for 1.2 High Blocks With Equal Spacing of Gaps Ahead and Behind.

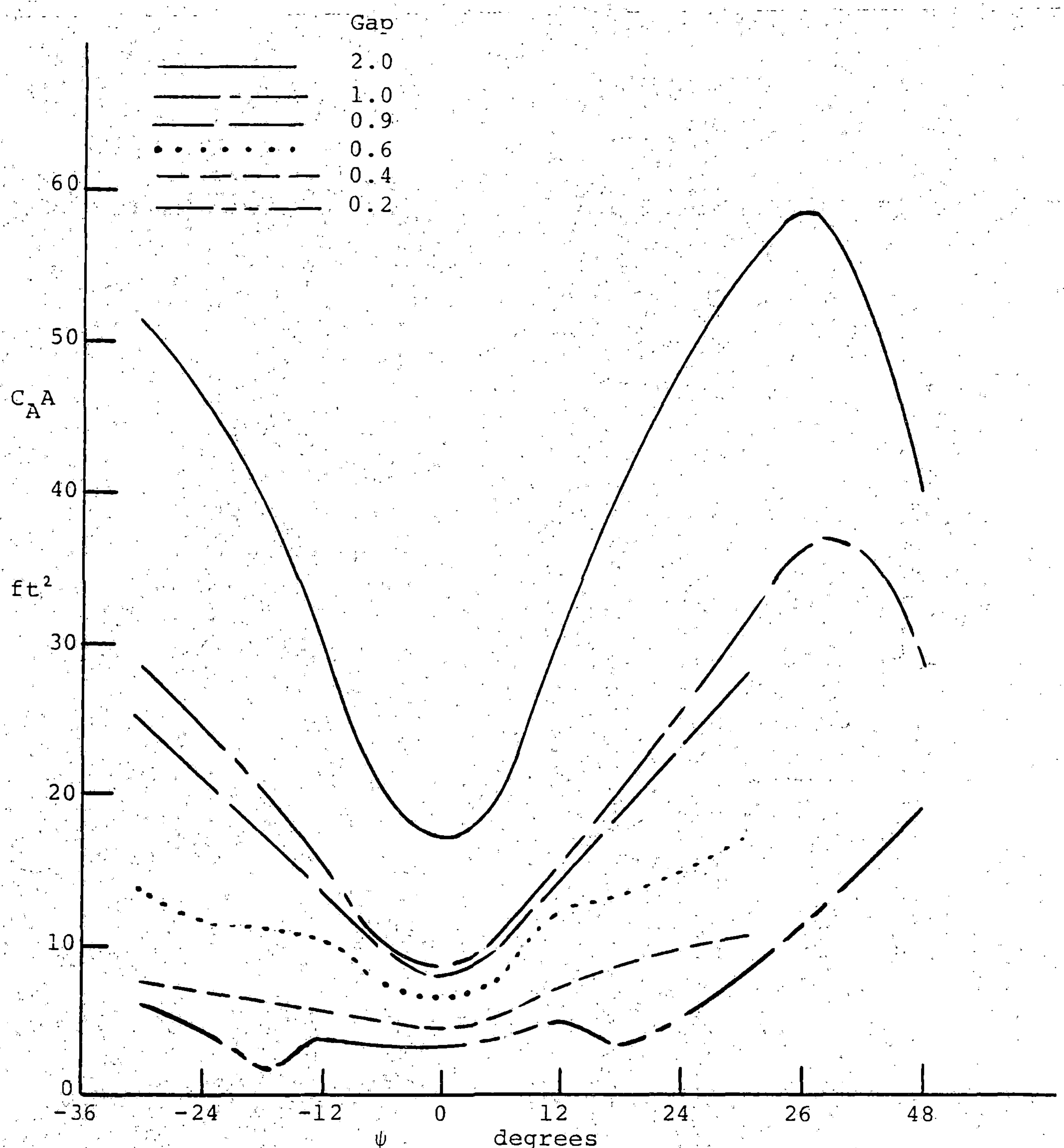

Figure 14. Axial Force Area Versus Yaw Angle for 1.4 High Blocks With Equal Spacing of Gaps Ahead and Behind.

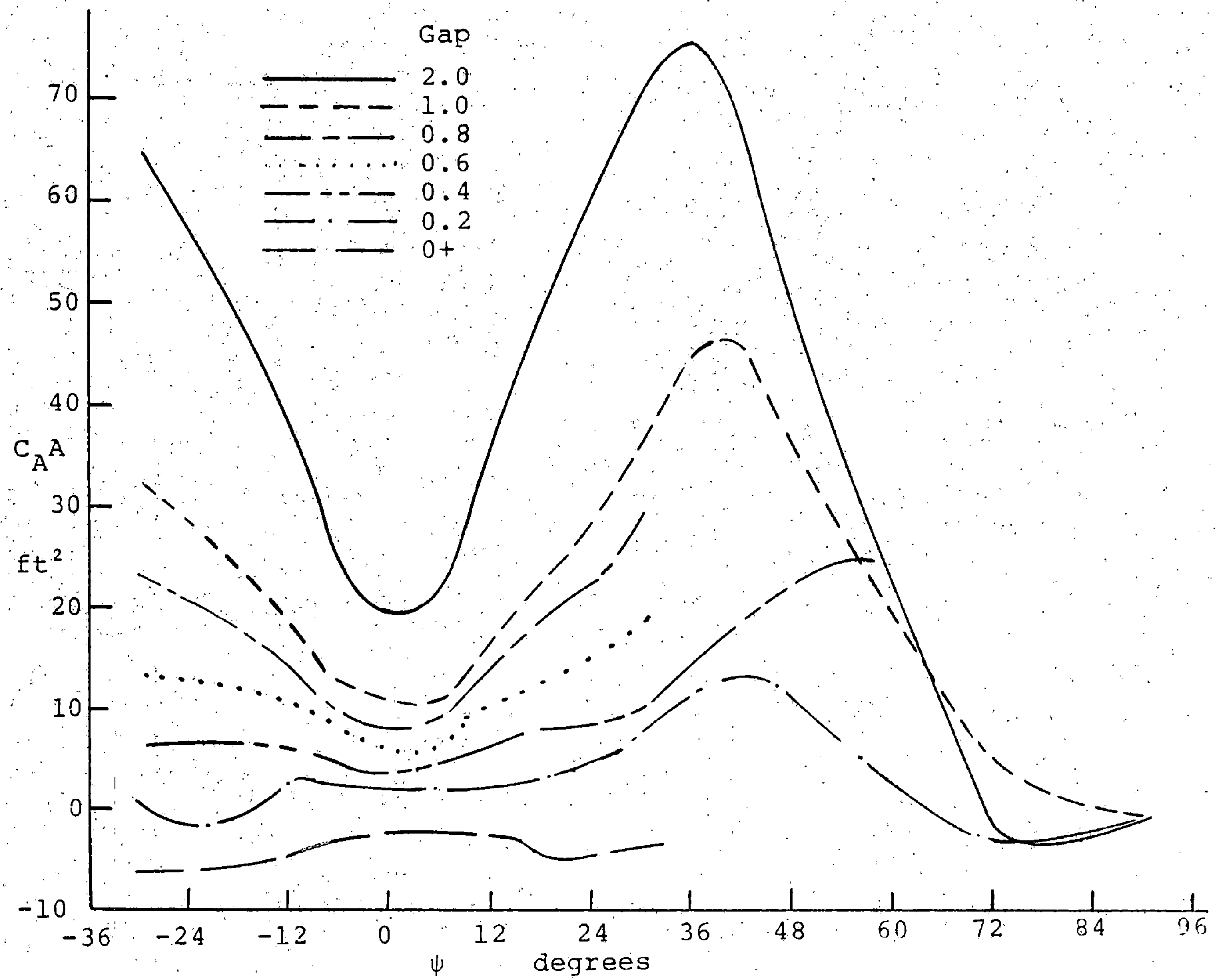

Figure 15. Axial Force Area Versus Yaw Angle for 1.7 High Blocks With Equal Spacing of Gaps Ahead and Behind.

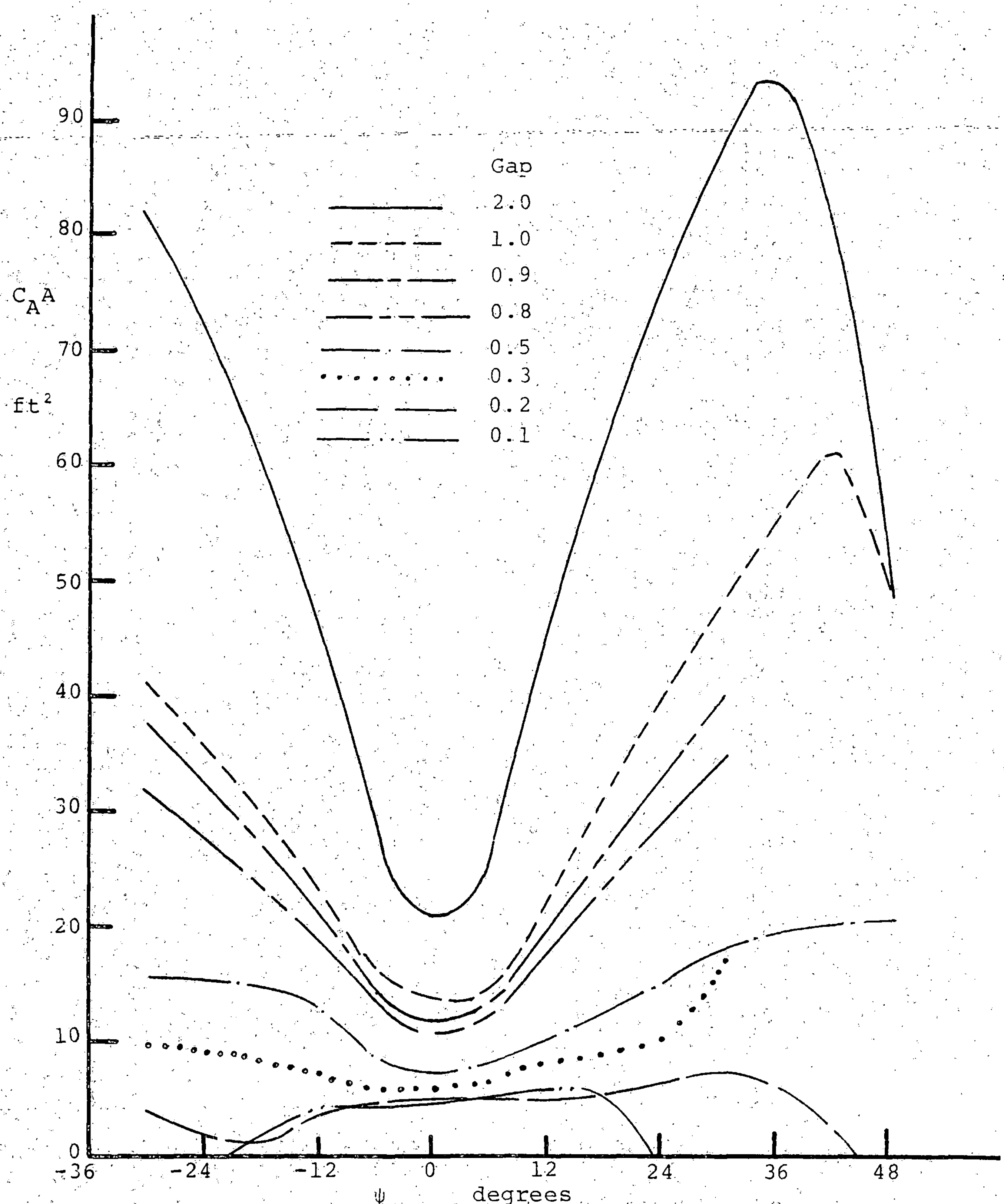

Figure 16. Axial Force Area Versus Yaw Angle for 2.0 High Blocks With Equal Spacing of Gaps Ahead and Behind.

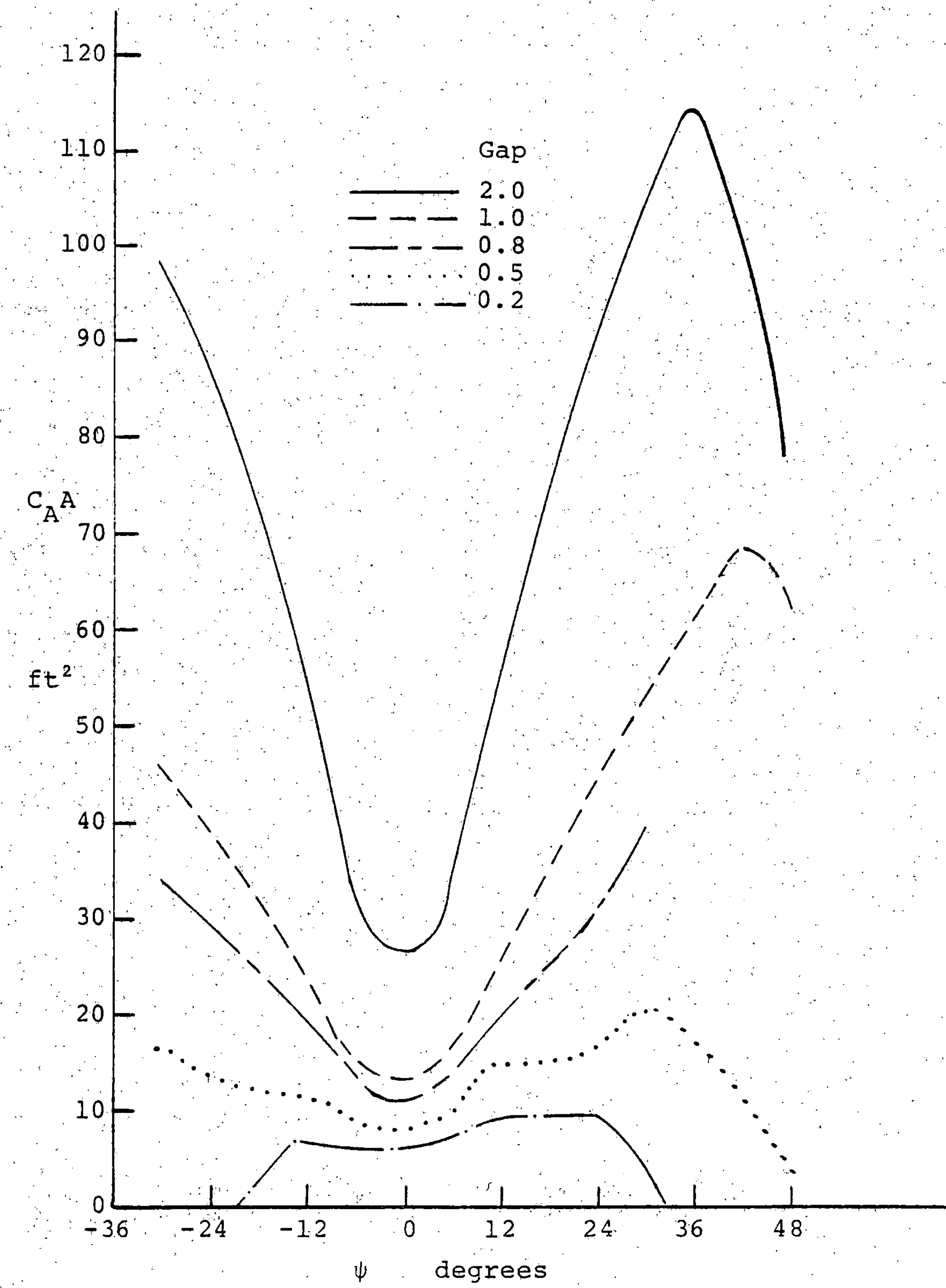

Figure 17. Axial Force Area Versus Yaw Angle for 2.4 High Blocks With Equal Spacing of Gaps Ahead and Behind.

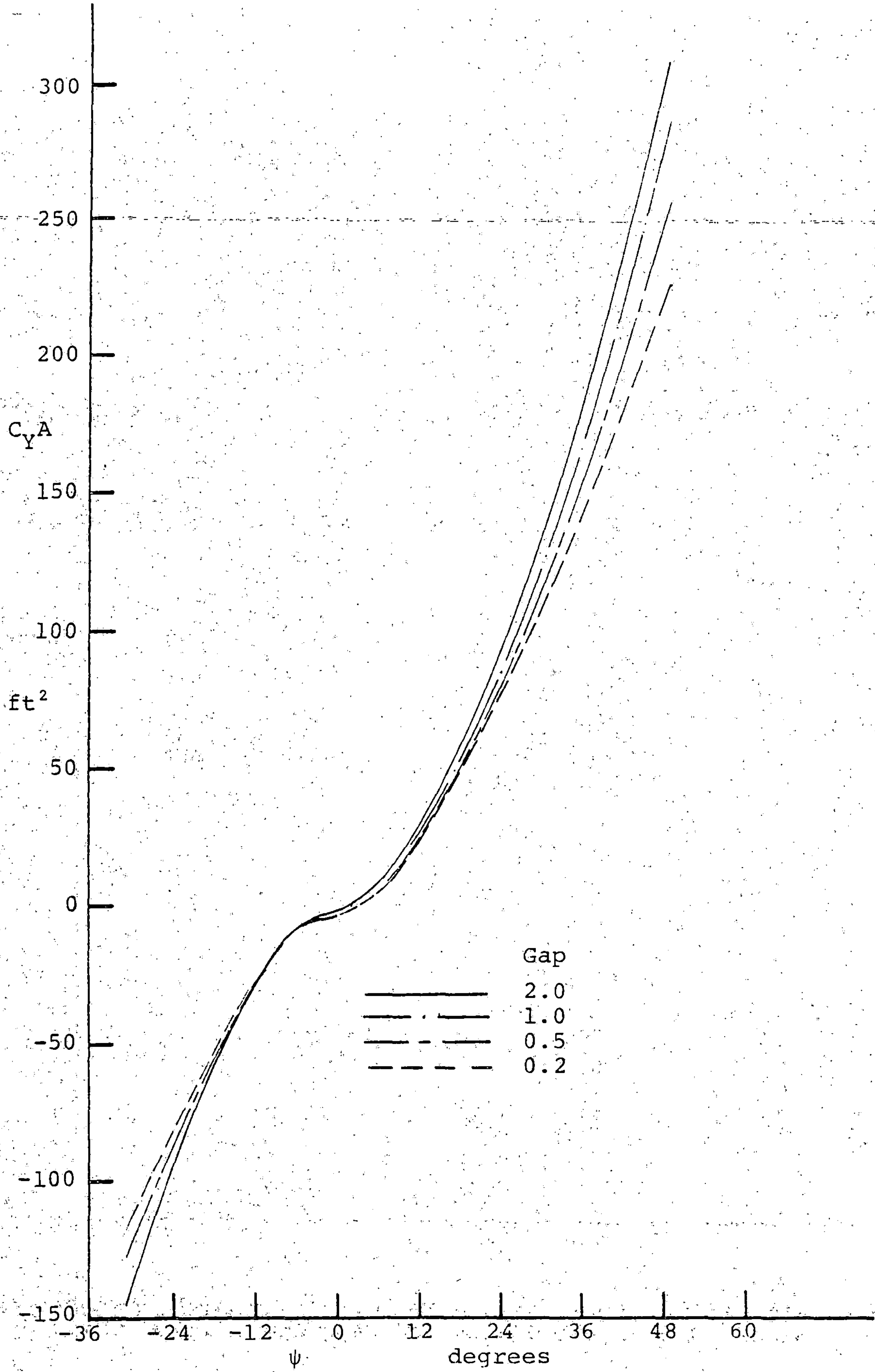

Figure 18. Side Force Area Versus Yaw Angle for 1.0 High Blocks With Equal Spacing of Gaps Ahead and Behind.

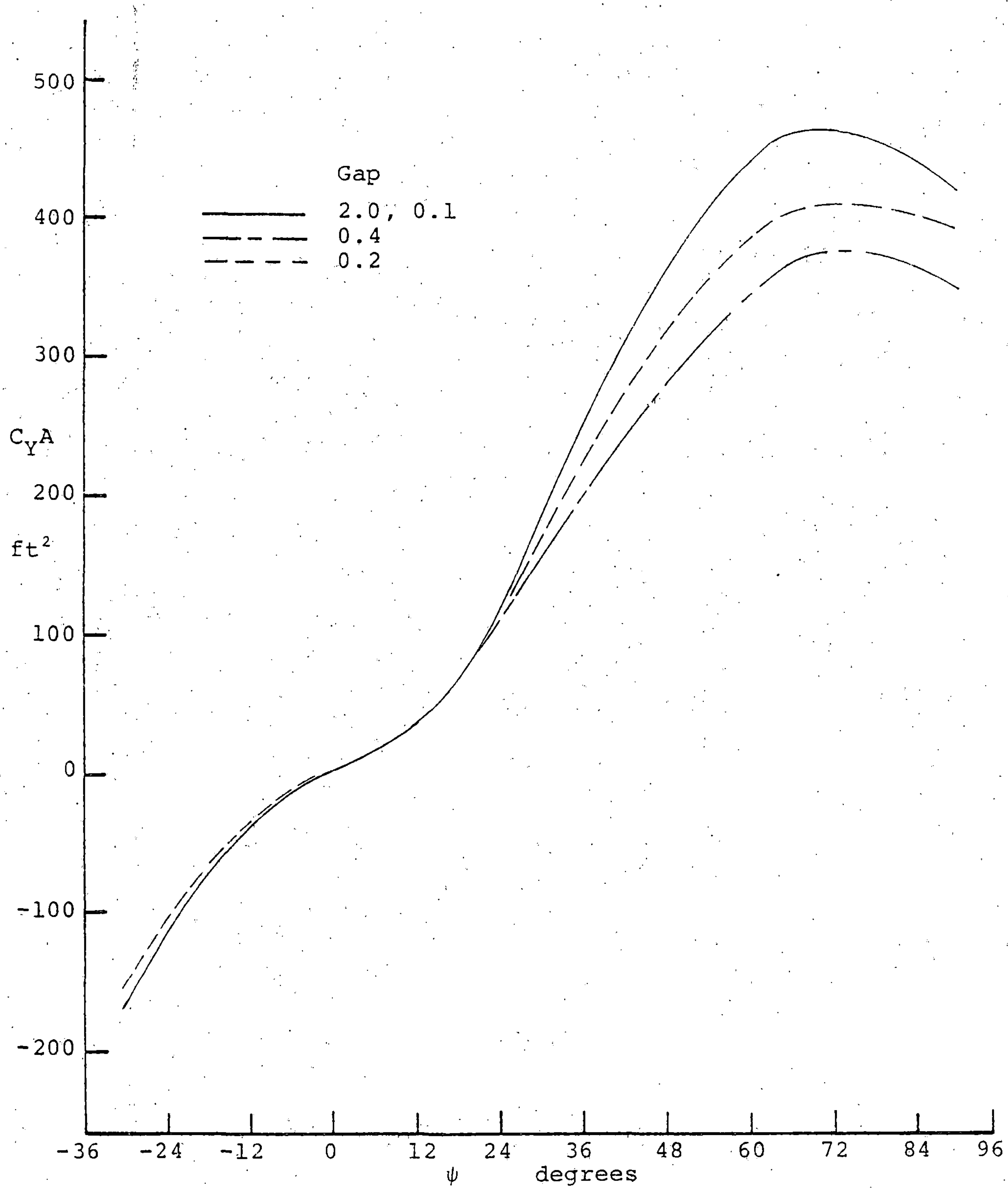

Figure 19. Side Force Area Versus Yaw Angle for 1.2 High Blocks With Equal Spacing of Gaps Ahead and Behind.

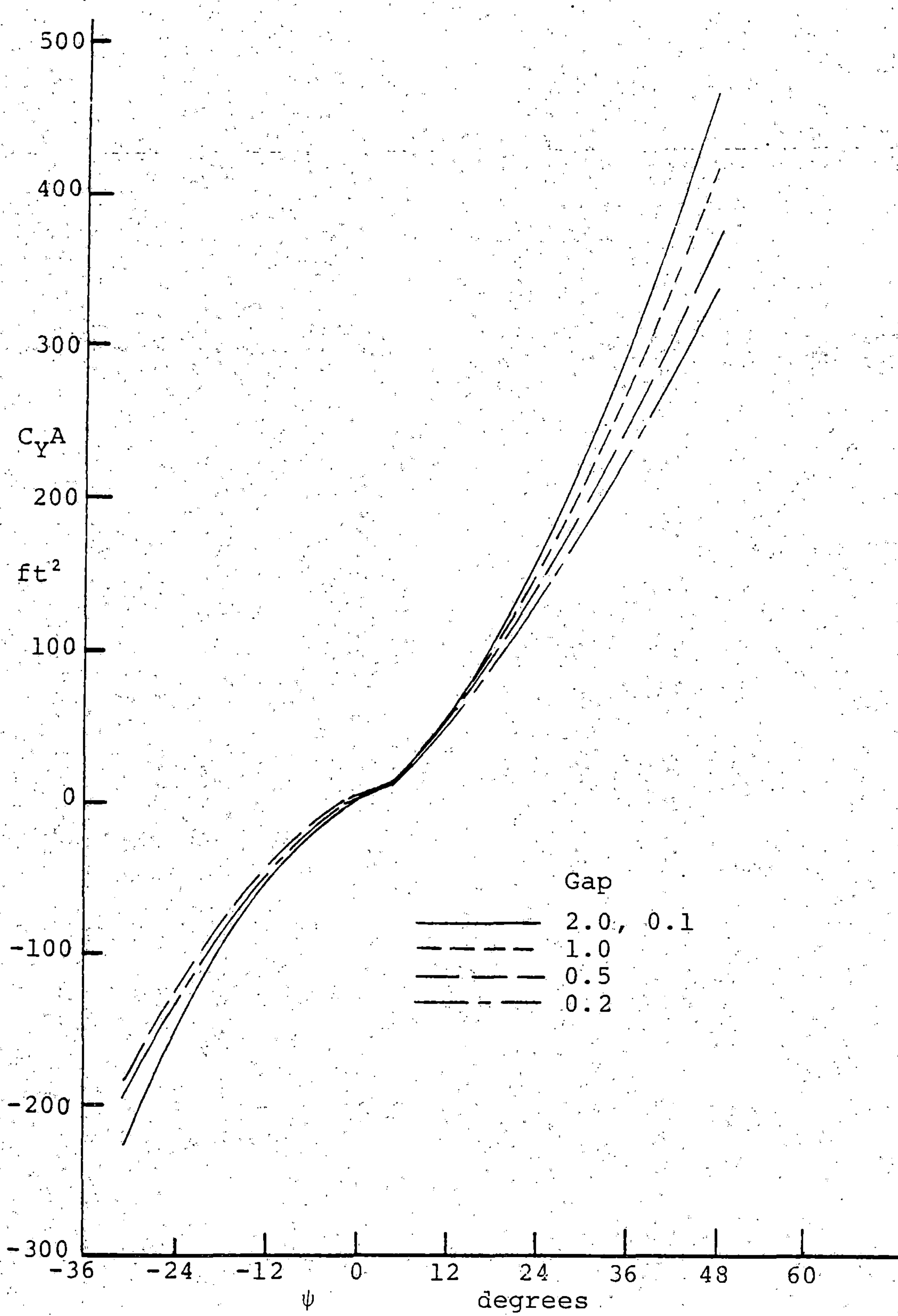

Figure 20. Side Force Area Versus Yaw Angle for 1.4 High Blocks With Equal Spacing of Gaps Ahead and Behind.

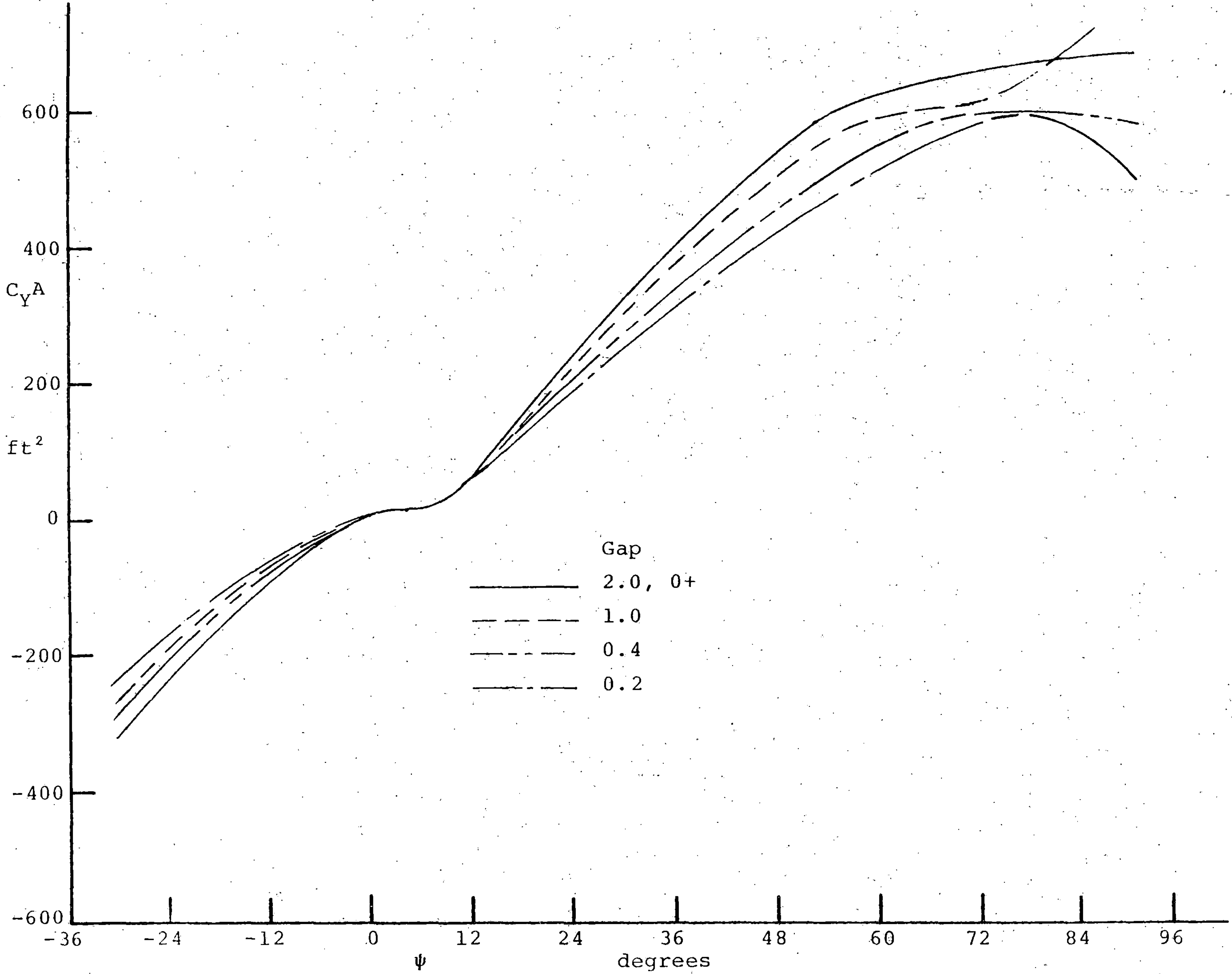

Figure 21. Side Force Area Versus Yaw Angle for 1.7 High Blocks With Equal Spacing of Gaps Ahead and Behind.

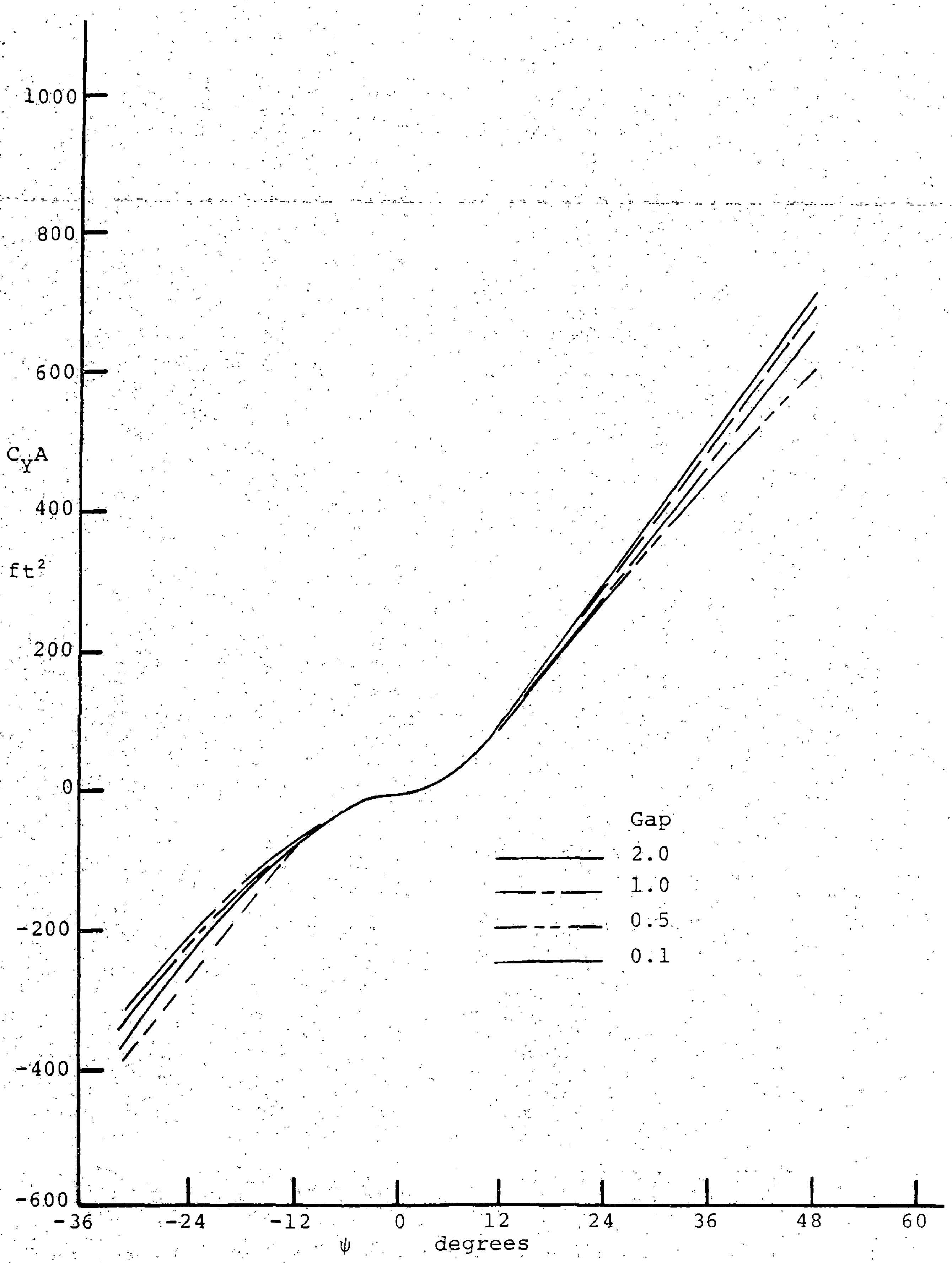

Figure 22. Side Force Area Versus Yaw Angle for 2.0 High Blocks With Equal Spacing of Gaps Ahead and Behind.

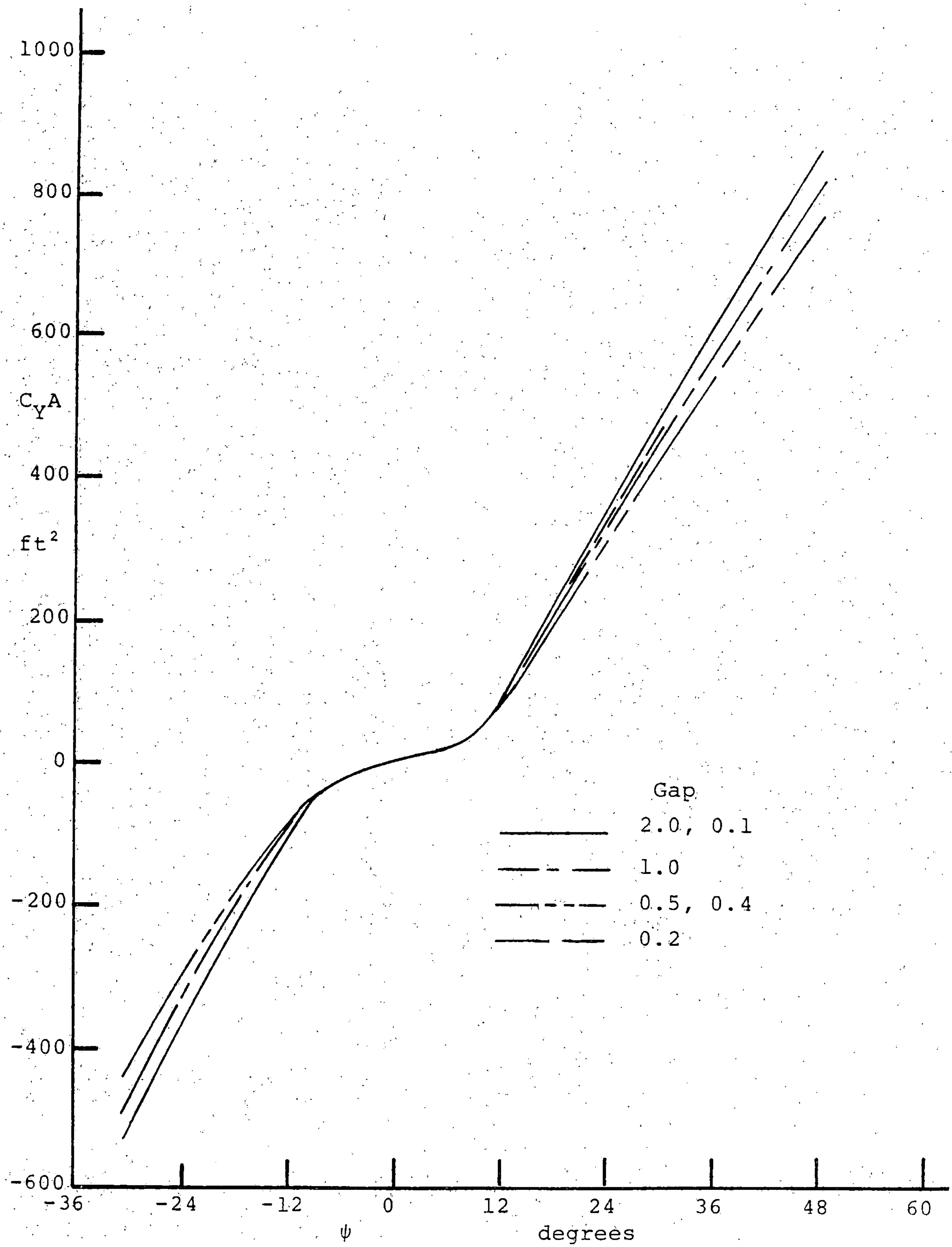

Figure 23. Side Force Area Versus Yaw Angle for 2.4 High Blocks With Equal Spacing of Gaps Ahead and Behind.

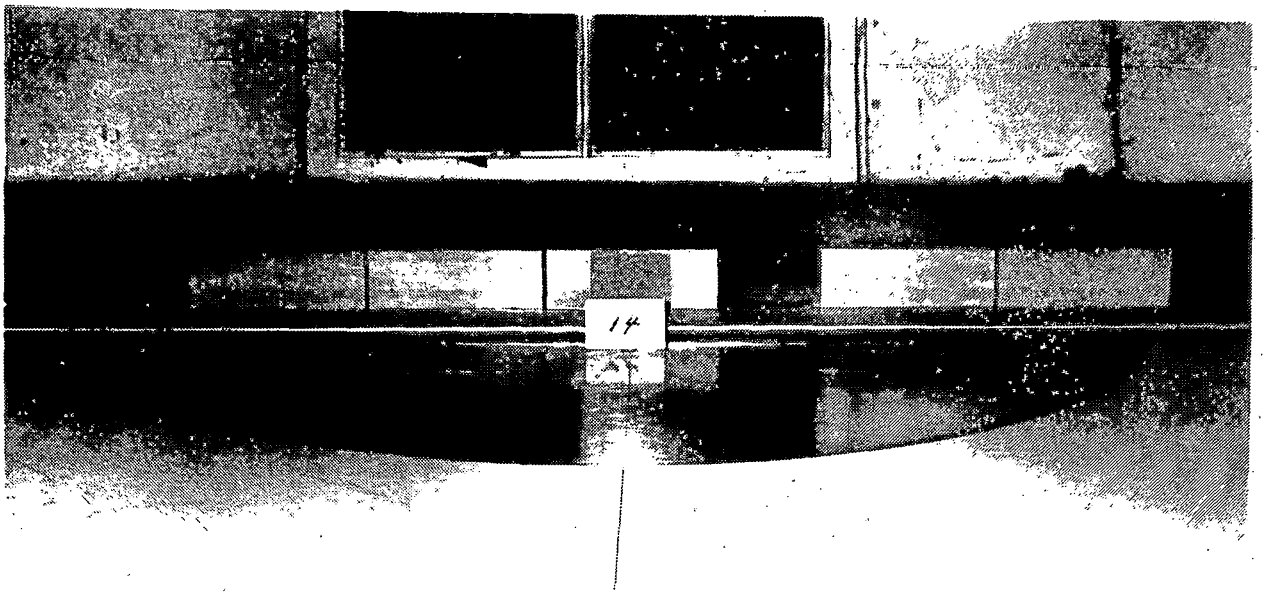

3.0 Behind Metric Block and Other Gaps 0.1.

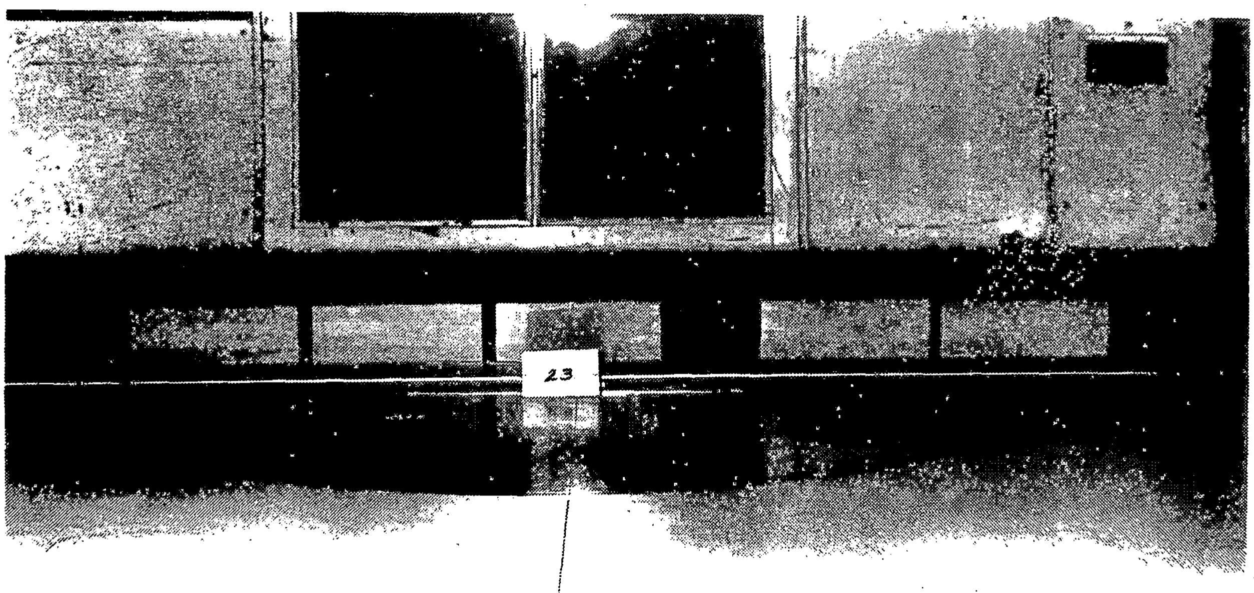

Figure 24. Photographs of 1.7 High Blocks With Variable Spacing of Gaps Behind Metric Block.

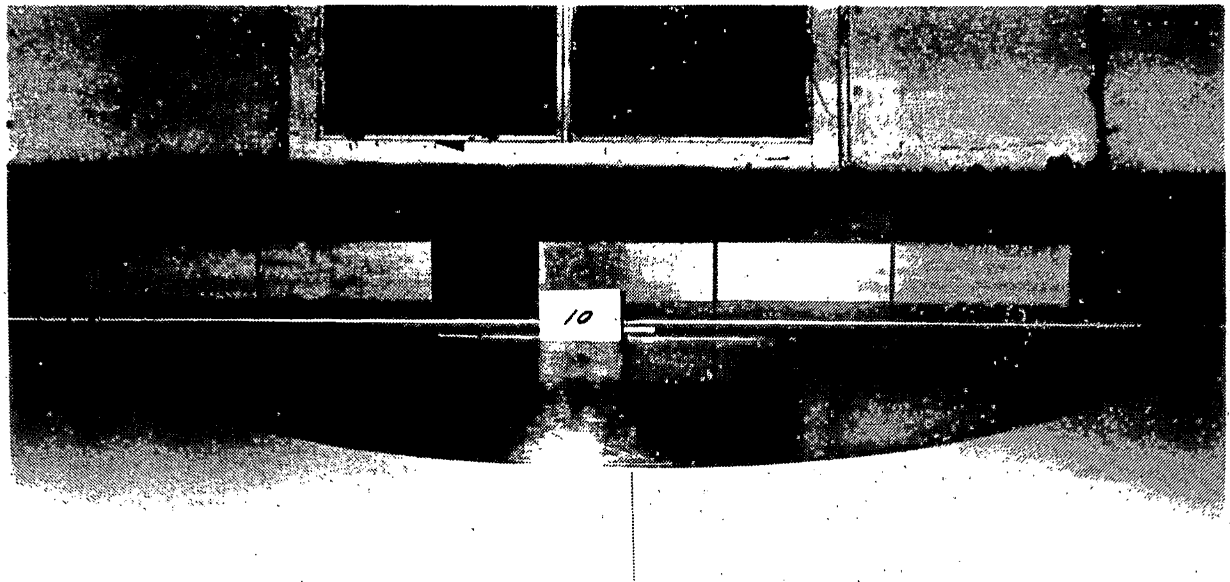

3.0 Ahead of Metric Block and Other Gaps 0.1.

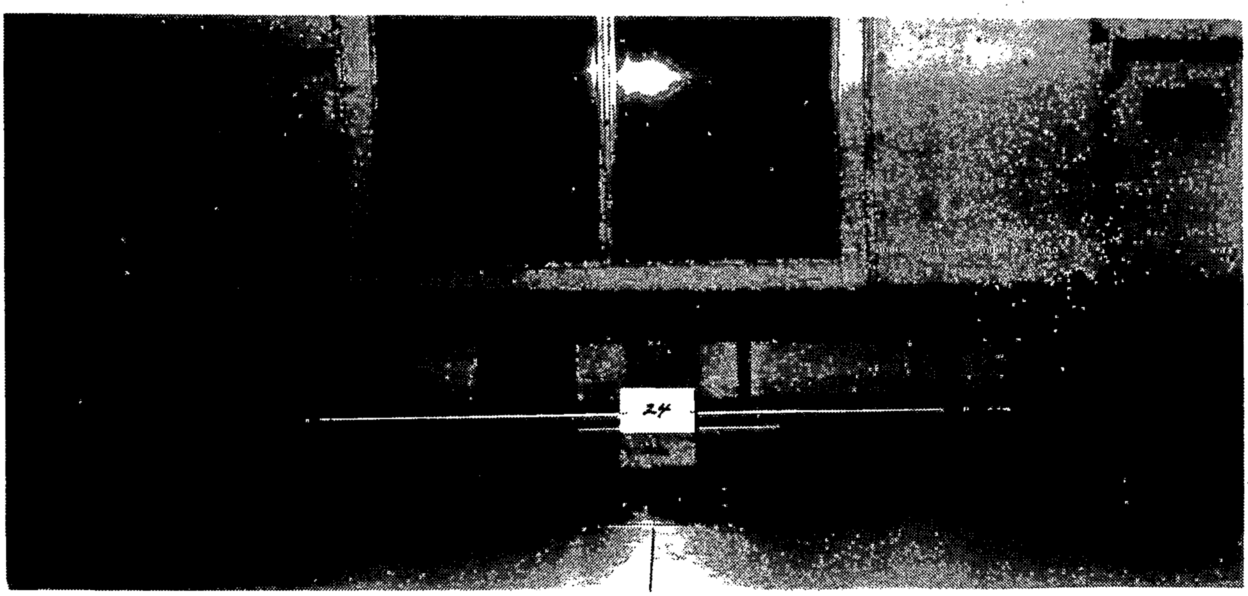

3.0 Ahead of Metric Block and Other Gaps 0.4

Figure 25. Photographs of 1.7 High Blocks With Variable Spacing of Gaps Ahead of Metric Block.

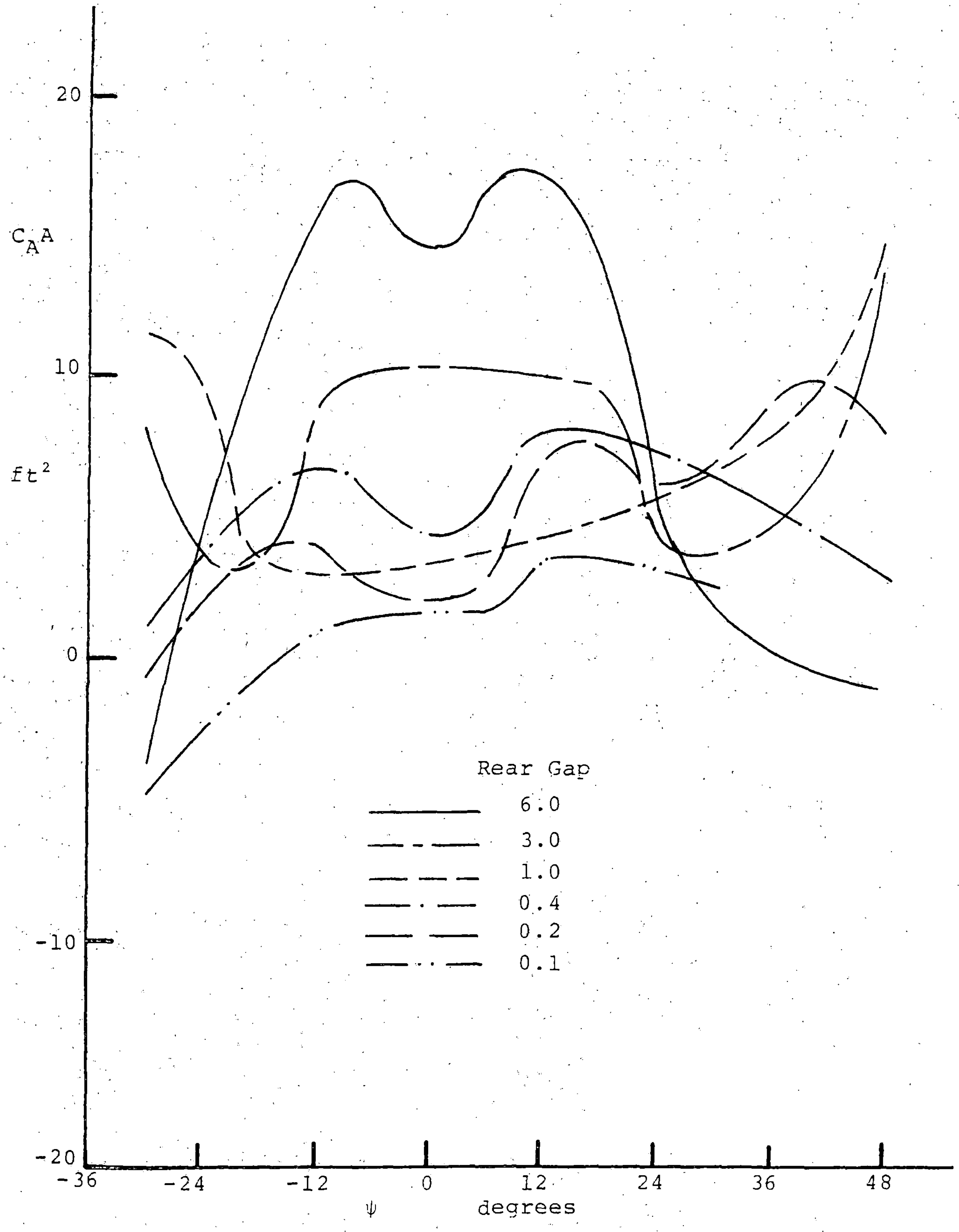

Figure 26. Axial Force Area Versus Yaw Angle for 1.7 High Blocks With Variable Spacing of Gaps Behind Metric Block. All Other Gaps 0.1.

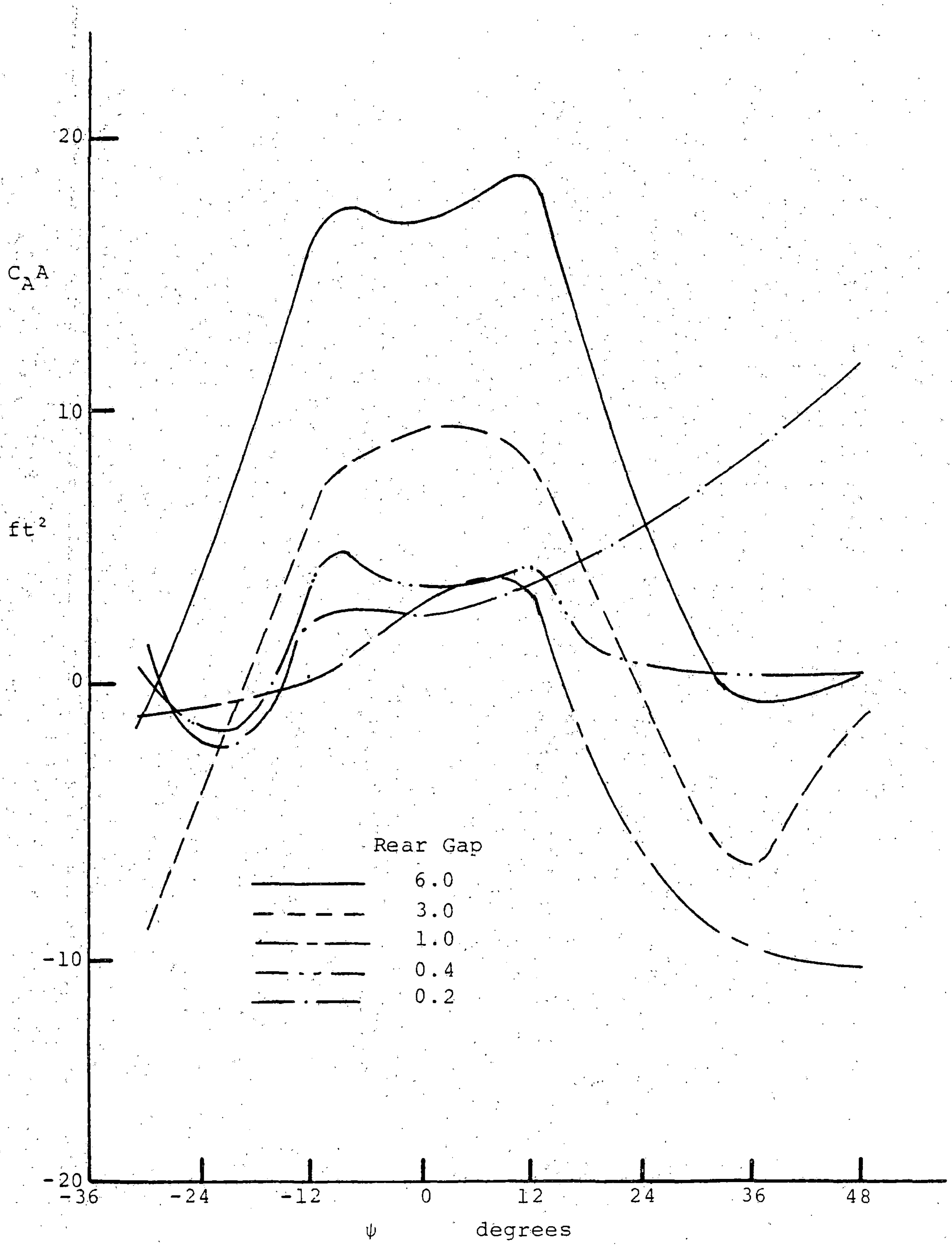

Figure 27. Axial Force Area Versus Yaw Angle for 1.7 High Blocks With Variable Spacing of Gaps Behind Metric Block. All Other Gaps 0.2.

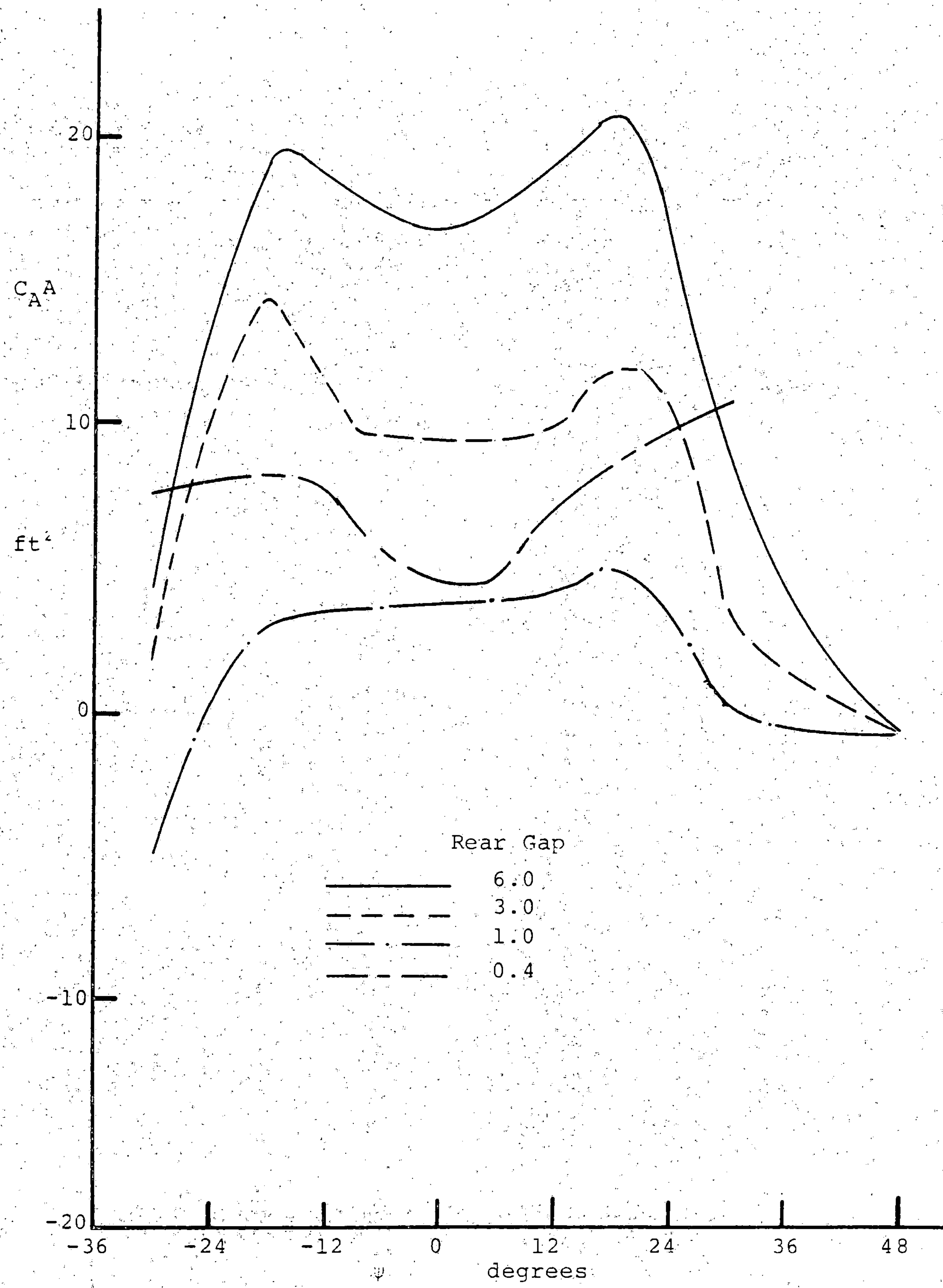

Figure 28. Axial Force Area Versus Yaw Angle for 1.7 High Blocks With Variable Spacing of Gaps Behind Metric Block. All Other Gaps 0.4.

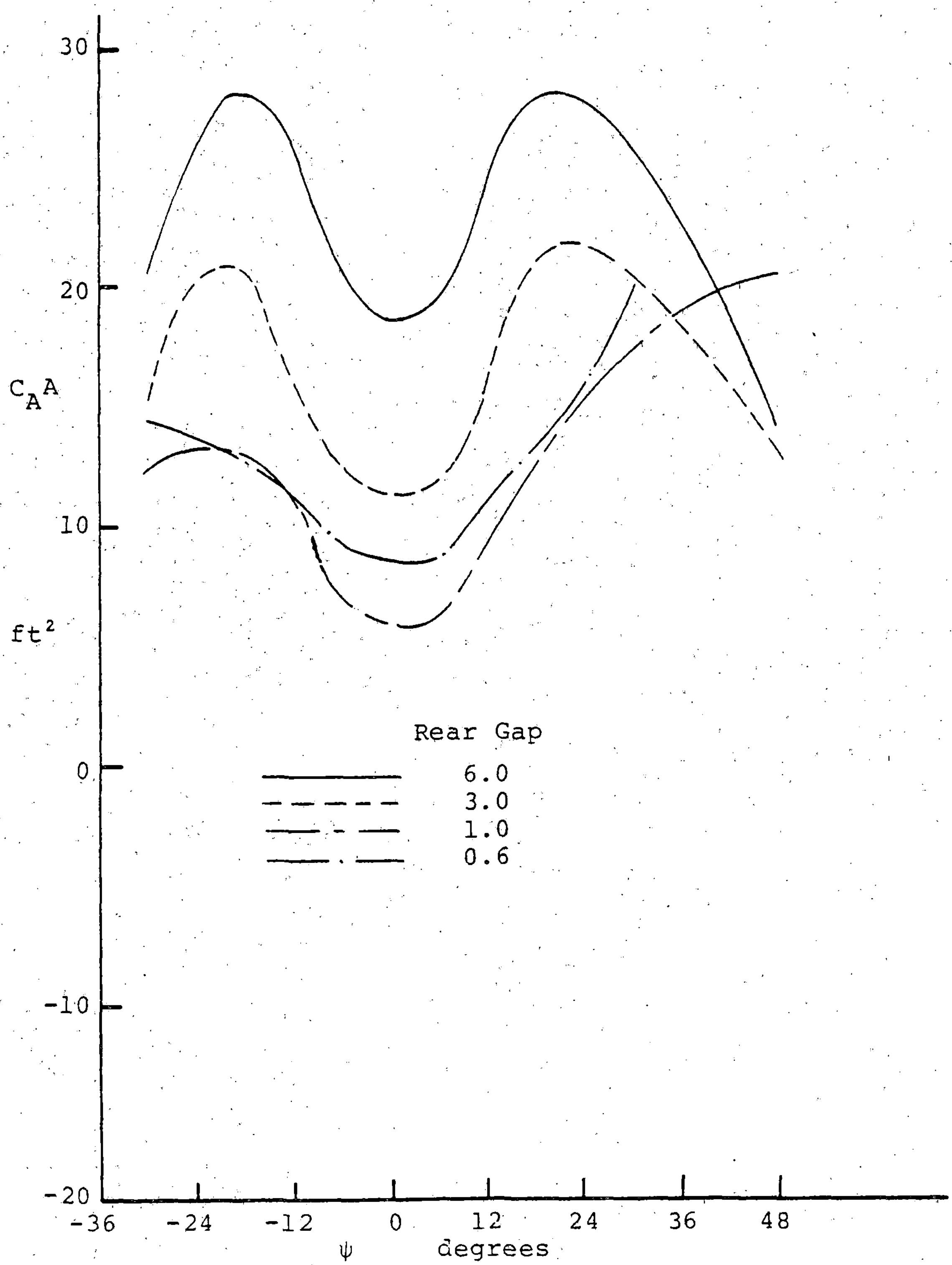

Figure 29. Axial Force Area Versus Yaw Angle for 1.7 High Blocks With Variable Spacing of Gaps Behind Metric Block. All Other Gaps 0.6.

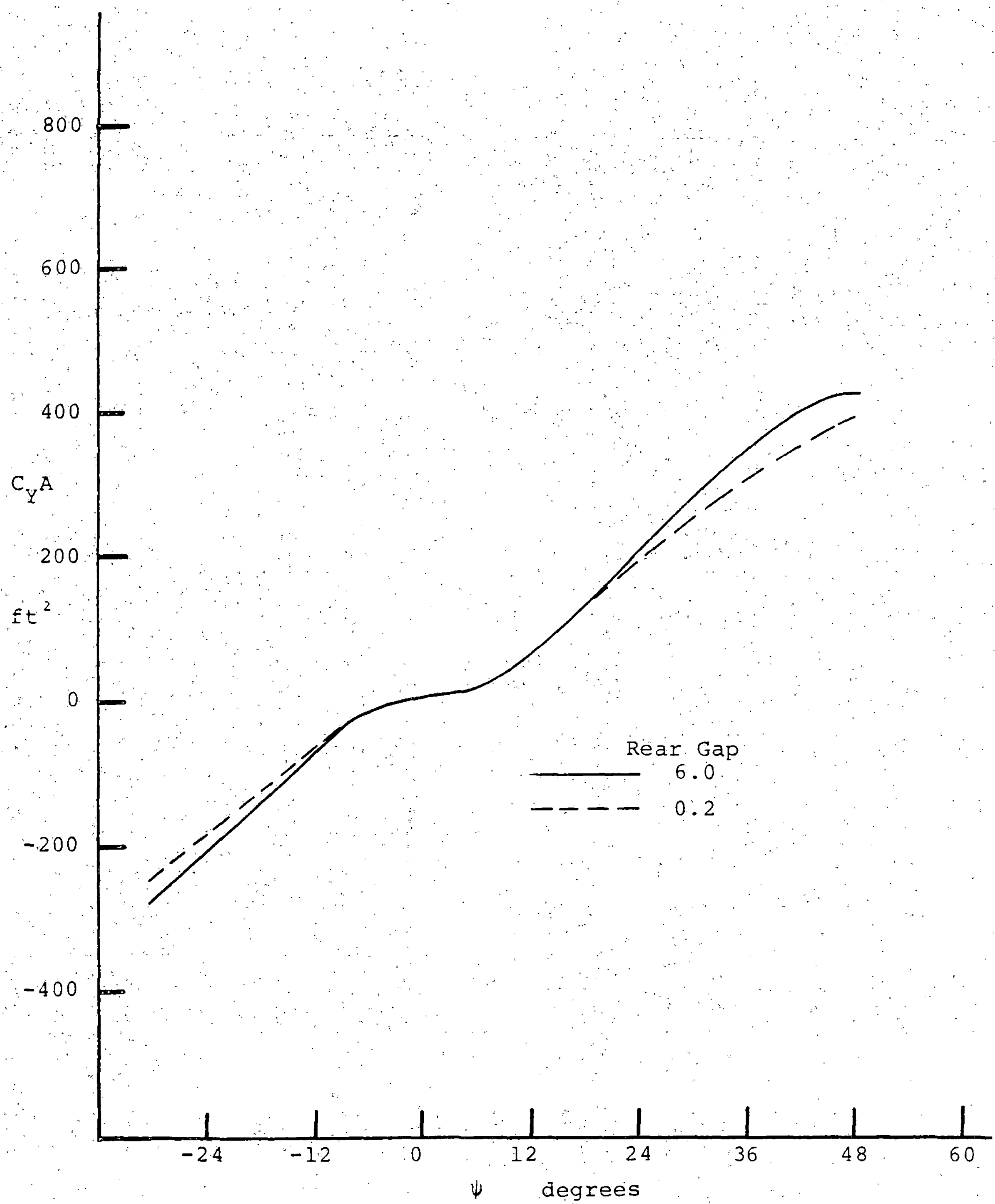

Figure 30. Side Force Area Versus Yaw Angle for 1.7 High Blocks With Variable Spacing of Gaps Behind Metric Block. All Other Gaps 0.1.

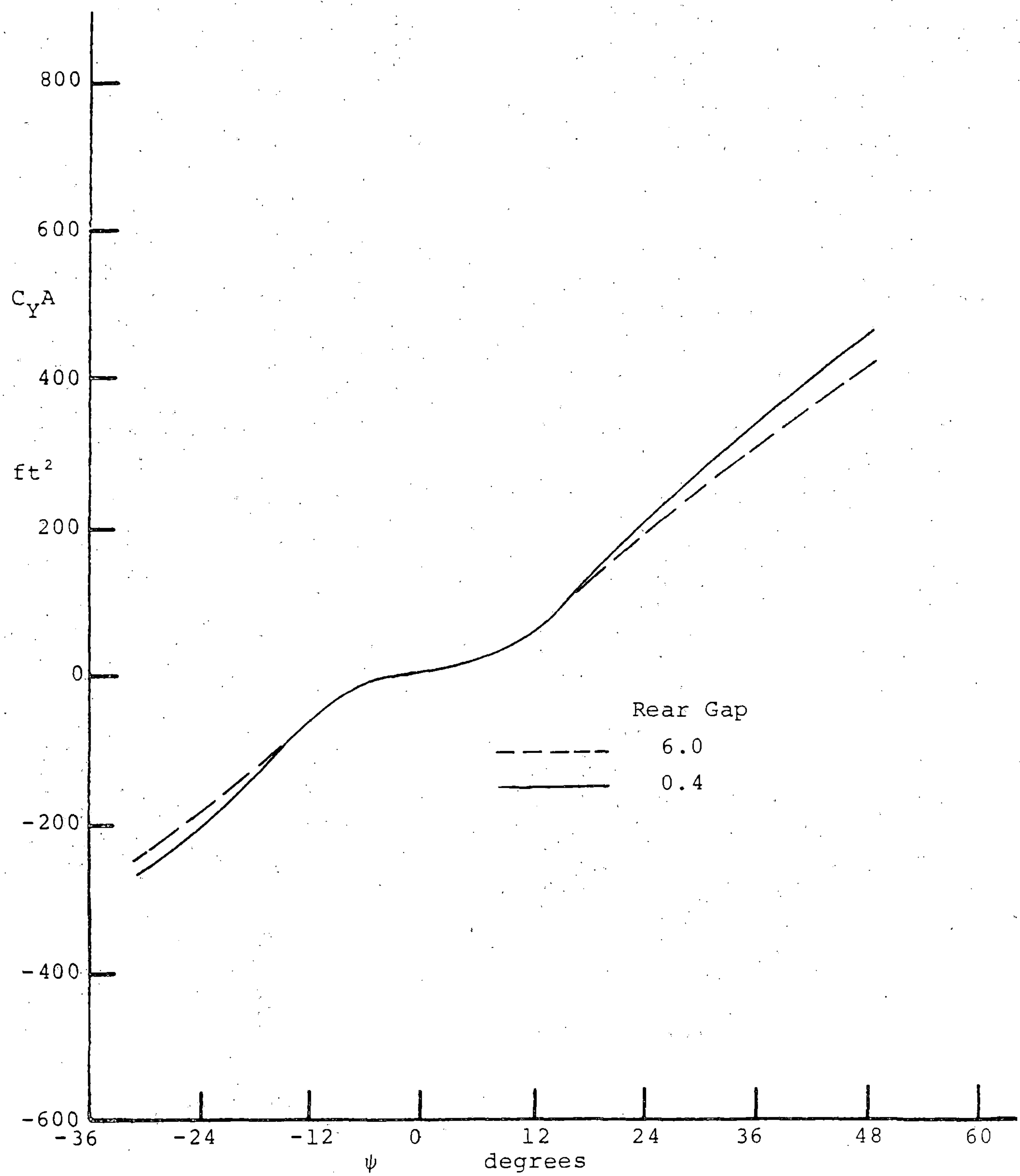

Figure 31. Side Force Area Versus Yaw Angle for 1.7 High Blocks With Variable Spacing of Gaps Behind Metric Block. All Other Gaps 0.2.

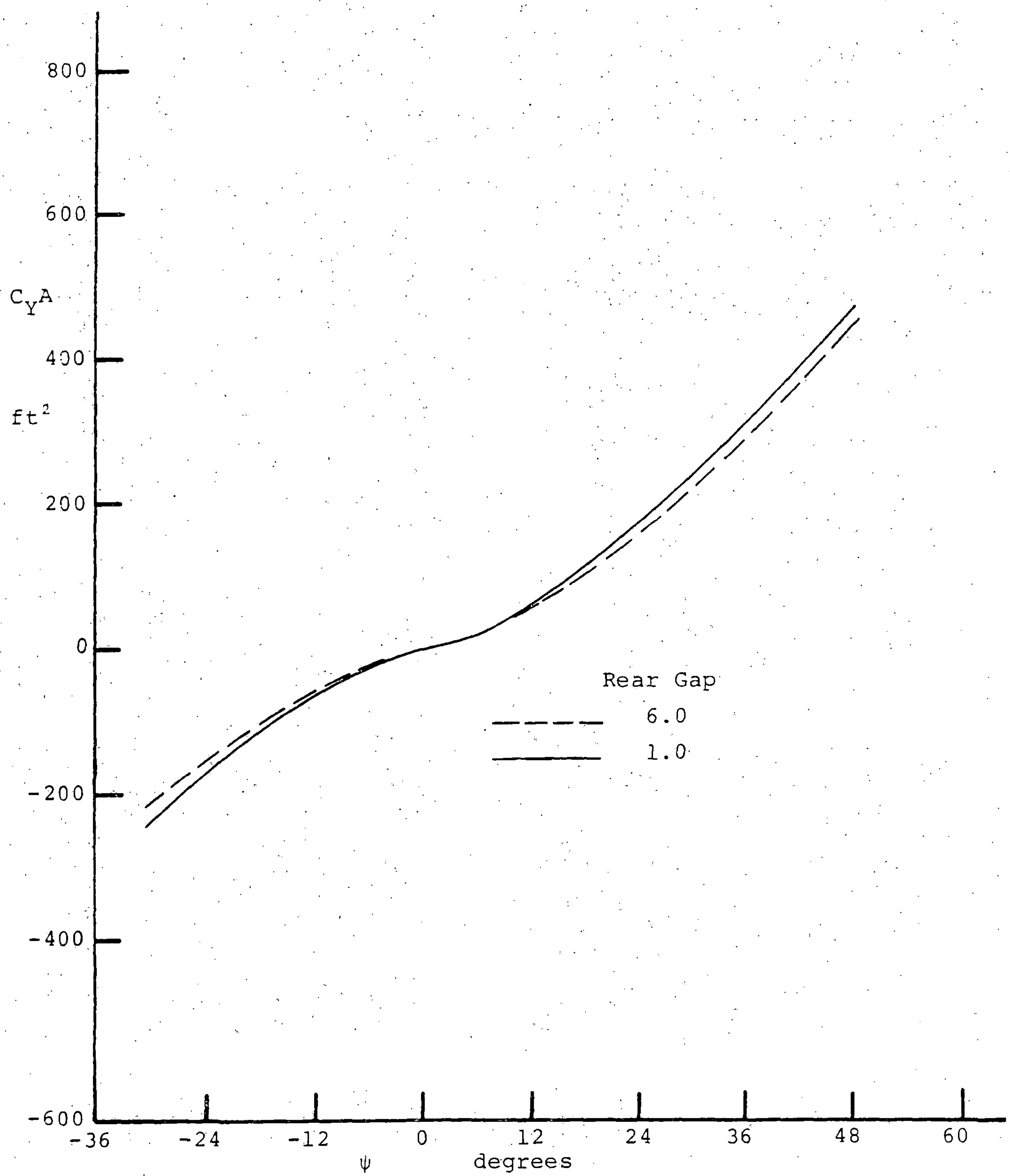

Figure 32. Side Force Area Versus Yaw Angle for 1.7 High Blocks With Variable Spacing of Gaps Behind Metric Block. All Other Gaps 0.4.

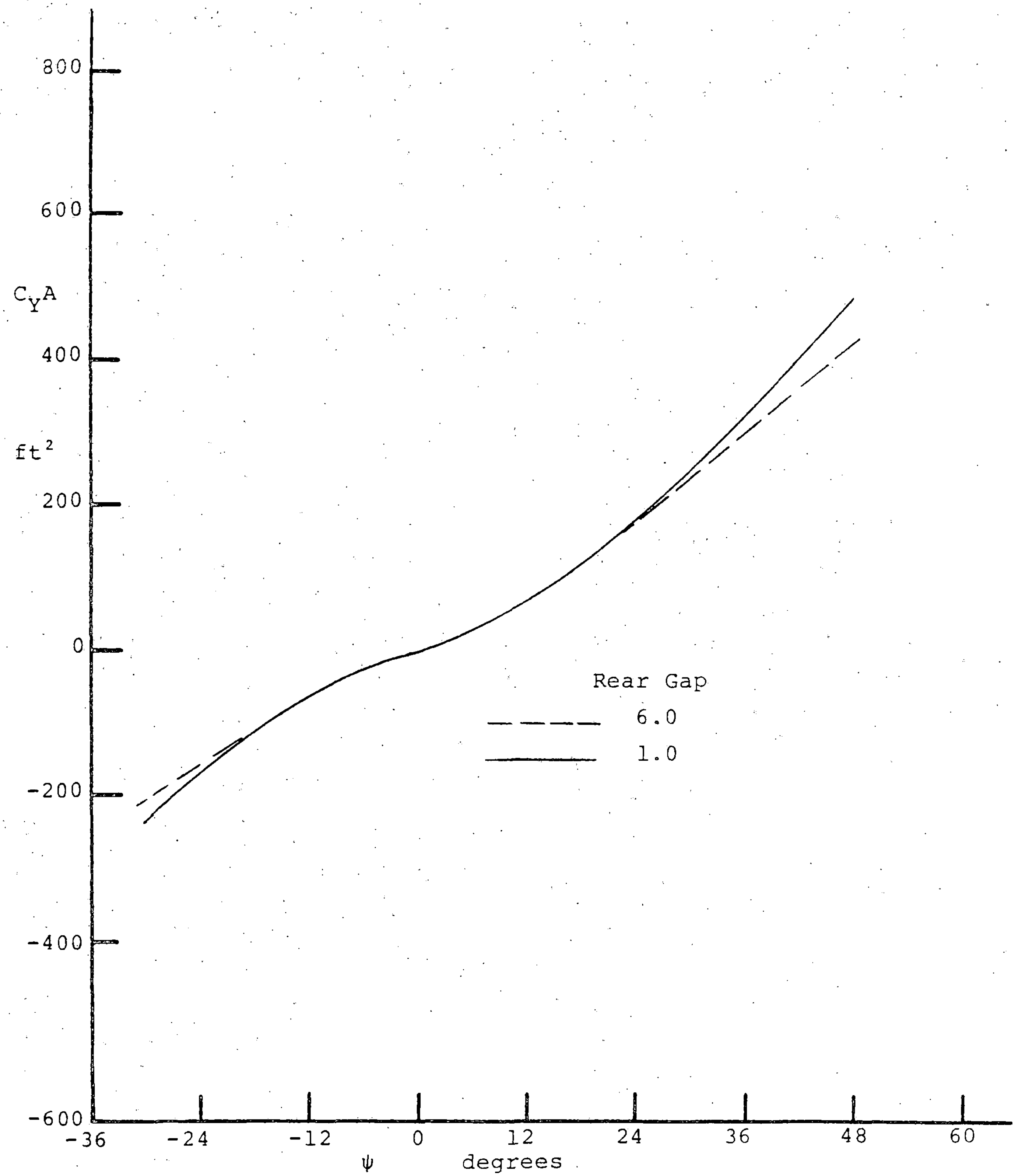

Figure 33. Side Force Area Versus Yaw Angle for 1.7 High Blocks With Variable Spacing of Gaps Behind Metric Block. All Other Gaps 0.6.

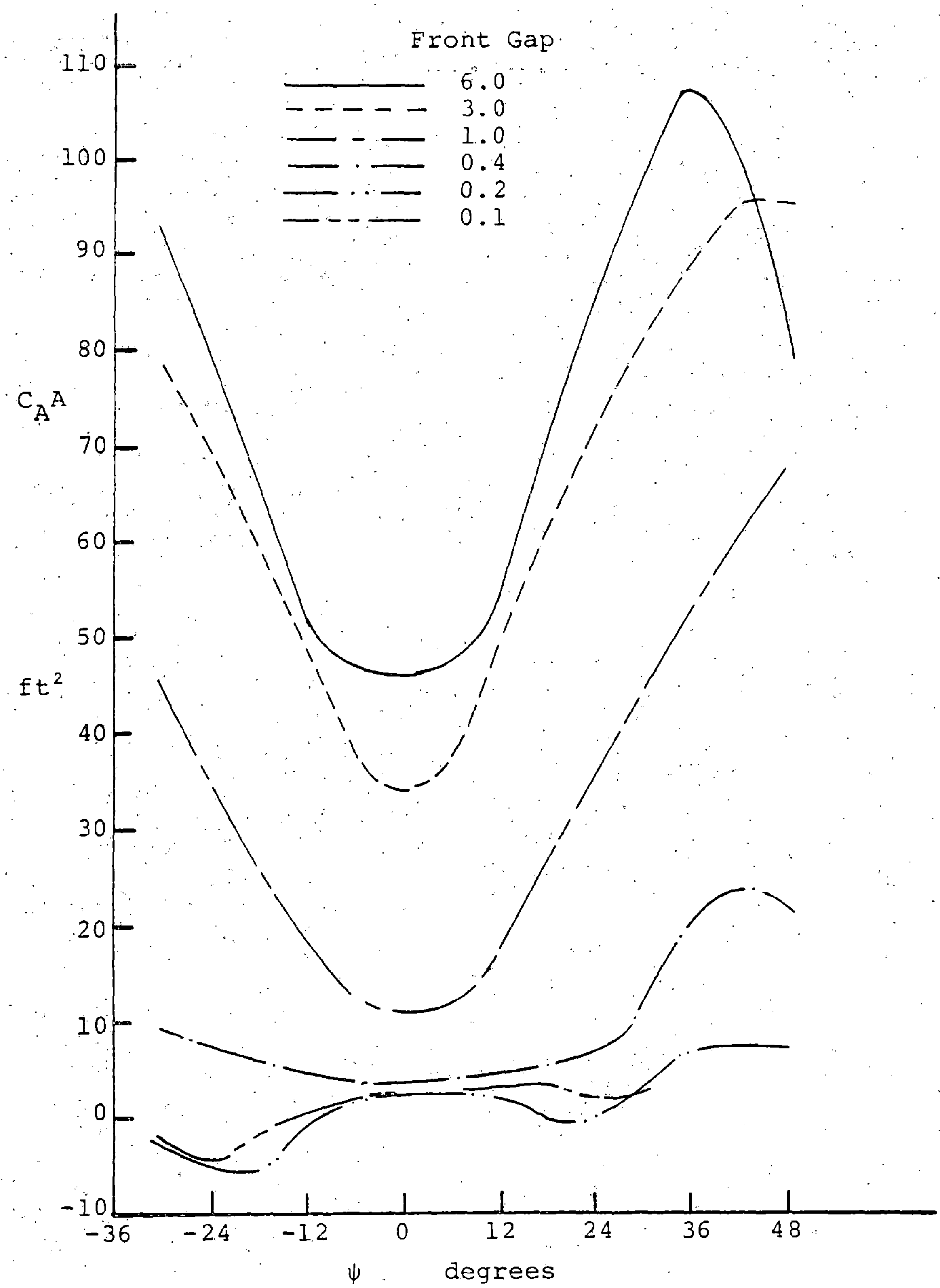

Figure 34. Axial Force Area Versus Yaw Angle for 1.7 High Blocks With Variable Spacing of Gaps Ahead of Metric Block. All Other Gaps 0.1.

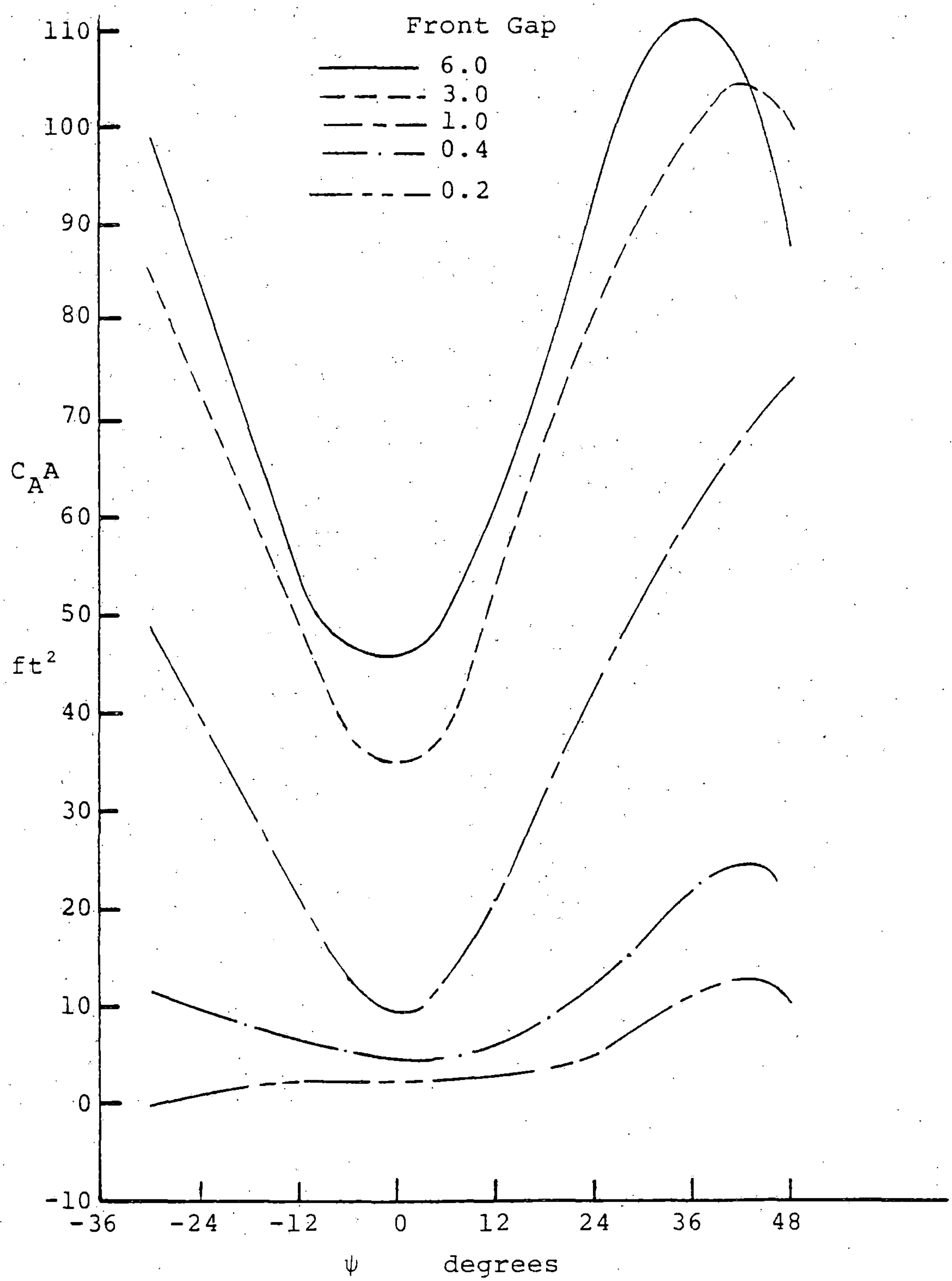

Figure 35. Axial Force Area Versus Yaw Angle for 1.7 High Blocks With Variable Spacing of Gaps Ahead of Metric Block. All Other Gaps 0.2.

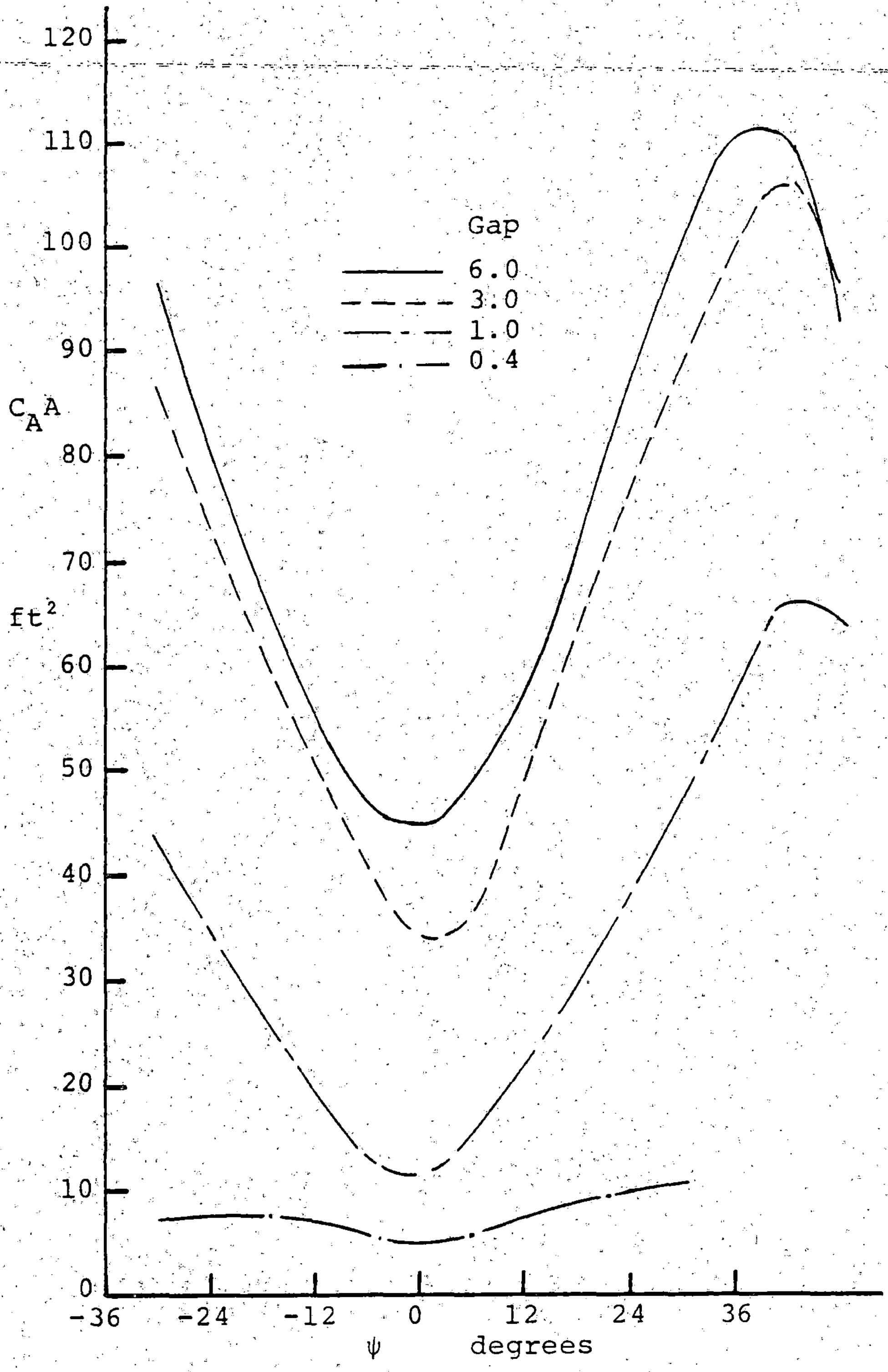

Figure 36. Axial Force Area Versus Yaw Angle for 1.7 High Blocks With Variable Spacing of Gaps Ahead of Metric Block. All Other Gaps 0.4

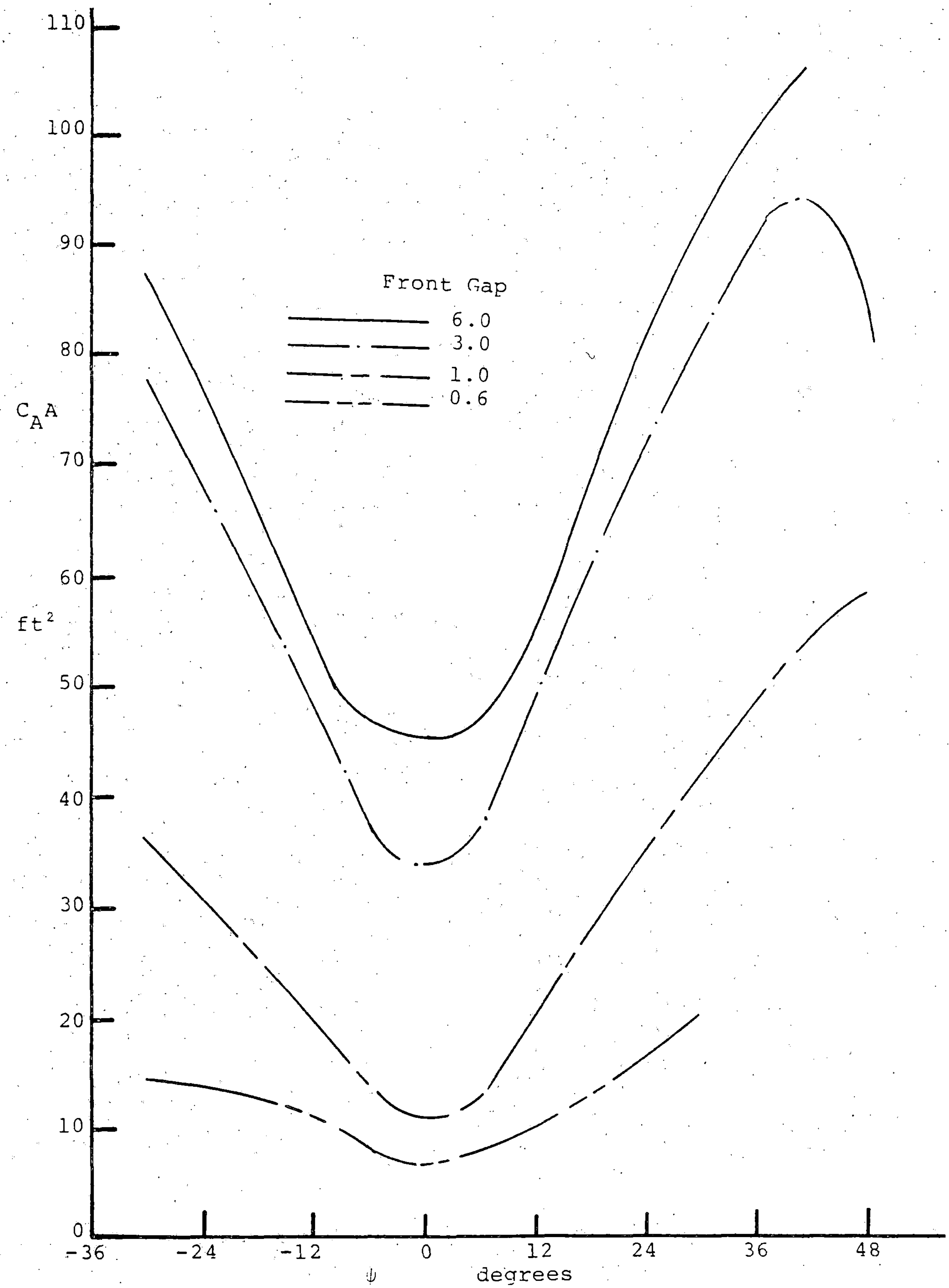

Figure 37. Axial Force Area Versus Yaw Angle for 1.7 High Blocks With Variable Spacing of Gaps Ahead of Metric Block. All Other Gaps 0.6.

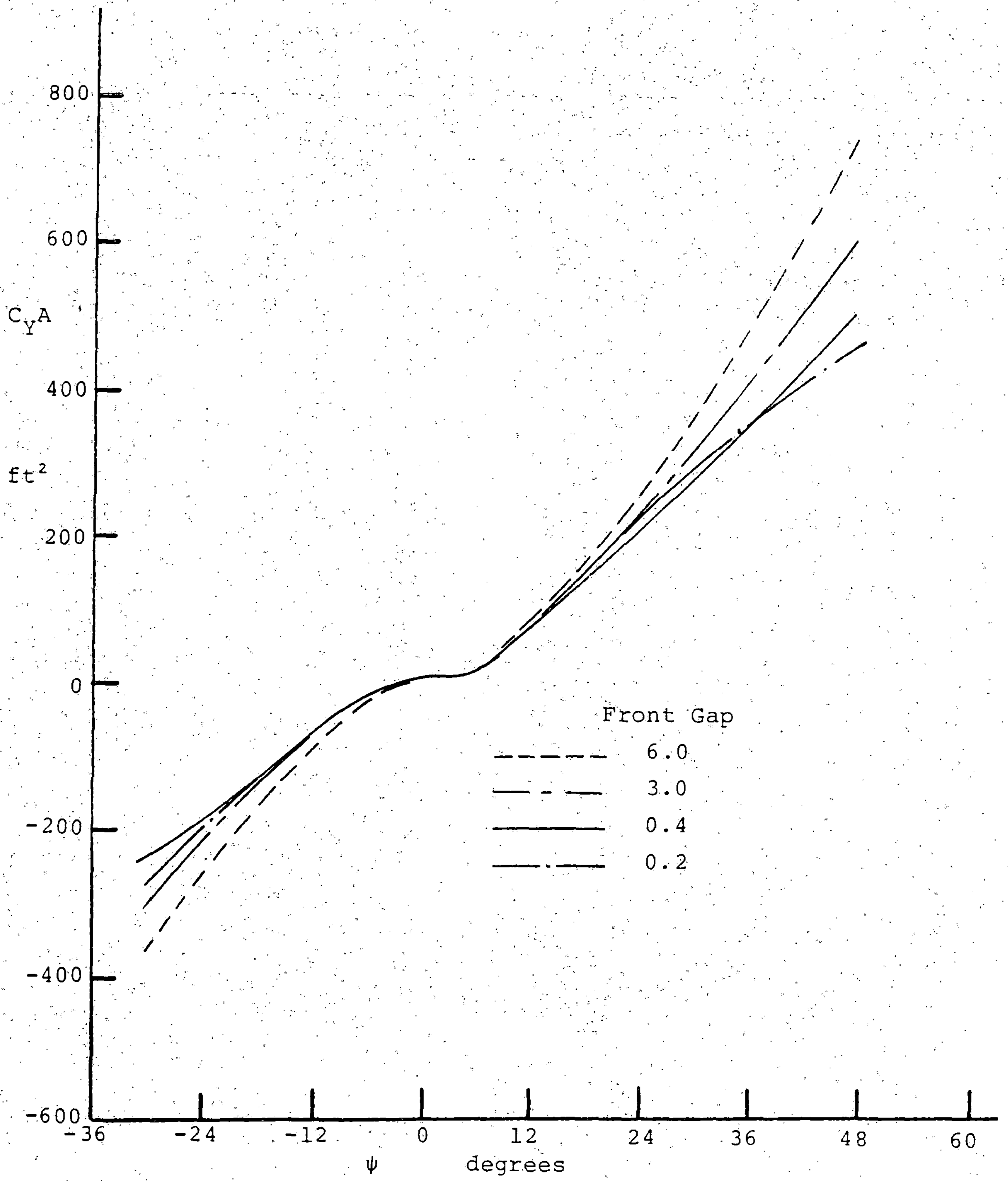

Figure 38. Side Force Area Versus Yaw Angle for 1.7 High Blocks With Variable Spacing of Gaps Ahead of Metric Block. All Other Gaps 0.1.

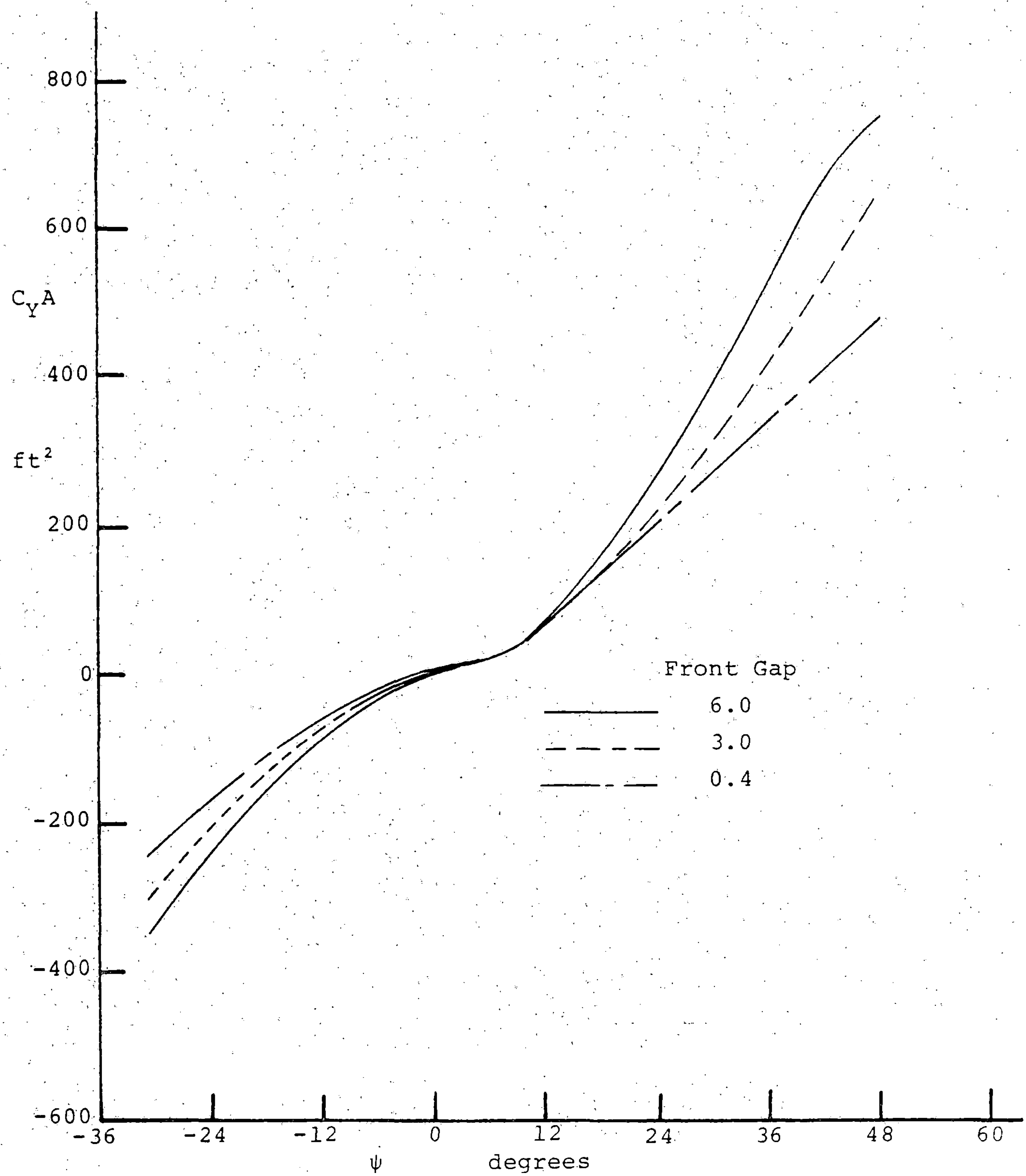

Figure 39. Side Force Area Versus Yaw Angle for 1.7 High Blocks With Variable Spacing of Gaps Ahead of Metric Block. All Other Gaps 0.2

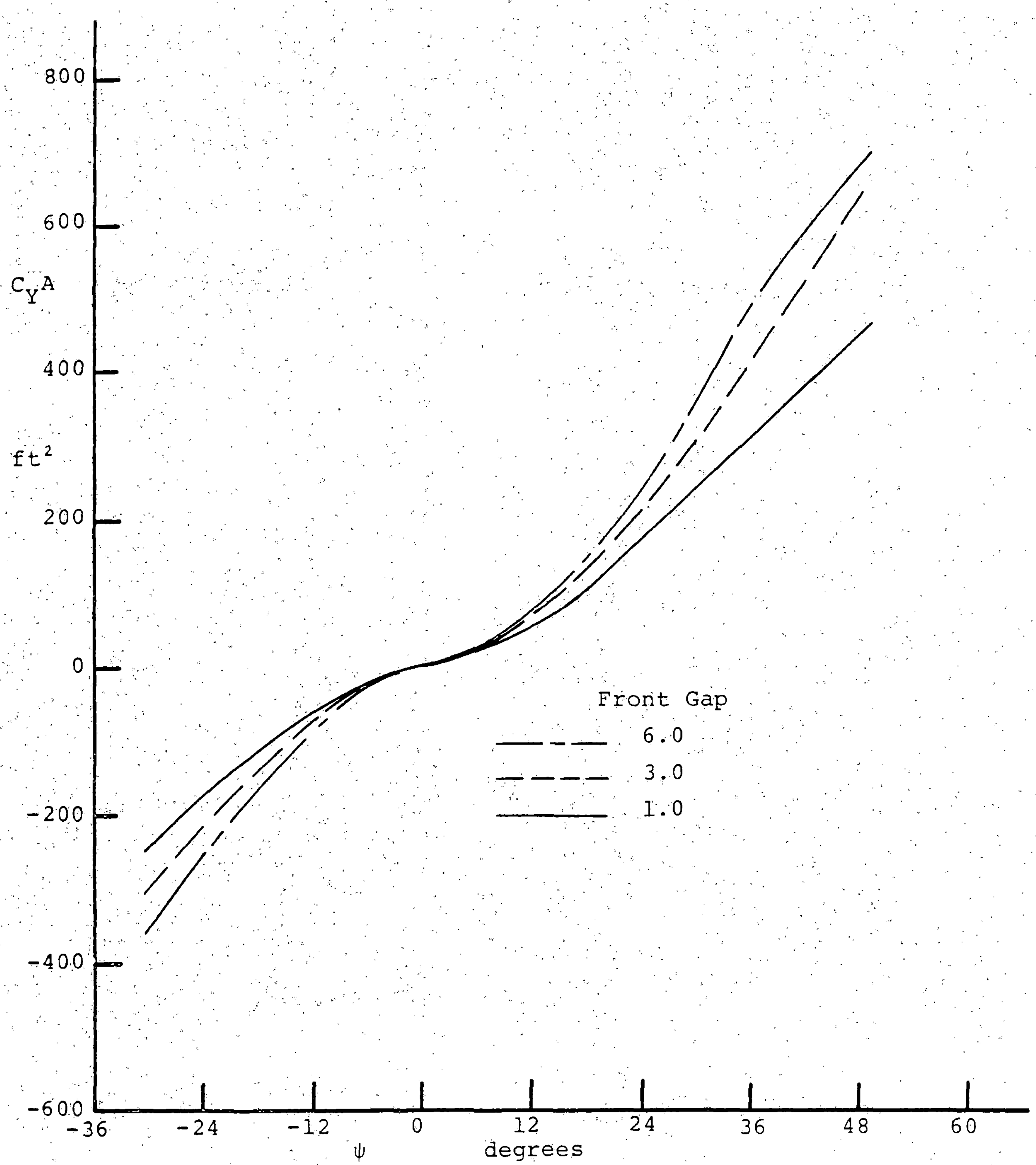

Figure 40. Side Force Area Versus Yaw Angle for 1.7 High Blocks With Variable Spacing of Gaps Ahead of Metric Block. All Other Gaps 0.4.

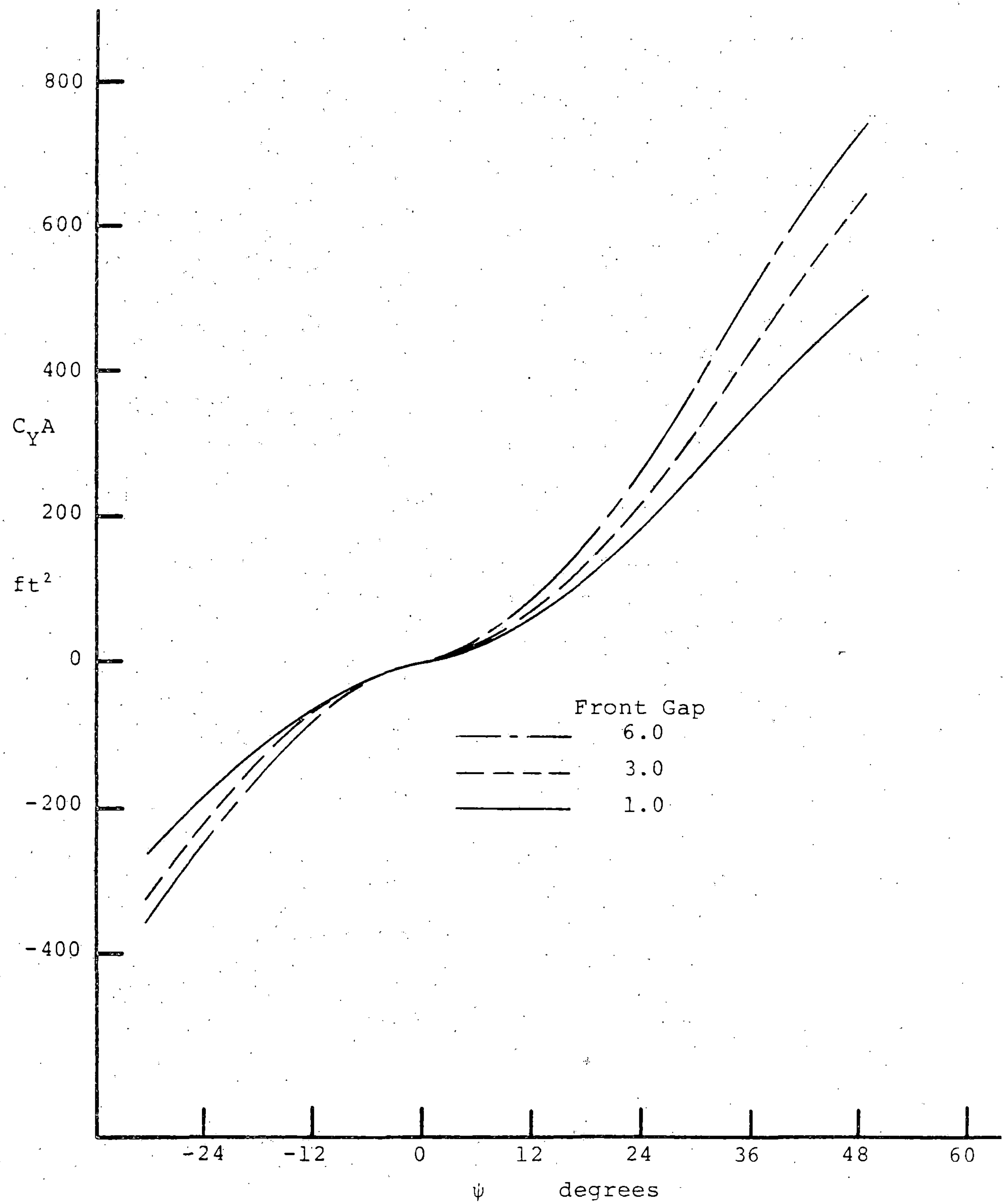

Figure 41. Side Force Area Versus Yaw Angle for 1.7 High Blocks With Variable Spacing of Gaps Ahead of Metric Block. All Other Gaps 0.6.

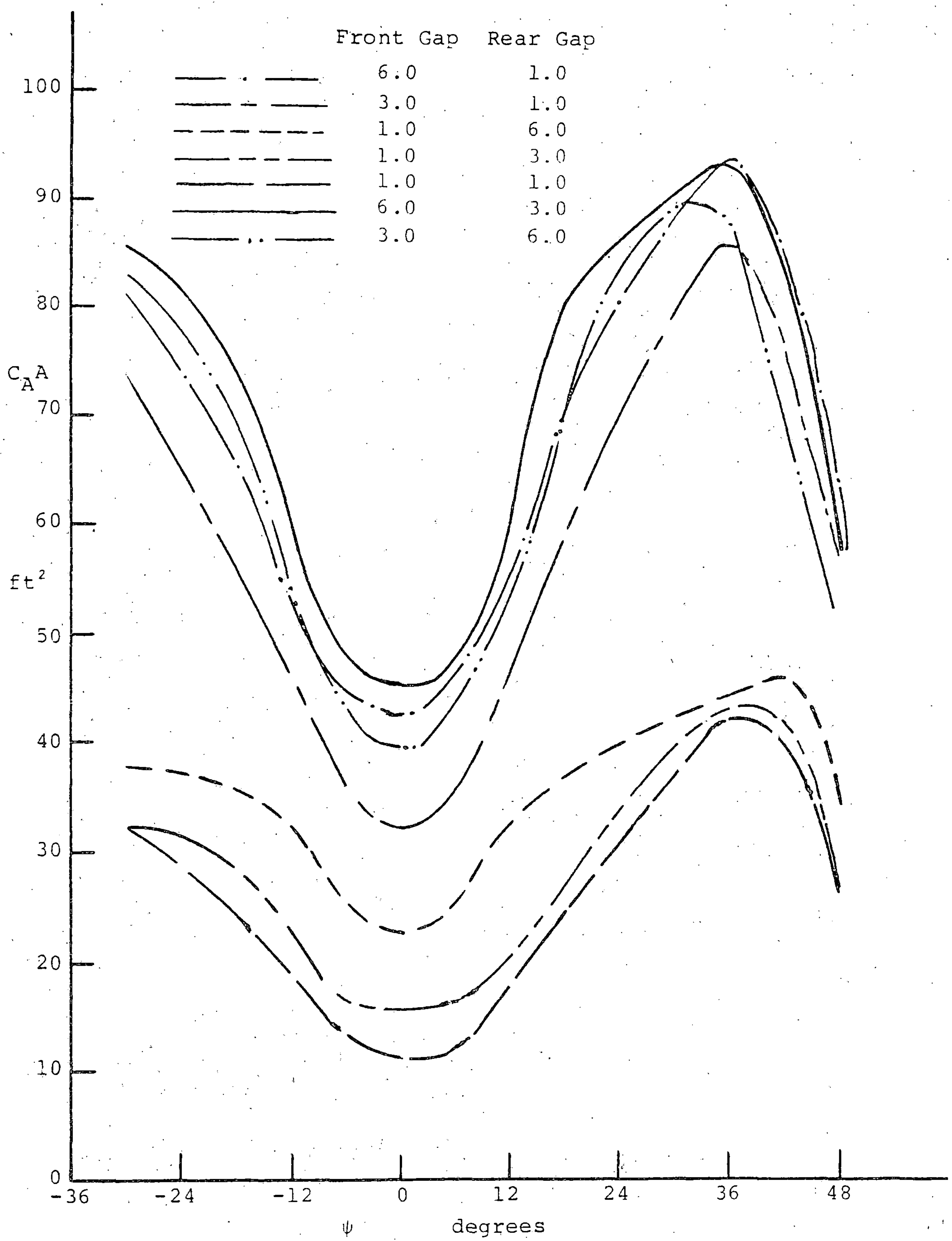

Figure 42. Axial Force Area Versus Yaw Angle for 1.7 High Blocks With Different Spacings of Gaps Ahead of and Behind the Metric Block as Shown.

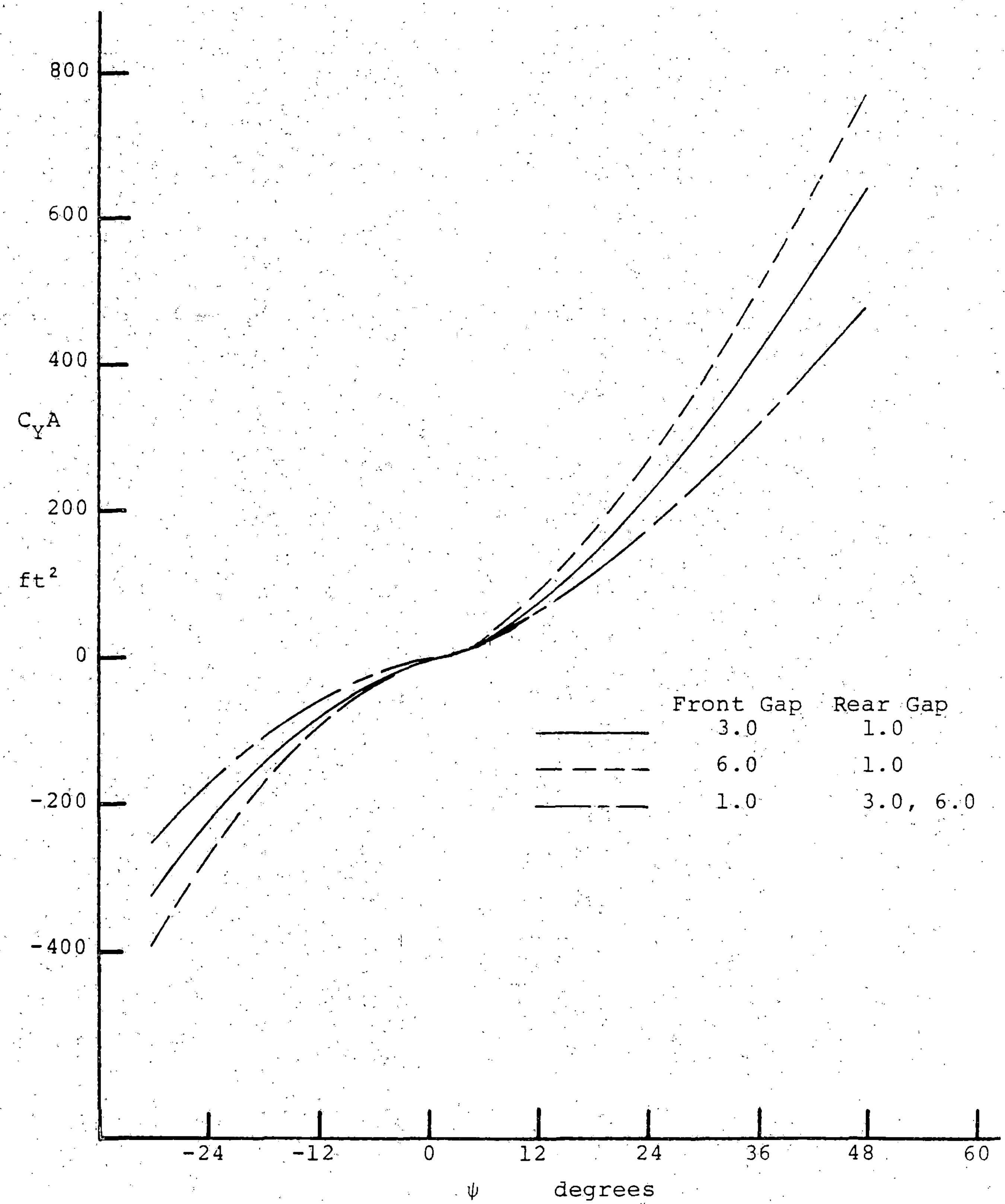

Figure 43. Side Force Area Versus Yaw Angle for 1.7 High Blocks With Different Spacings of Gaps Ahead of and Behind the Metric Block as Shown.

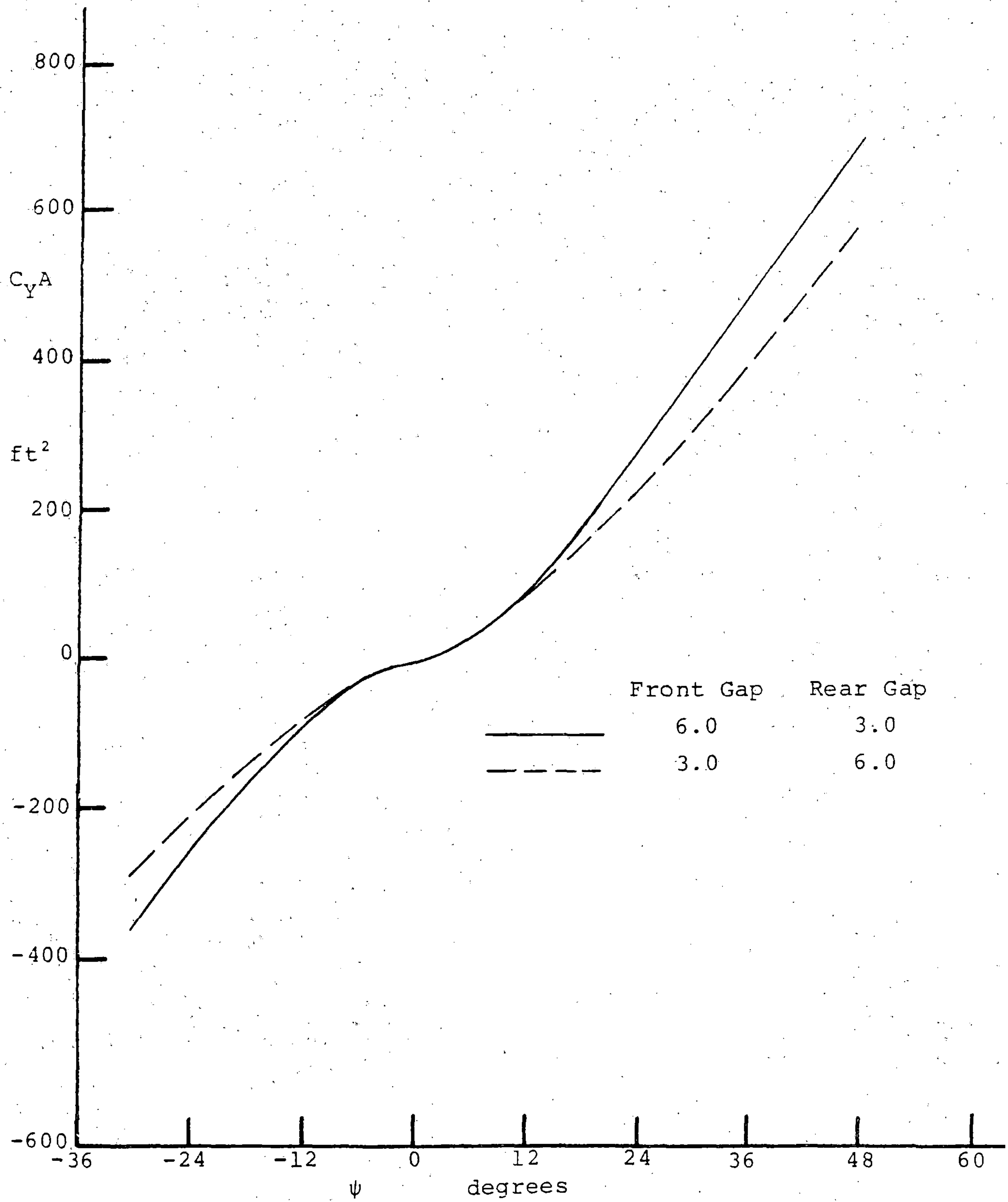

Figure 44. Side Force Area Versus Yaw Angle for 1.7 High Blocks With Different Spacings of Gaps Ahead of and Behind the Metric Block as Shown.

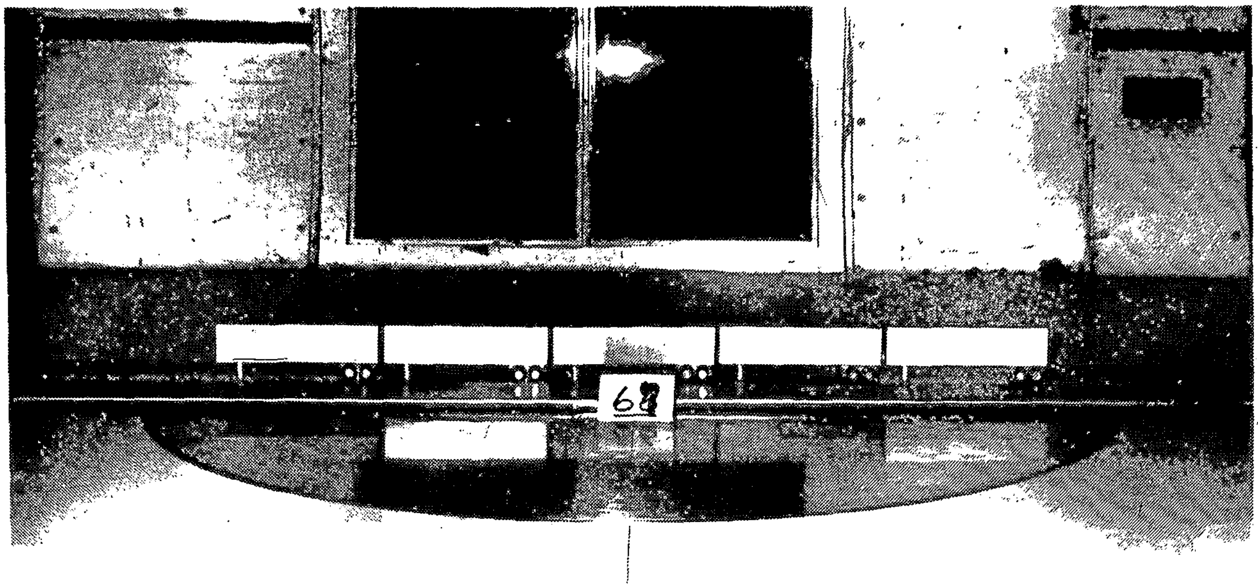

Figure 45. Photograph of Forward Facing Trailers With Spacing of Gaps Ahead and Behind of 0.1 and 0% Shielding.

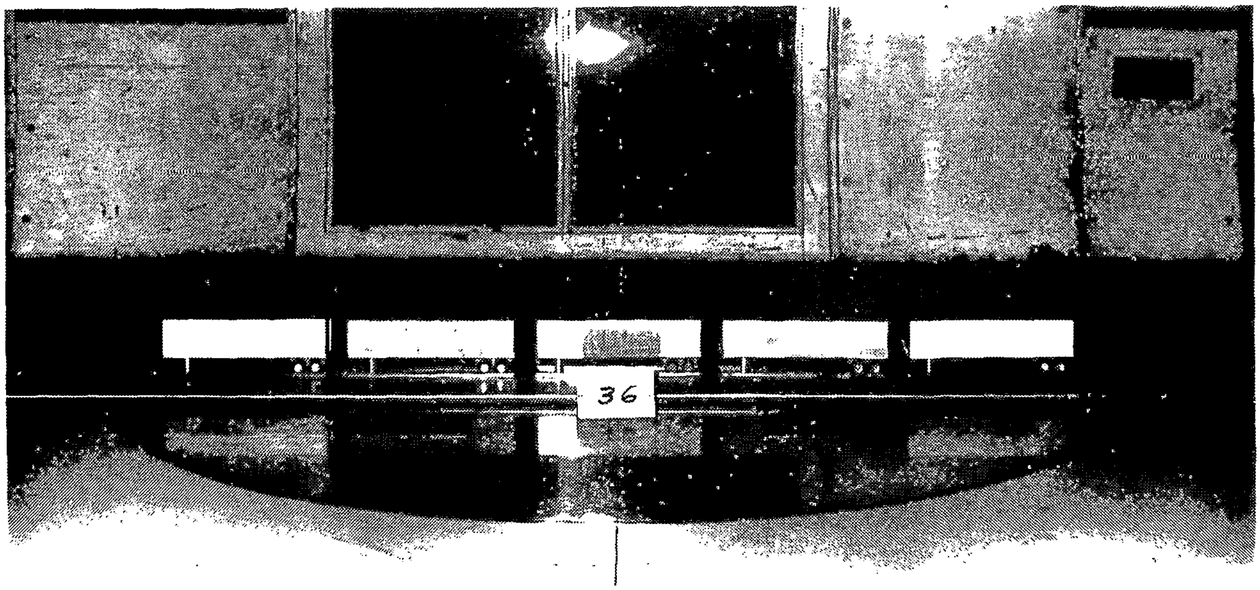

Figure 46. Photograph of Forward Facing Trailers With Spacing of Gaps Ahead and Behind of 0.6 and 25% Shielding.

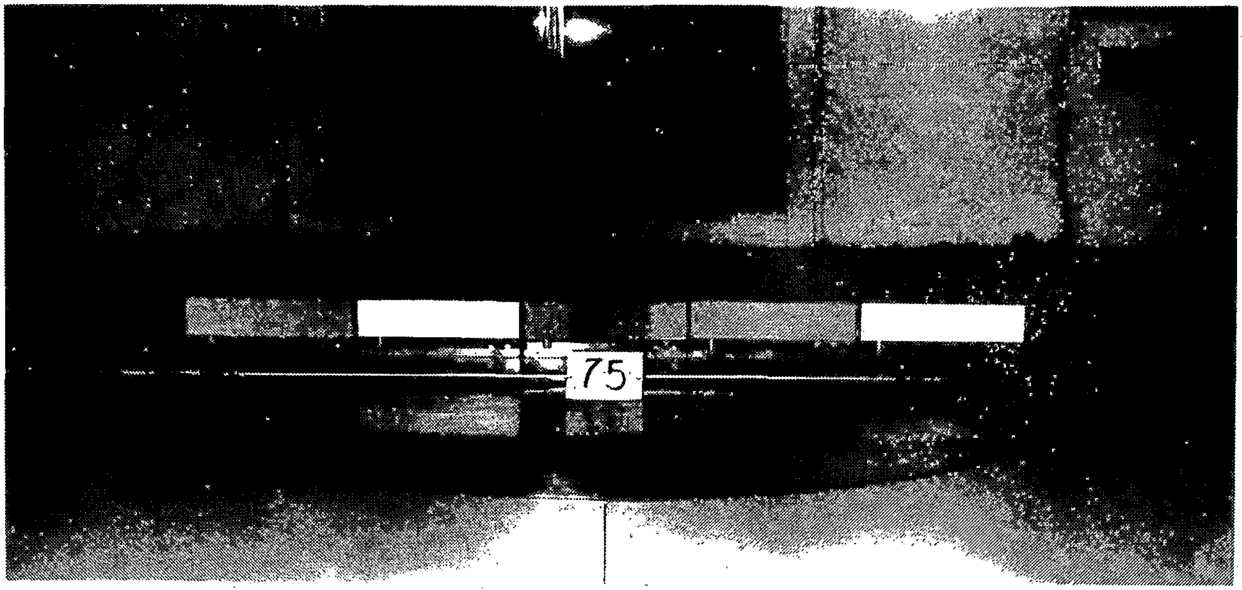

Figure 47. Photograph of Forward Facing Trailers With Spacing of Gaps Ahead and Behind of 0.1 and 50% Shielding.

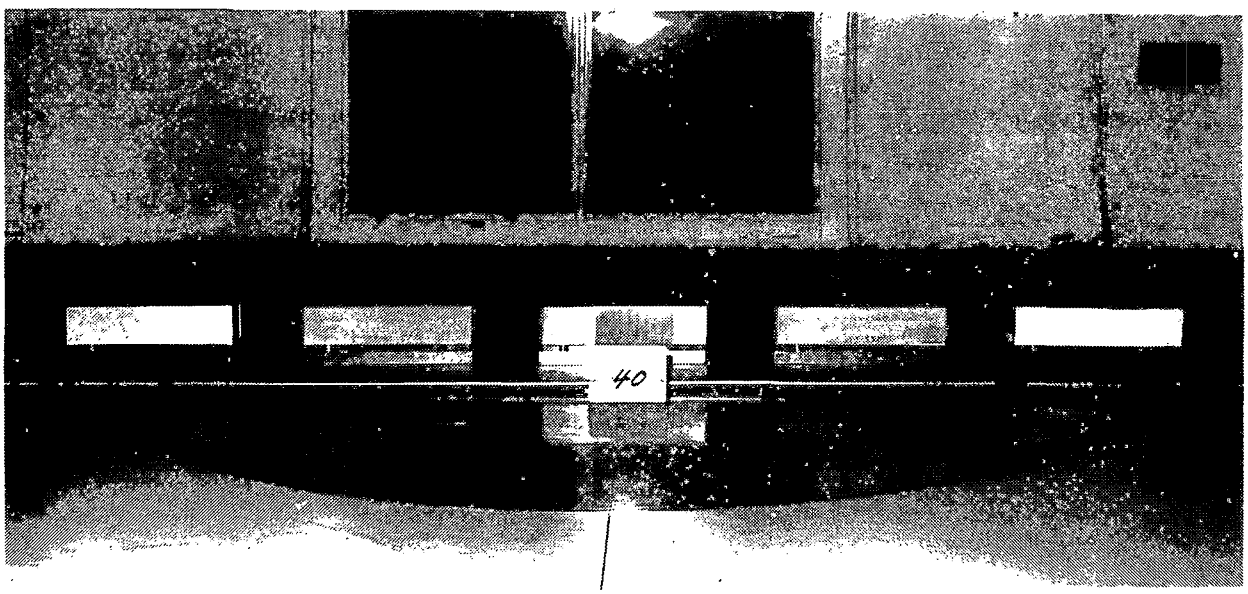

Figure 48. Photograph of Forward Facing Trailers With Spacing of Gaps Ahead and Behind of 2.0 and 75% Shielding.

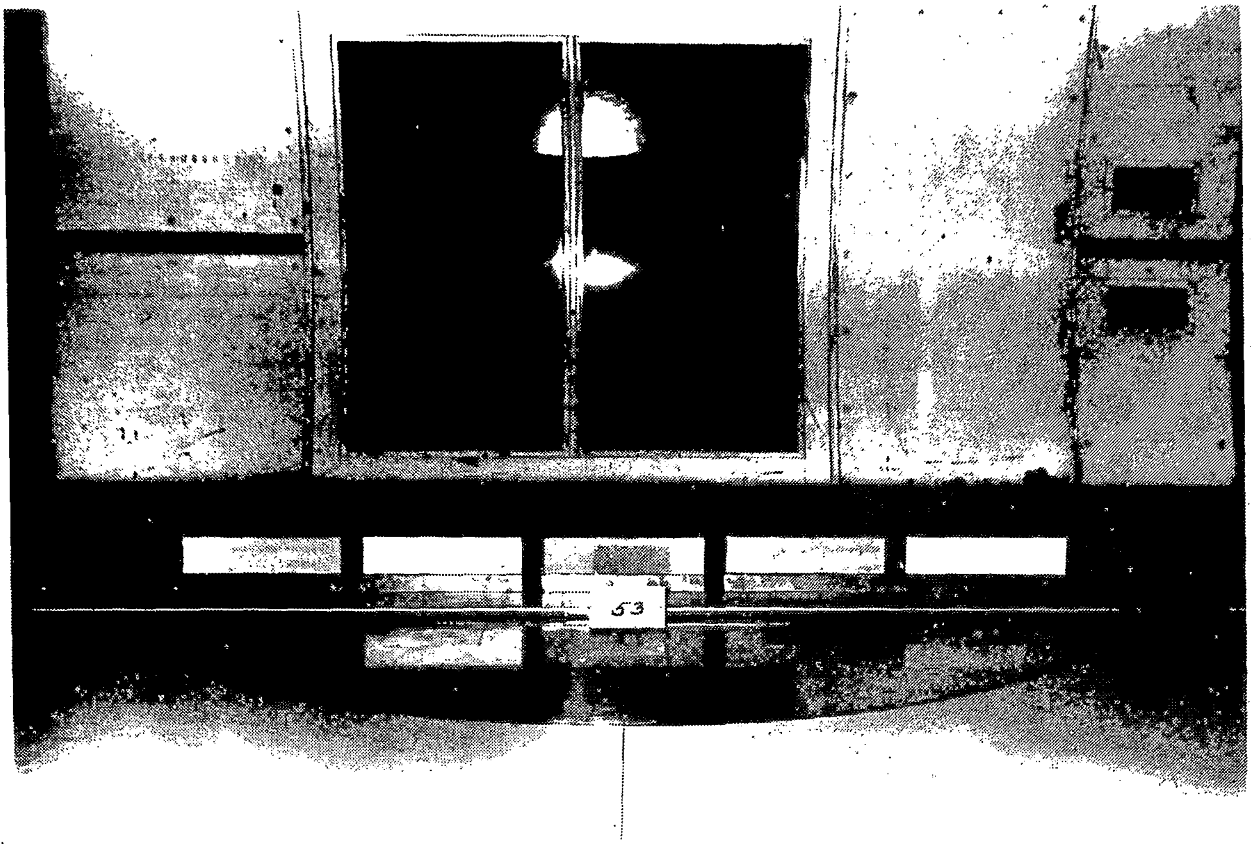

Figure 49. Photograph of Forward Facing Trailers With Spacing of Gaps Ahead and Behind of 1.0 and 100% Shielding.

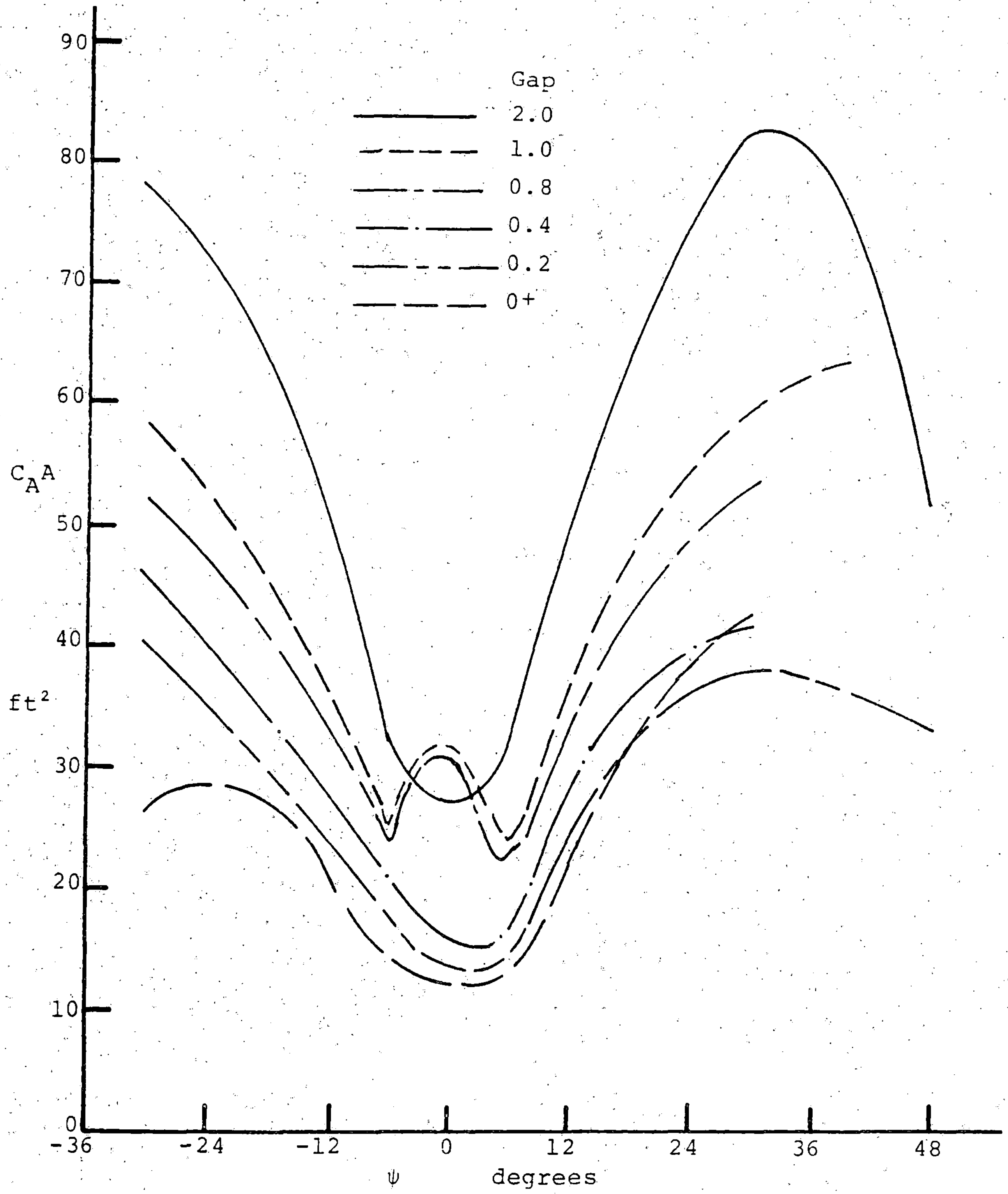

Figure 50. Axial Force Area on Forward Facing Trailers With Equal Spacing of Gaps Ahead and Behind. 0% Shielding.

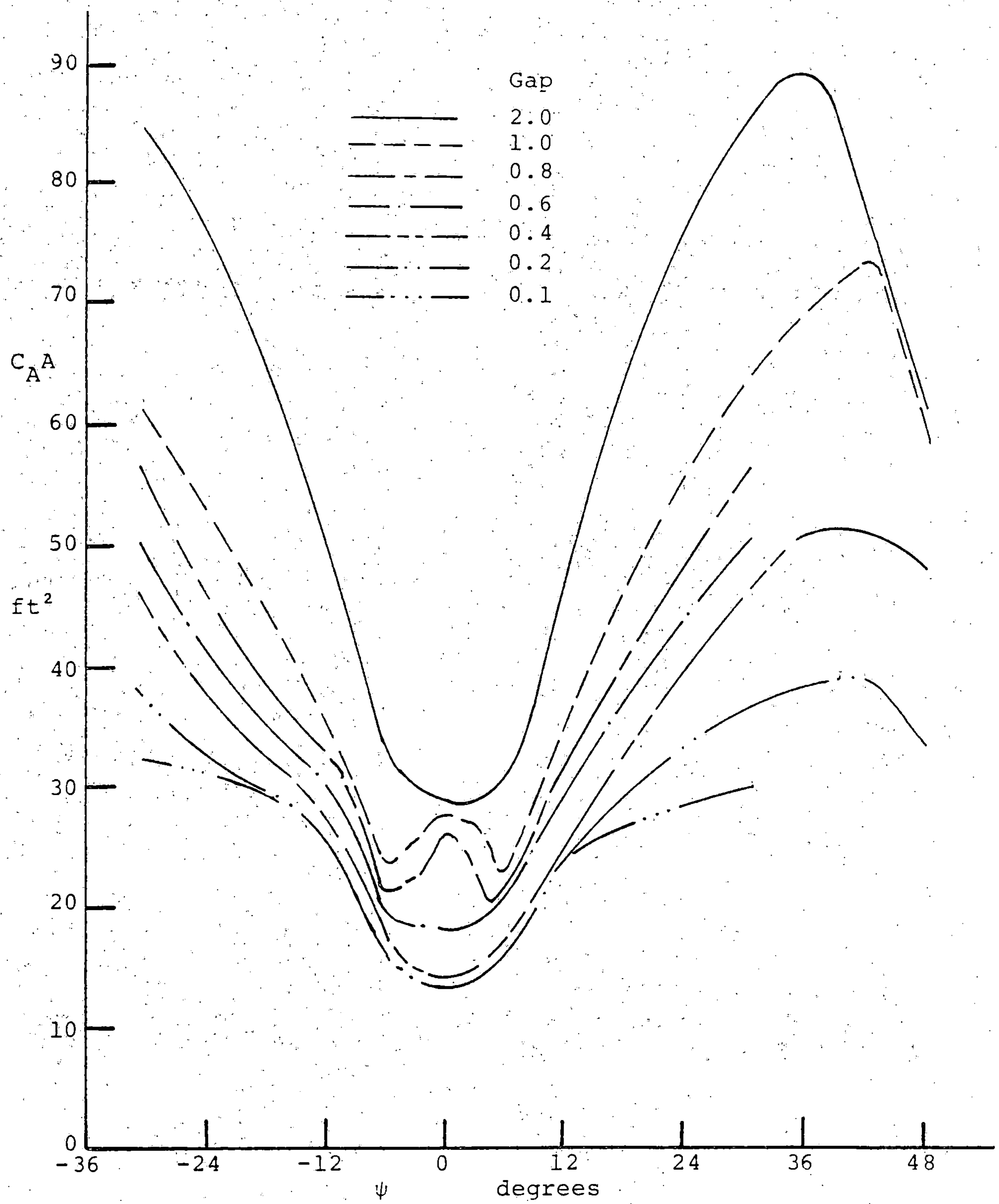

Figure 51. Axial Force Area on Forward Facing Trailers With Equal Spacing of Gaps Ahead and Behind. 25% Shielding.

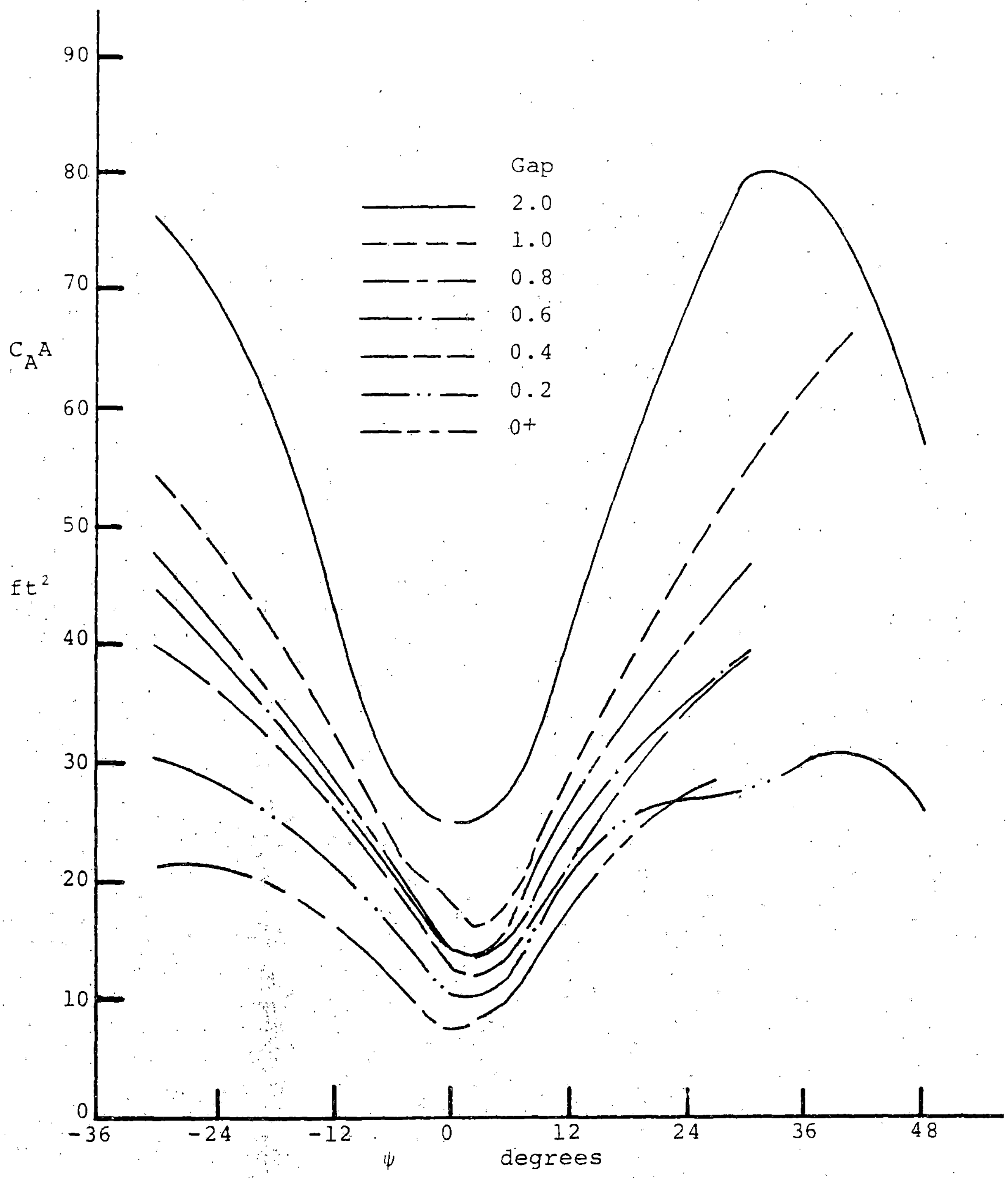

Figure 52. Axial Force Area on Forward Facing Trailers With Equal Spacing of Gaps Ahead and Behind. 50% Shielding.

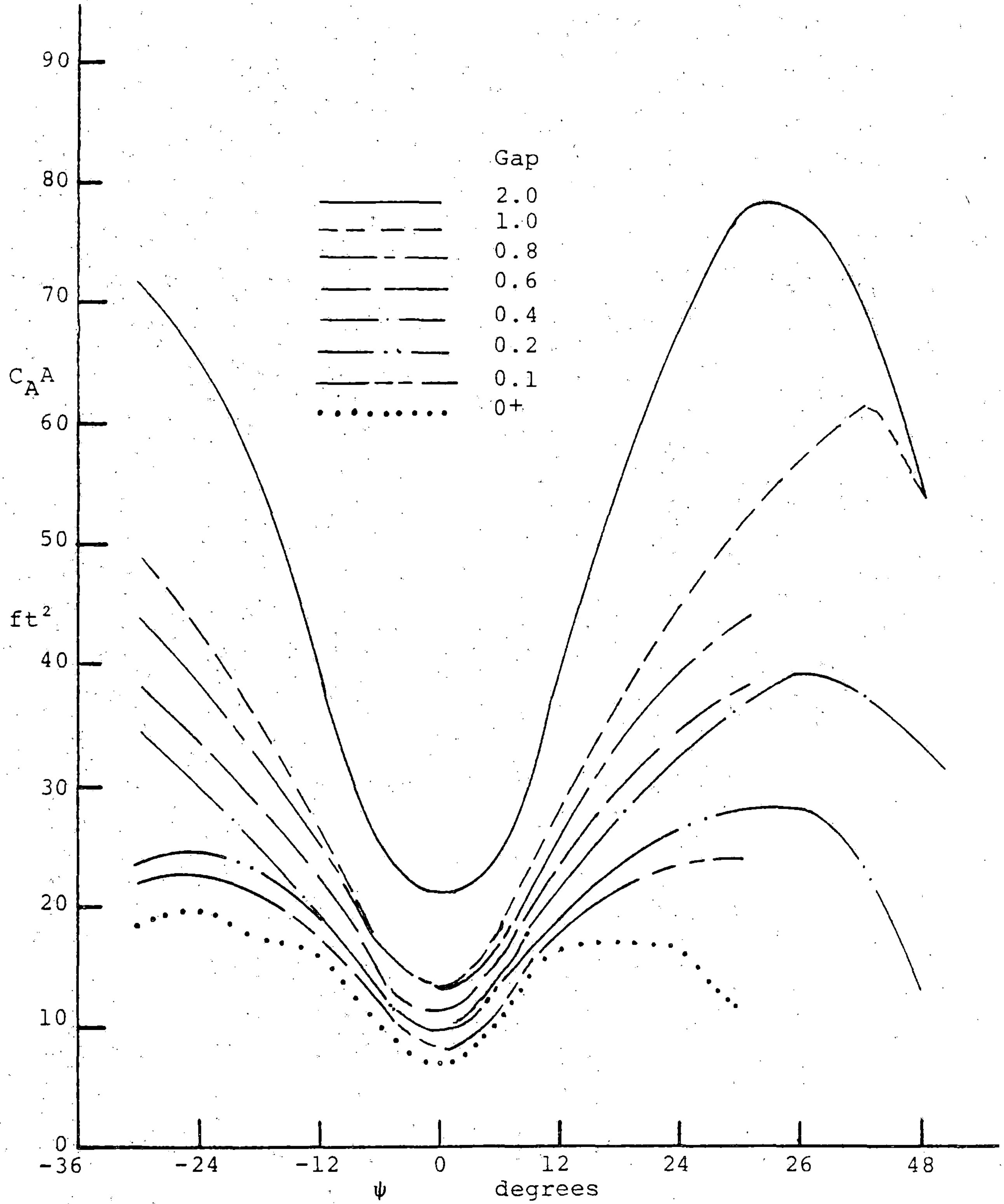

Figure 53. Axial Force Area on Forward Facing Trailers With Equal Spacing of Gaps Ahead and Behind. 75% Shielding.

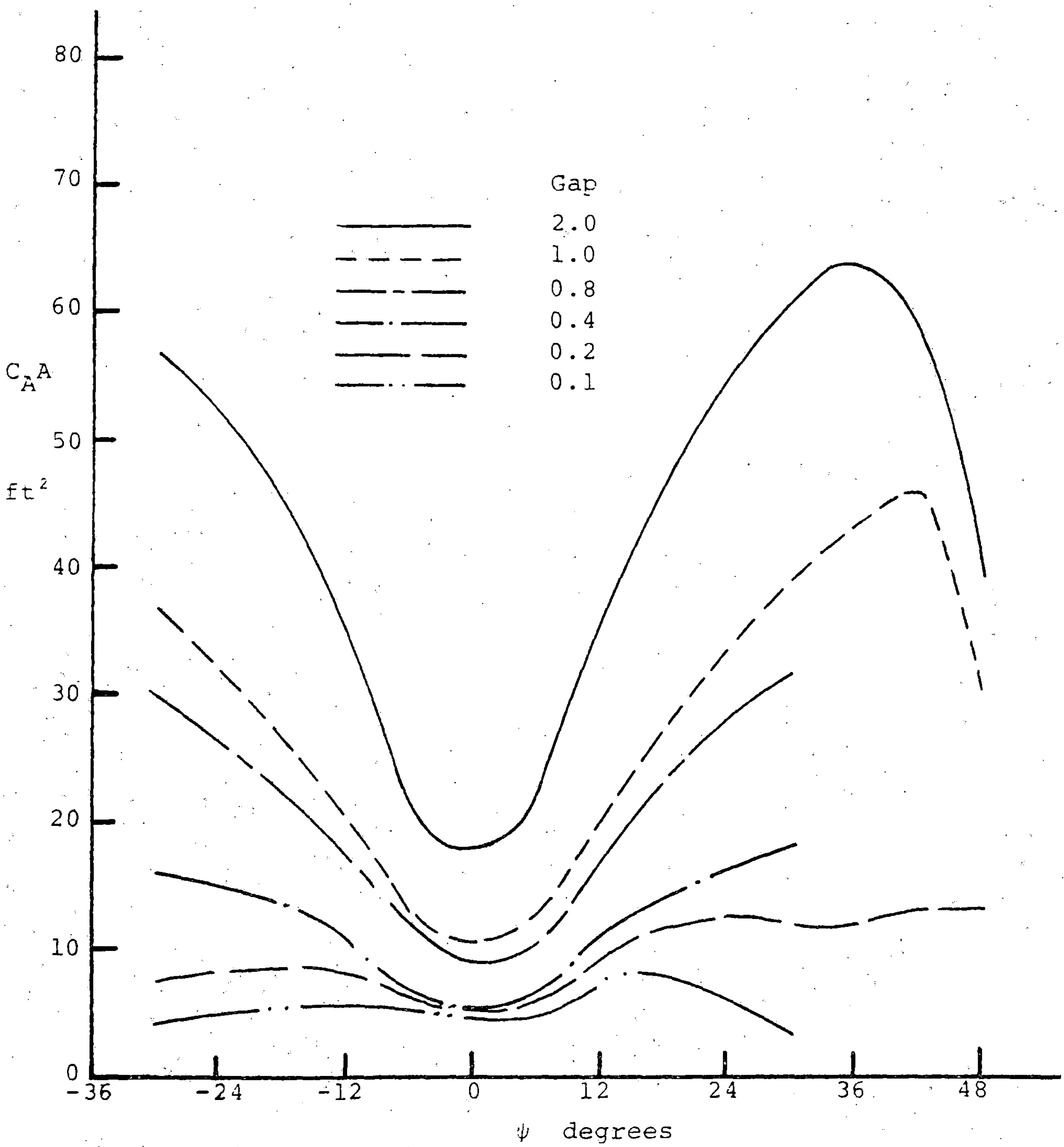

Figure 54. Axial Force Area on Forward Facing Trailers With Equal Spacing of Gaps Ahead and Behind. 100% Shielding.

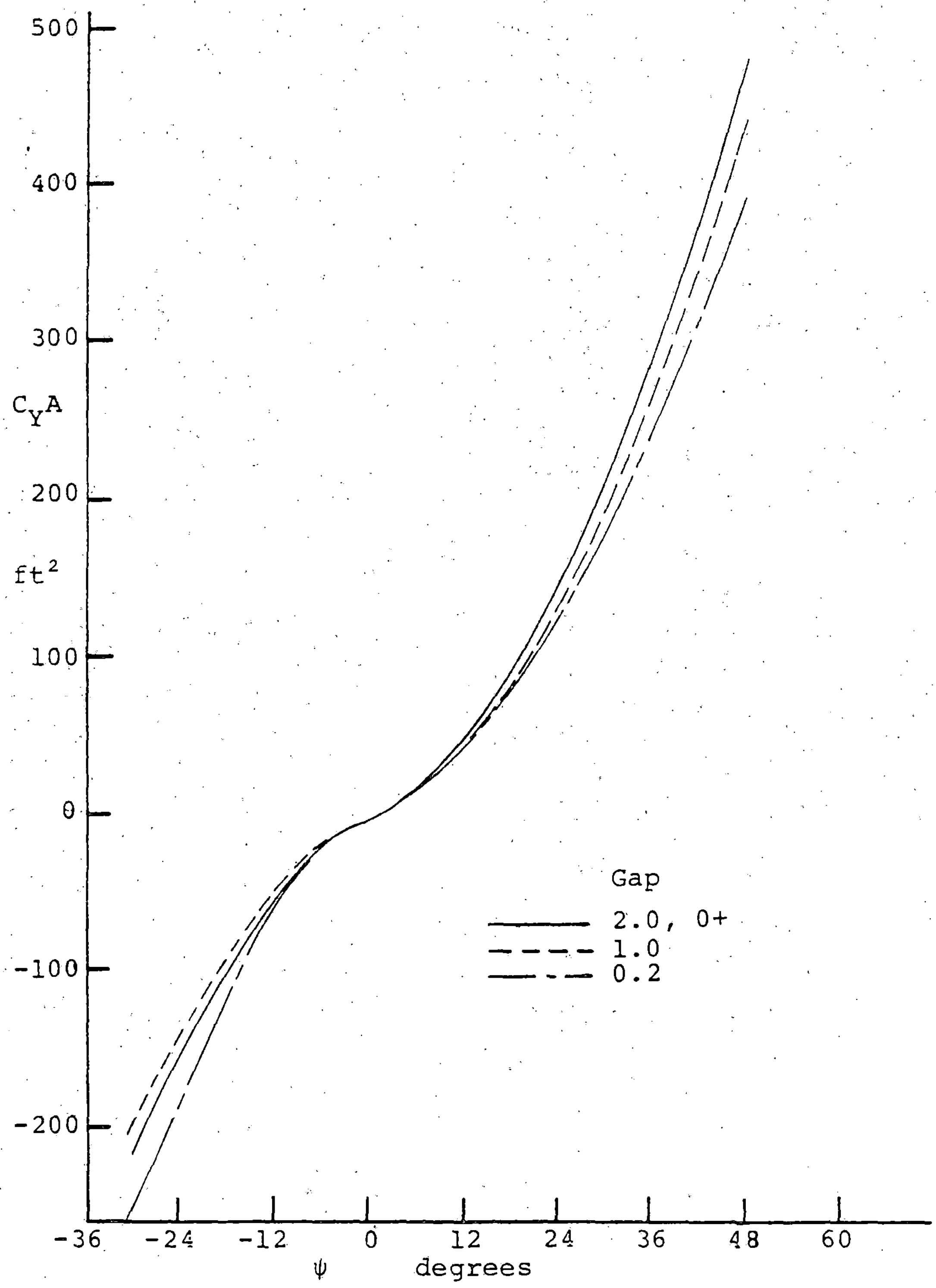

Figure 55. Side Force Area on Forward Facing Trailers With Equal Spacing of Gaps Ahead and Behind. 0% Shielding.

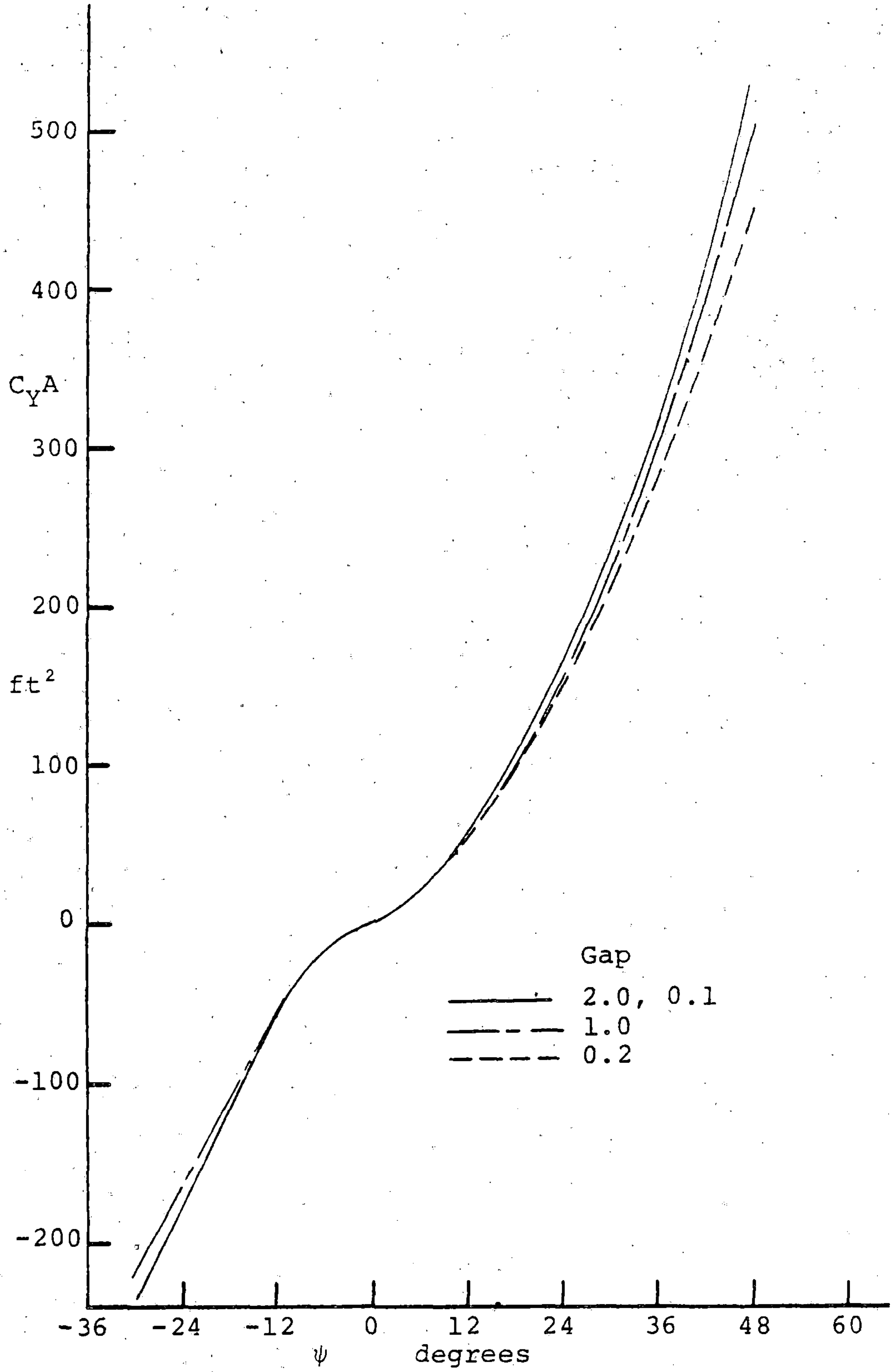

Figure 56. Side Force Area on Forward Facing Trailers With Equal Spacing of Gaps Ahead and Behind. 25% Shielding.

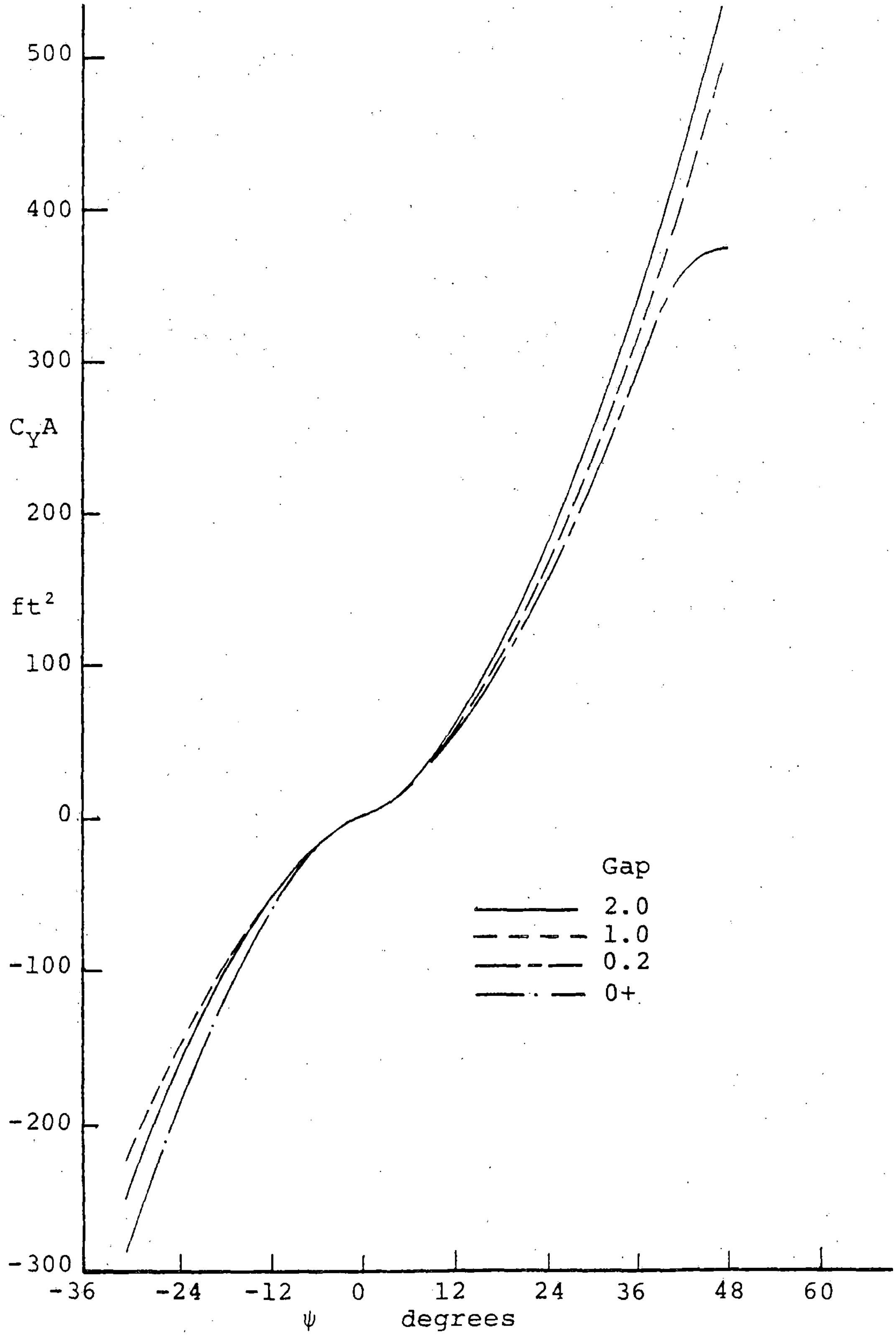

Figure 57. Side Force Area on Forward Facing Trailers With Equal Spacing of Gaps Ahead and Behind. 50% Shielding.

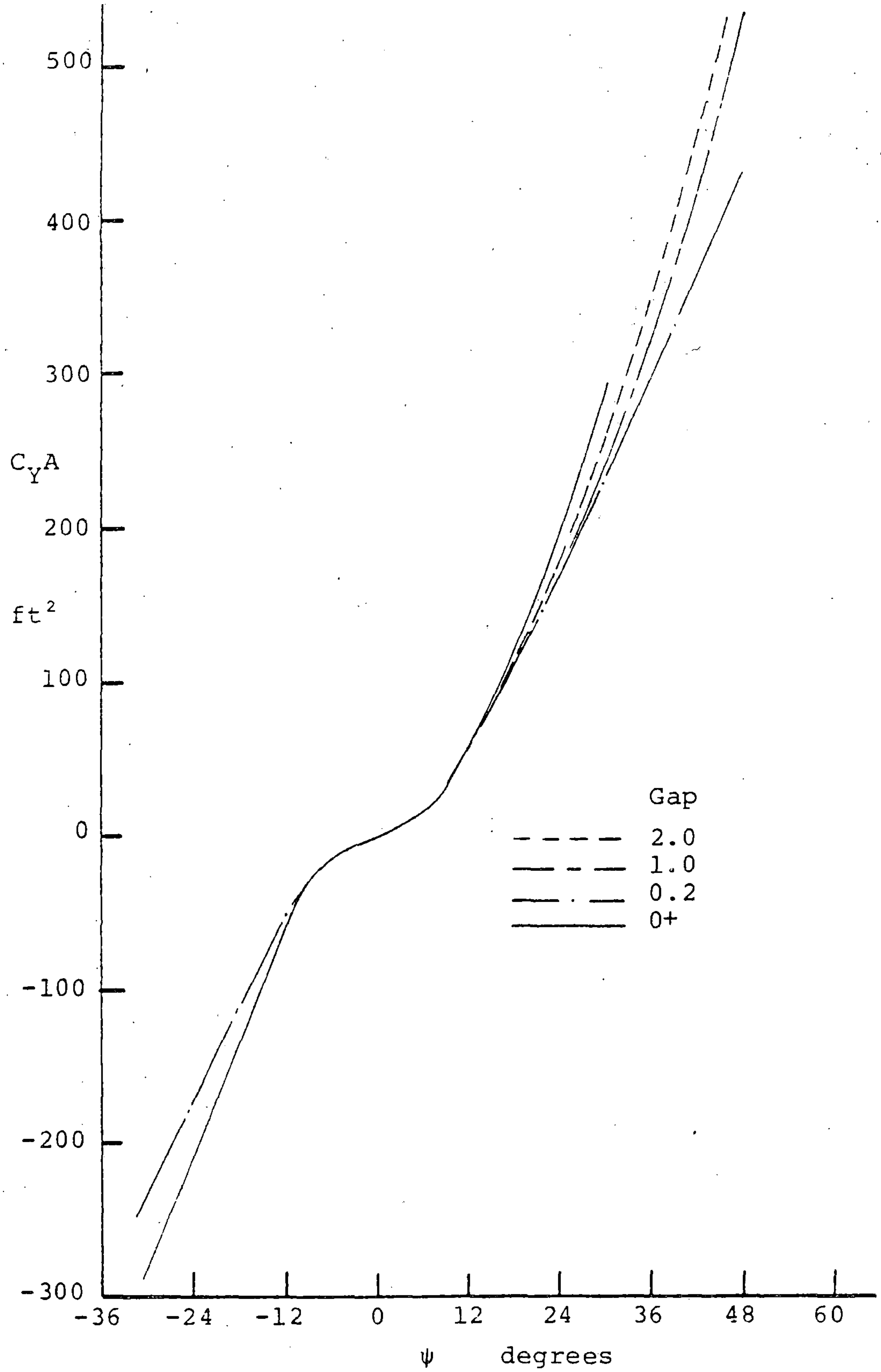

Figure 58. Side Force Area on Forward Facing Trailers With Equal Spacing of Gaps Ahead and Behind. 75% Shielding.

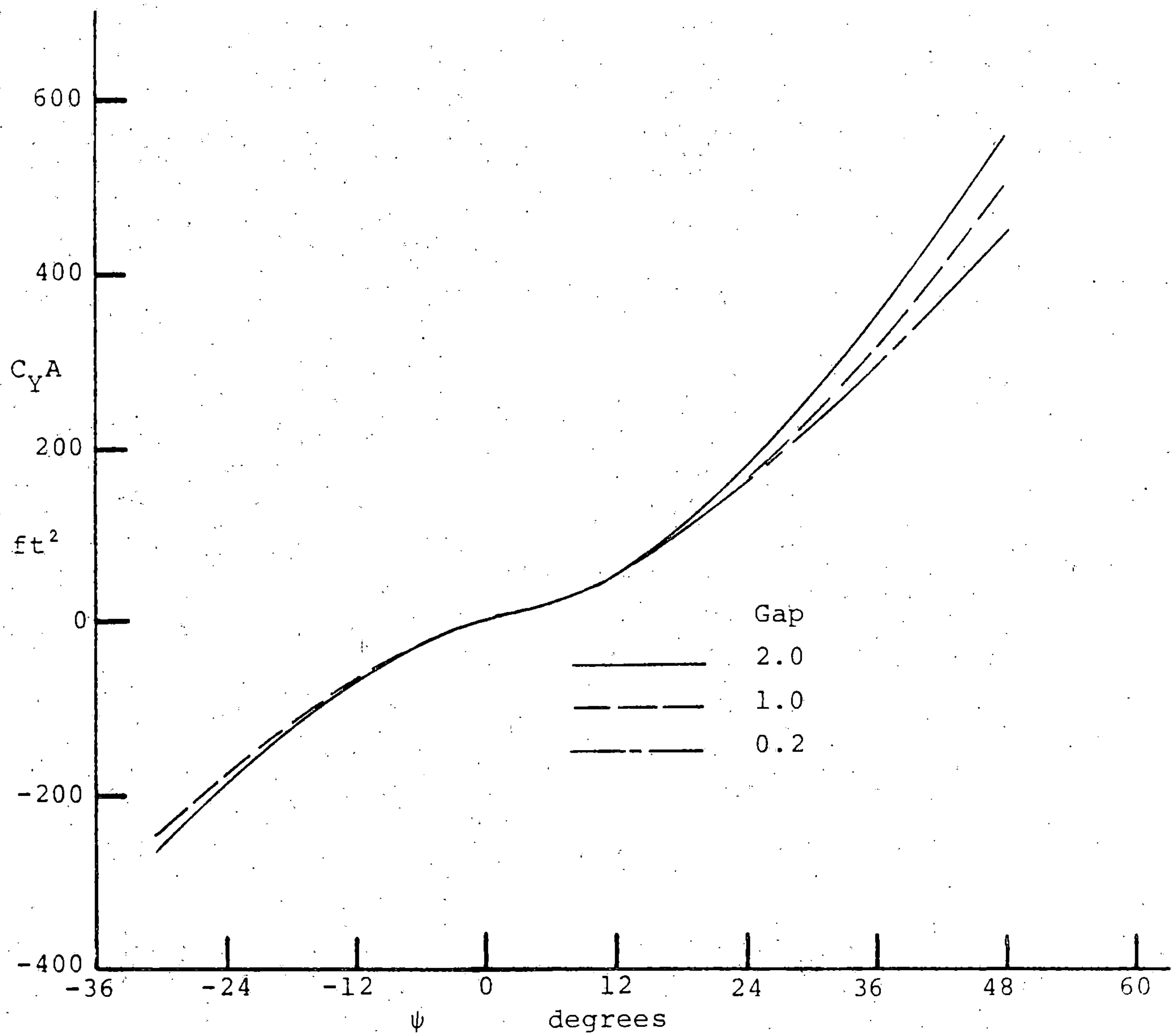

Figure 59. Side Force Area on Forward Facing Trailers With Equal Spacing of Gaps Ahead and Behind. 100% Shielding.

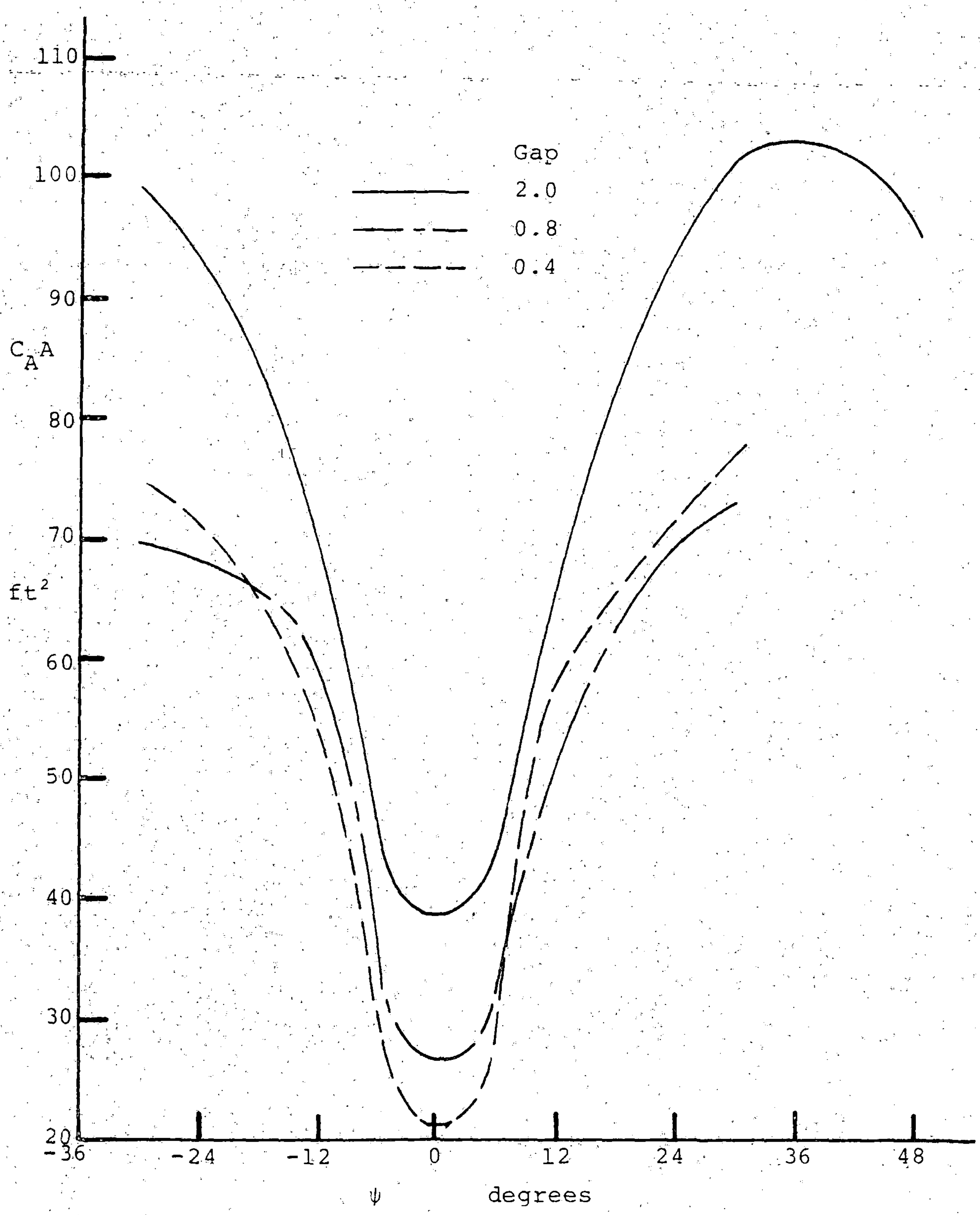

Figure 60. Axial Force Area on Rearward Facing Trailers With Equal Spacing of Gaps Ahead and Behind. 0% Shielding.

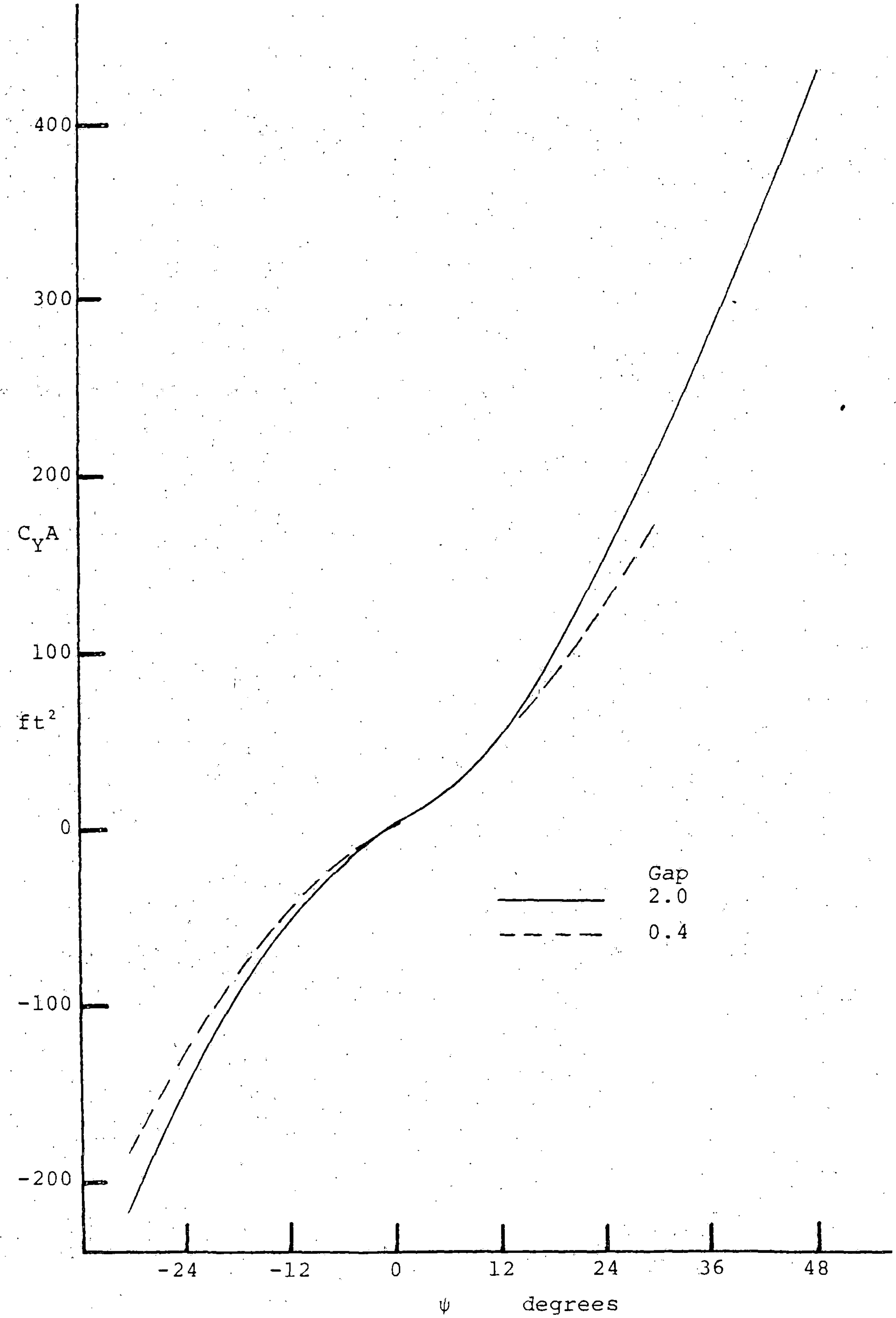

Figure 61. Side Force Area on Rearward Facing Trailers With Equal Spacing of Gaps Ahead and Behind. 0% Shielding.

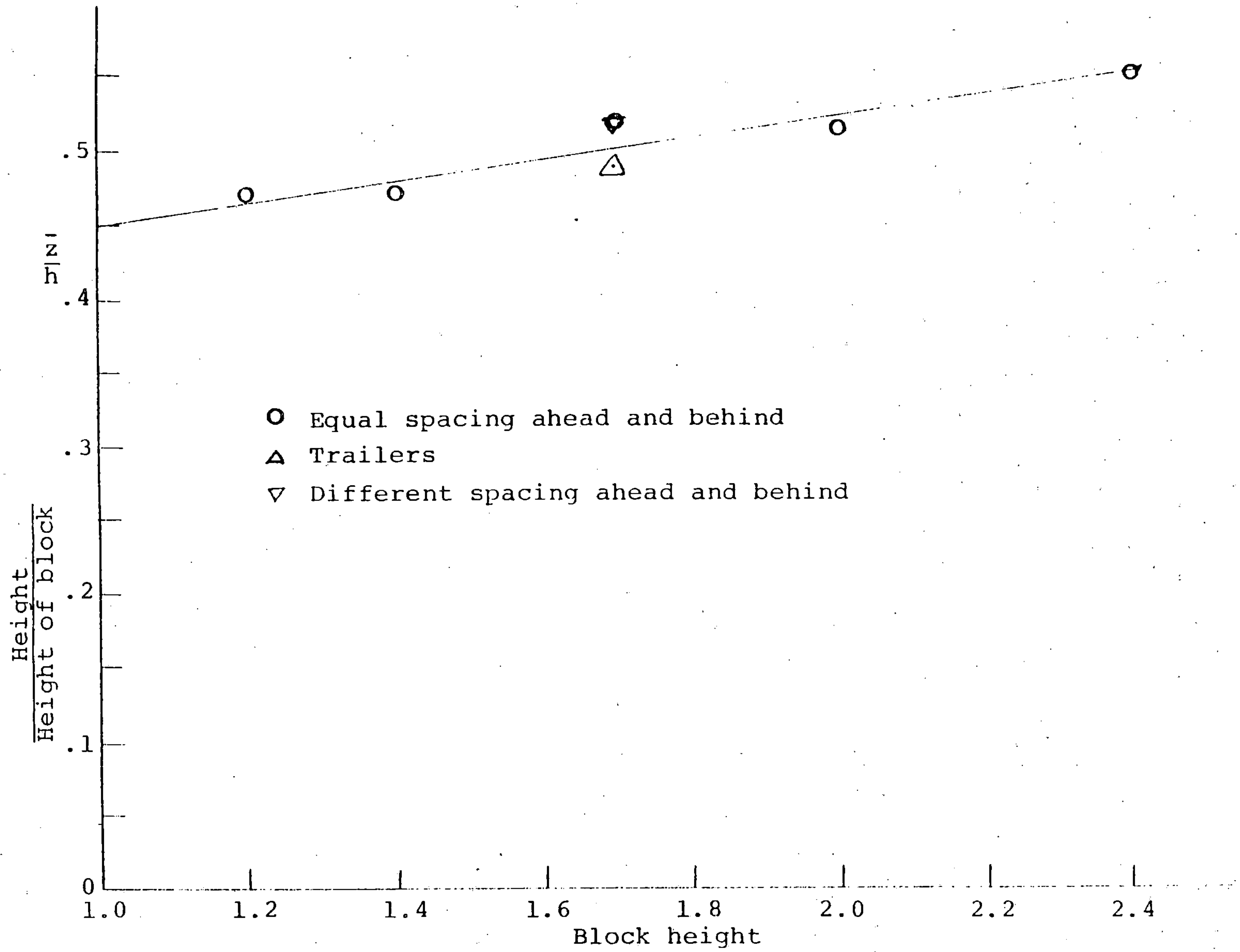

Figure 62. Height of the Point of Application of the Side Force on the Container Blocks and Trailers as a Function of Block Height.

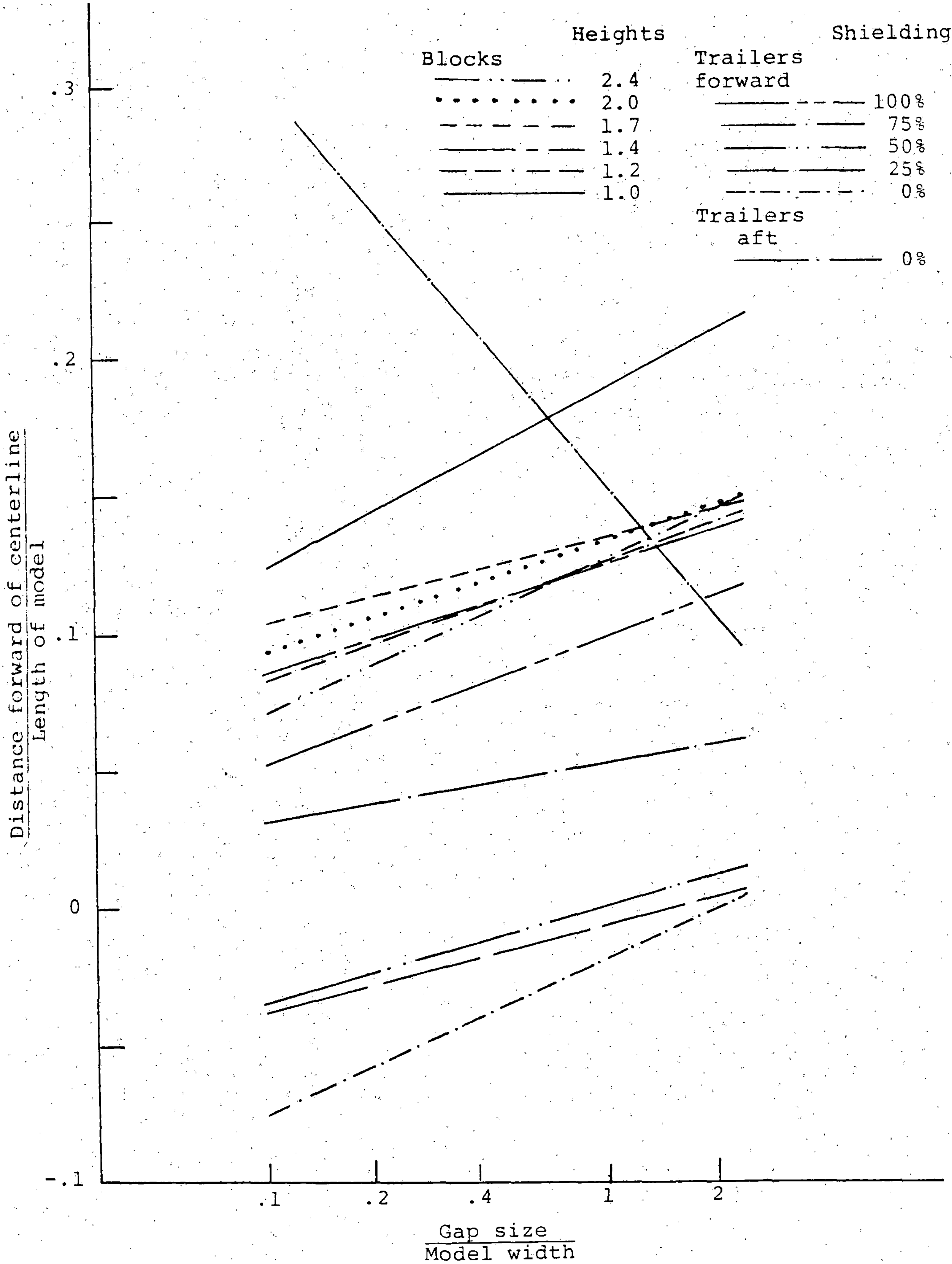

Figure 63. Longitudinal Location of the Point of Application of the Side Force on the Container Blocks and Trailers as a Function of Gap Spacing.

TABLE 1

DYNAMIC PRESSURE q AS A FUNCTION OF RELATIVE WIND VELOCITY V_R

V_R(mph)	q(#/ft^2)
10	.2553
20	1.0214
30	2.298
40	4.085
50	6.384
60	9.193
70	12.513
80	16.343
90	20.684
100	25.536

TABLE 2

MATRIX OF TEST CONDITIONS

A. Container Blocks with Equal Spacing Front and Rear

Spacing \ Height	1.0	1.2	1.4	1.7	2.0	2.4
	Yaw Angles					
0+				0-30°		
0.1	0-30°	0-30°	0-30°	0-30°	0-30°	0-30°
0.2	0-48°	0-48° 42-90°	0-48°	0-48° 42-90°	0-48°	0-48°
0.3	0-30°		0-30°		0-30°	0-30°
0.4	0-30°	0-48° 42-90°	0-30°	0-30° 42-90°	0-30°	0-30°
0.5	0-48°		0-48°		0-48°	0-48°
0.6	0-30°	0-30°	0-30°	0-30°	0-30°	0-30°
0.7	0-30°		0-30°		0-30°	0-30°
0.8	0-30°	0-30°	0-30°	0-30°	0-30°	0-30°
0.9	0-30°		0-30°		0-30°	0-30°
1.0	0-48°	0-48° 42-90°	0-48°	0-48° 42-90°	0-48°	0-48°
2.0	0-48°	0-48° 42-90°	0-48°	0-48° 42-90°	0-48°	0-48°

B. Container Blocks 1.7 High with Different Spacing Front and Rear

Front	Rear	Yaw Angles
0.2	0.1	0-48°
0.4	0.1	0-48°
1.0	0.1	0-48°
3.0	0.1	0-48°
6.0	0.1	0-48°
0.1	0.2	0-48°
0.1	0.4	0-48°
0.1	1.0	0-48°
0.1	3.0	0-48°
0.1	6.0	0-48°

TABLE 2 (continued)

B. (continued)

Front	Rear	Yaw Angles
0.4	0.2	0-48°
1.0	0.2	0-48°
3.0	0.2	0-48°
6.0	0.2	0-48°
0.2	0.4	0-48°
0.2	1.0	0-48°
0.2	3.0	0-48°
0.2	6.0	0-48°
1.0	0.4	0-48°
3.0	0.4	0-48°
6.0	0.4	0-48°
0.4	1.0	0-48°
0.4	3.0	0-48°
0.4	6.0	0-48°
1.0	0.6	0-48°
3.0	0.6	0-48°
6.0	0.6	0-48°
0.6	1.0	0-48°
0.6	3.0	0-48°
0.6	6.0	0-48°
3.0	1.0	0-48°
6.0	1.0	0-48°
1.0	3.0	0-48°
1.0	6.0	0-48°
6.0	3.0	0-48°
3.0	6.0	0-48°

TABLE 2 (continued)

C. Trailers Facing Forward

Spacing \ Shielding	Yaw Angles 0%	25%	50%	75%	100%
0	0-30°		0-30°	0-30°	
0.1	0-30°	0-30°	0-30°	0-30°	0-30°
0.2	0-48°	0-48°	0-48°	0-48°	0-48°
0.3					0-30°
0.4	0-30°	0-48°	0-30°	0-48°	0-30°
0.5					0-48°
0.6	0-30°	0-30°	0-30°	0-30°	0-30°
0.7	0-30°				0-30°
0.8	0-30°	0-30°	0-30°	0-30°	0-30°
0.9	0-30°				0-30°
1.0	0-48°	0-48°	0-48°	0-48°	0-48°
2.0	0-48°	0-48°	0-48°	0-48°	0-48°

Trailers Facing Aft

0.4	0-30°
0.8	0-30°
2.0	0-48°

TABLE 3

VERTICAL LOCATION OF SIDE FORCE

A. Different Height Blocks - Equal Spacing Front and Rear

Block Height	Height / Block Height	Standard Deviation
1.0	.45	.021
1.2	.47	.017
1.4	.48	.016
1.7	.52	.011
2.0	.52	.016
2.4	.55	.039

B. 1.7 High Blocks - Different Spacing Front and Rear

Equal spacing front, variable rear

Front Spacing	Height / Block Height	Standard Deviation
0.1	.50	.049
0.2	.53	.023
0.4	.52	.013
0.6	.52	.018
1.0	.51	.015

Equal spacing rear, variable front

Rear Spacing	Height / Block Height	Standard Deviation
0.1	.53	.010
0.2	.54	.029
0.4	.53	.012
0.6	.53	.0077
1.0	.52	.050
All cases	.52	.012

TABLE 3 (continued)

C. Trailers facing forward

Shielding	Height / Trailer Height	Standard Deviation
0%	.49	.017
25%	.51	.021
50%	.46	.011
75%	.48	.0091
100%	.46	.012
Trailers facing aft		
0%	.50	.0084
All cases	.49	.021

APPENDIX

RELATIVE WIND

The aerodynamic effects on the train depend upon the relative velocity of the wind with respect to the train. This velocity can be caused by either the wind over the ground or the motion of the train. The relative wind is found from a vector addition of these two quantities as shown in Figure A-1. The relative wind and yaw angle can be calculated using the following relations.

$$V_R = \sqrt{(V_w \sin\alpha)^2 + (V_t + V_w \cos\alpha)^2}$$

$$\psi = \arctan\left(\frac{V_w \sin\alpha}{V_t + V_w \cos\alpha}\right)$$

BOUNDARY LAYER CONSIDERATIONS

A calculation of the boundary layer for the series of freight car tests run in the CIT wind tunnel was given in Reference 1 and repeated here as Figure A-2. This figure shows that the boundary layer is an appreciable fraction of the height of the unloaded multimodal cars recently tested. It is not until quite close to the wall that the boundary layer velocity drops appreciable from free stream velocity (0.8 free stream velocity at 0.2 of the boundary layer height from the wall).

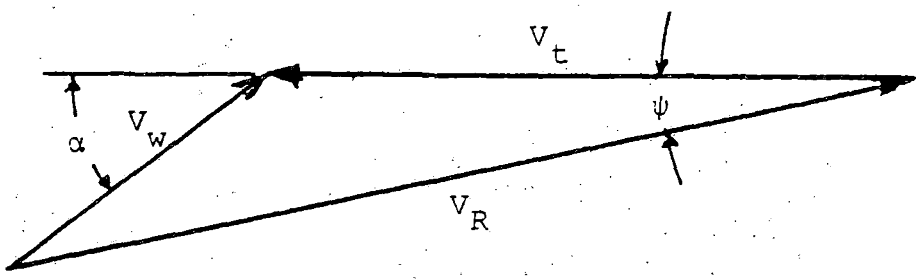

Figure A-1. Diagram Illustrating Relative Wind as Determined by Actual Wind and Train Speed.

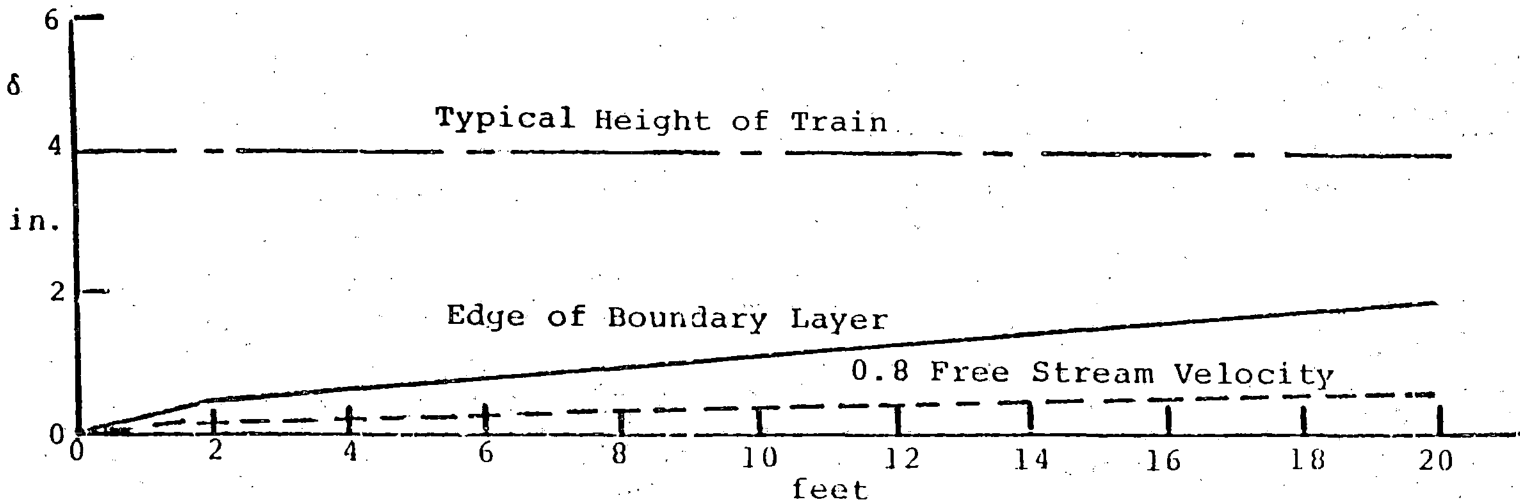

Figure A-2. Boundary Layer on Ground Board Compared With Train Height.

REFERENCES

1. Hammitt, A.G. "Aerodynamic Forces on Freight Trains. Volume I - Wind Tunnel Tests of Containers and Trailers on Flatcars," PB 264304, December 1976.

2. Hammitt, A.G. "Aerodynamic Forces on Freight Trains. Volume IV - Wind Tunnel Tests of Freight Cars and New Trailer and Container Car Designs," PB June 1979.